Miller, K.G., Sugarman, P.J., Browning, J.V., et al.
Proceedings of the Ocean Drilling Program, Initial Reports Volume 174AX (Suppl.)

2. OCEAN VIEW SITE[1]

Kenneth G. Miller, Peter J. Sugarman, James V. Browning, Stephen F. Pekar, Miriam E. Katz, Benjamin S. Cramer, Donald Monteverde, Jane Uptegrove, Peter P. McLaughlin Jr., Stefanie J. Baxter, Marie-Pierre Aubry, Richard K. Olsson, Bill Van Sickel, Keith Metzger, Mark D. Feigenson, Sarah Tiffin, Francine McCarthy[2]

SECTION AUTHORSHIP

The following, who are listed in alphabetical order, are responsible for the given section:

Chief Scientists: Miller, Sugarman
Staff Scientists: Browning, Pekar
Operations: Miller
Lithostratigraphy: Cramer, Katz, Metzger, Miller, Monteverde, Mullikin, Pekar, Skinner, Sugarman, Uptegrove, Van Sickel
Biostratigraphy:
- Foraminifers: Browning (Miocene), Pekar (Oligocene), Olsson (Miocene, Eocene)
- Calcareous nannofossils: Aubry
- Dinocysts: McCarthy, Tiffin

Logging: Baxter, McLaughlin
Isotopic stratigraphy: Feigenson, Monteverde, Pekar, Sugarman

SITE SUMMARY

The Ocean View Site (September and October 1999) was the sixth continuously cored borehole drilled as part of the New Jersey Coastal Plain Drilling Project and the third site drilled as part of Ocean Drilling Program (ODP) Leg 174AX, complementing shelf drilling during Leg 174A. Located between the Leg 150X Atlantic City and Cape May Sites,

[1]Miller, K.G., Sugarman, P.J., Browning, J.V., Pekar, S.F., Katz, M.E., Cramer, B.S., Monteverde, D., Uptegrove, J., McLaughlin, Jr., P.P., Baxter, S.J., Aubry, M.-P., Olsson, R.K., Van Sickel, B., Metzger, K., Feigenson, M.D., Tiffin, S., McCarthy, F., 2001. Ocean View Site. *In* Miller, K.G., Sugarman, P.J., Browning, J.V., et al., *Proc. ODP, Init. Repts.,* 174AX (Suppl.), 1–72 [Online]. Available from World Wide Web: <http://www-odp.tamu.edu/publications/174AXSIR/VOLUME/CHAPTERS/174AXS_2.PDF>. [Cited YYYY-MM-DD]
[2]**Scientific Party addresses.**

Ms 174AXSIR-102

drilling at Ocean View (39°10′43.826″N, 74°43′31.643″W; elevation = 9.4 ft [2.87 m]; Sea Isle City, United States Geological Survey [USGS] 7.5-min quadrangle; Dennis Township, Cape May County, New Jersey) targeted upper Miocene through middle Eocene sequences. Recovery was very good (mean recovery = 81%), ending at a total depth (TD) of 1575 ft (480.06 m) in lowermost middle Eocene sediments. A full suite of slimline logs was obtained to 1123 ft (342.29 m), and a gamma-ray log was obtained to 1560 ft (475.49 m). The scientific team provided descriptions of sedimentary textures, structures, colors, and fossil content and identified lithostratigraphic units, lithologic contacts, and sequences (unconformity-bounded units). Sr-isotopic analyses of the numerous shell beds found at Ocean View provide excellent age control, supplemented by biostratigraphic (planktonic foraminiferal, nannofossil, and dinocyst) studies.

The Cape May Formation (5–107.5 ft; 1.5–32.8 m; ?middle-late Pleistocene–Holocene) consists primarily of sands and subordinate gravels and clays that represent nearshore environments. Gravels (0–16.1 ft [0.00–4.91 m]) comprise the terrace that has been dated at Cape May as oxygen isotope Stage 5e. Below this (to 107.5 ft; 32.8 m), the Cape May Formation consists primarily of very fine to medium occasionally gravelly quartz sands, deposited in nearshore barrier complex environments. Sands assigned provisionally (107.5–166.7 ft; 32.8–50.81 m) and definitively (166.7–220.55 ft; 50.81–67.2 m) to the Cohansey Formation represent three or four sequences that either were not represented in previous New Jersey boreholes or were very poorly defined in estuarine sediments at Cape May. At Ocean View, these sands were deposited in nearshore and estuarine environments. Dinocysts indicate that they can be assigned to either Zone DN8 (upper middle Miocene) or DN6 (upper Miocene). These sequences should complement the fully marine upper middle to upper Miocene sequences sampled by the Leg 174AX Bethany Beach, Delaware, borehole.

The Kirkwood Formation (220.55–1002.8 ft; 67.22–305.65 m) at Ocean View is comprised of three middle Miocene (Kw/Co, Kw3, Kw2b) and four lower Miocene (Kw2a, Kw1b, Kw1a, and Kw0) sequences. Sequences Kw2c and Kw1c are not represented at Ocean View but are truncated between this site and Cape May. Sequences Kw2 and Kw1a are each provisionally subdivided into three higher-order sequences (Kw2a1, Kw2a2, and Kw2a3; Kw1a1, Kw1a2, and Kw1a3, respectively). The preservation of higher-order lower-middle Miocene sequences can be explained by higher sediment supply and accommodation space provided by loading; alternatively, the great thickness of the section is consistent with an autocyclical cause (lobe switching) for these apparent sequences. Analyses of nearshore seismic profiles recently collected near Ocean View should reveal if the higher-order cyclicity is due to base level lowering, and hence, if these are true sequences or due to autocyclical processes. Possible lowstand deposits are identified for the first time in the Kirkwood Formation in both Sequences Kw2a and Kw1a.

The Kirkwood sequences have many more shell beds than were previously found at other onshore New Jersey boreholes; these shells provided Sr-isotopic age estimates that are critical in dating sequences, sequence boundaries, and their relationship to glacioeustasy. The relatively complete lower to middle Miocene section at Ocean View will allow (1) comparison with those to the north (Atlantic City and Island Beach) and to the south (Cape May and Bethany Beach, Delaware, boreholes) to evaluate the effects of regional tectonics on the preservation

and architecture of sequences and (2) evaluation of the stratigraphic response to eustasy estimated from both backstripped and global $\delta^{18}O$ records.

The thick Oligocene section (895.55–1171.5 ft; 272.96–357.07 m) at Ocean View consists of six to eight sequences. Numerous shell beds in the Oligocene section provide detailed Sr-isotopic age estimates. Integration of Sr-isotopic ages with lithostratigraphy suggests correlation with Sequences O6, O5, possibly O4, O3, O2b, O2a, O1, and possibly ML of Pekar et al. (1997a), indicating that the Ocean View borehole provides the most complete record of Oligocene deposition in New Jersey. Further analysis of the Oligocene section will (1) test a model that explains the patchy distribution of onshore Oligocene strata by clinoform progradation, (2) develop a more detailed Oligocene eustatic estimate using two-dimensional backstripping, and (3) evaluate the stratigraphic response to eustasy estimated from both the backstripped and global $\delta^{18}O$ records.

The upper Eocene section at Ocean View (1171.5–1434.4 ft; 357.07–437.21 m) is the thickest cored in New Jersey. At least two sequences were identified, correlating with Sequences E11 and E10 of Browning et al. (1997a), both of which are assigned to the Absecon Inlet Formation. This section is significant because it is quite fossiliferous, exhibits minimal diagenetic alteration, and was deposited in the deepest paleodepth of any upper Eocene section in New Jersey. This upper Eocene section provides an excellent opportunity to develop a stable isotopic stratigraphy and a eustatic record, allowing us to test a first-order link between glacio-eustatic change and unconformities for this interval. Whereas these goals have been achieved for the Oligocene and younger record, is it unclear if glacioeustasy, in fact, controlled the development of late Eocene sequences. The lithologic assignment of the upper Eocene section between 1374.4 and 1402.9 ft (418.92 and 427.60 m) is equivocal, though we provisionally identify it as the Absecon Inlet Formation and a newly recognized sequence, E10a. Intercalations of nannofossil Zones N19/N20 and NP18 in this sequence suggest reworking, possibly associated with the Chesapeake Bay impact event. However, the underlying sequence (1402.9–1434.4 ft; 427.60–437.21 m) contains upper Eocene nannofossils (Zone NP18) mixed with middle Eocene acarininids and is correlated with Sequence E9; this sequence elsewhere in New Jersey has been correlated with the impact event. Further evaluation of the regional and global correlations of this event in New Jersey are needed, especially considering that previous studies have failed to find the correlative microtektites in New Jersey that are predicted for this event.

We recovered a relatively complete middle Eocene section (1434.4–1575 ft; 437.21–480.06 m) with the borehole TD in the lowermost middle Eocene. At least four sequences were recognized, and three were correlated with Sequences E8, E7, and E6 of Browning et al. (1997b). The middle Eocene section is significant because it was deposited further downdip than any previously cored middle Eocene section in New Jersey, providing a record of the full range of water depth variations for this interval. The section from 1521 ft (463.60 m) and below contains an interesting mix of lower Eocene planktonic foraminifers (Zones P6b/P7; *Morozovella formosa, Morozovella gracilis,* and various acarininids) and middle Eocene nannofossils (Zone NP15) and planktonic foraminifers (Zone P10 or younger). Such pervasive reworking is generally uncommon in New Jersey Coastal Plain subsurface boreholes and may point to a slumping event. Although much of the section below 1480 ft (451.10 m) suffers from silica diagenesis that may preclude stable isoto-

pic studies, the section above appears to be suitable for isotopic studies that will evaluate the link between glacio-eustatic change and sequences for the middle Eocene.

The Ocean View borehole was a tremendous success in meeting scientific goals. We obtained the following:

1. Upper Neogene sequences that provide a foundation for future drilling in the Delmarva peninsula, correlating to offshore Leg 174AX, and evaluating sea-level change for this interval;
2. A remarkably complete lower-middle Miocene section that allows evaluation of sea-level changes and tectonic effects when compared with the coeval sections to the north and south;
3. A thick fossiliferous Oligocene section that will allow testing of sequence stratigraphic models and the continued development of an Oligocene eustatic record using two-dimensional backstripping; and
4. Middle to upper Eocene sequences that allow the evaluation of the link between glacioeustasy and the formation of sequences.

BACKGROUND AND OBJECTIVES

This chapter is the site report for the sixth continuously cored and logged borehole drilled on the New Jersey Sea Level Transect. The JOIDES Planning Committee and Science Committee endorsed onshore drilling as an ODP-related activity. The first three sites (Fig. F1) were drilled at Island Beach (March–April 1993), Atlantic City (June–August 1993), and Cape May (March–April 1994) as Ocean Drilling Program Leg 150X (Miller et al., 1994a, 1994b, 1996a), the landward continuation of slope drilling by ODP Leg 150 (Mountain, Miller, Blum, et al., 1994). ODP Leg 174A continued the transect by drilling on the shelf (Fig. F1) (Austin, Christie-Blick, Malone, et al., 1998). Drilling continued onshore as Leg 174AX at Bass River (October–November 1996) (Miller, Sugarman, Browning, et al., 1998), Ancora (July–August 1998) (Miller et al., 1999b), and Ocean View, New Jersey (September–October 1999), and Bethany Beach, Delaware (May–June 2000) (Fig. F1). Bass River and Ancora were drilled updip, targeting Upper Cretaceous to Paleogene strata, whereas Ocean View and Bethany Beach were drilled downdip, targeting younger strata. Onshore drilling of the Legs 150X and 174AX boreholes was sponsored by the National Science Foundation, Earth Science Division, Continental Dynamics, and Ocean Drilling Programs, and the New Jersey Geological Survey (NJGS).

The New Jersey Sea Level/Mid-Atlantic Transect was designed to document the response of passive continental margin sedimentation to glacio-eustatic changes during the Oligocene to Holocene "Icehouse World," a time when glacioeustasy was clearly operating (see Miller and Mountain, 1994, for summary). Legs 150X (coastal plain) and 150 (slope) were extremely successful in dating Eocene–Miocene sequences, correlating them to the $\delta^{18}O$ proxy for glacioeustasy and causally relating sequence boundaries to glacioeustatic falls (Miller et al., 1996b, 1998). Onshore drilling was also designed to evaluate mechanisms for sea-level change during the Late Cretaceous to Eocene, an interval that purportedly lacked glacio-eustatic changes (e.g., Sea-Level Working Group, 1992) (see Miller et al., 1999a, for discussion).

F1. Location map showing existing ODP boreholes analyzed as a part of the New Jersey transect, p. 47.

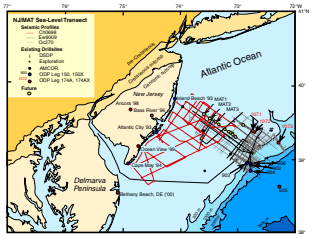

The Ocean View borehole targeted middle Eocene though Miocene sequences to document their regional distribution and in particular, to verify the ages and significance of several sequences that were sampled only at one previous borehole. For example, the Cape May borehole provided the key section for Miocene sequence stratigraphic and $\delta^{18}O$ comparisons (Miller et al., 1997) but three Miocene sequences have been recognized only at this site (Sequences Kw1c, Kw2c, and Kw-Cohansey) and their regional significance is uncertain. In addition, de Verteuil (1997) used dinocysts to identify one additional upper middle Miocene sequence (Ch2) and four upper Miocene sequences (Ch3–Ch6). These upper middle to upper Miocene sequences have been identified only at the Cape May borehole, and additional sampling is required to establish their regional significance.

Drilling at Ocean View and Bethany Beach was devised specifically to differentiate among potential controls on sequence distribution. The Ocean View and Bethany Beach boreholes and other onshore records (Fig. **F1**) provide an extensive regional database of Oligocene–Miocene sequences that can be integrated with nearshore seismic profiles (Fig. **F1**) (Monteverde et al., 2000). This regional view will allow mapping of regional depocenters and delineation of tectonic features (e.g., faults and differential basin evolution) and their effects on sediments. For example, the regional depocenter shifted from New Jersey during the early Miocene to Maryland (Owens et al., 1988) during the middle Miocene to Pliocene, whereas Oligocene strata show a remarkably "patchy" regional distribution (Pekar et al., 2000). Owens and coauthors (e.g., Owens and Sohl, 1969; Owens et al., 1997) argued that the Miocene pattern reflected differential warping on the basins and arches on the Atlantic continental margin, although the pattern could be ascribed to switching of sediment lobes. Similarly, the patchy regional distribution of Oligocene strata in the mid-Atlantic region have been attributed to lobe switching (Miller et al., 1997), faulting (Benson, 1994), or clinoform progradation (Pekar et al., 2000).

Drilling at Ocean View was also designed to test models of sedimentation within sequences, integrating borehole facies information with seismic facies information derived from seismic profiles collected on the continental shelf (Monteverde et al., 2000) (Fig. **F1**). Drilling at Bethany Beach, Cape May, Ocean View, Atlantic City, and Island Beach provides an along-strike view of numerous lower Miocene sequences that reach their maximum thickness and development in nearshore profiles (Monteverde et al., 2000). New seismic ties (Ch0698 profiles) (Fig. **F1**) allow direct correlation of ages and depositional environments to the nearshore grid. The boreholes also provide information on middle Miocene sequences that can be tied to the middle shelf where they are best developed (e.g., Mountain, Miller, Blum et al., 1994; Austin, Christie-Blick, Malone, et al., 1998).

The Ancora, Bass River, and Ocean View boreholes had another major objective: to evaluate the stratigraphic continuity and hydrogeological potential of aquifers and confining units. The NJGS funded direct drilling costs for Bass River and partially funded drilling at Ancora and Ocean View to address hydrogeological objectives. Bass River and Ancora targeted Cretaceous aquifers in the Mount Laurel, Englishtown, and Potomac-Raritan-Magothy (PRM) Formations (see Zapecza, 1989, for discussion of these aquifers). Ocean View targeted Miocene aquifers (e.g., the Atlantic City 800-ft sand aquifer of Zapecza, 1989) and confining units between Cape May and Atlantic City. Continuous coring in the New Jersey Coastal Plain has shown that aquifer-confining unit

couplets are sequences bounded by unconformities (Sugarman and Miller, 1997). Thus, sequence stratigraphy provides a means to predict the continuity and regional distribution of aquifer-confining units (Sugarman and Miller, 1997). However, the updip-downdip and alongstrike relationships of aquifer-confining units is not clear in many cases. For example, the Atlantic City 800-ft sand near Atlantic City is comprised of two sand bodies that make up the highstand systems tracts of Sequences Kw1a and Kw1b (Sugarman and Miller, 1997). However, at Cape May, there are three sand bodies that could be mapped as the Atlantic City 800-ft sand. The highest of these aquifer sands is associated with Sequence Kw1c and pinches out between Cape May and Atlantic City. Although this aquifer does not correlate with the Atlantic City 800-ft sand at Atlantic City, it has been mapped as its equivalent throughout the Cape May peninsula. Drilling at Ocean View was designed to answer outstanding questions about Cenozoic aquifers, including the Atlantic City 800-ft sand.

OPERATIONS

Drilling at Ocean View, New Jersey (39°10′43.826″N, 74°43′31.643″W; elevation = 9.4 ft [2.87 m]; USGS, Sea Isle City, 7.5-min quadrangle, Dennis Township, Cape May County) began in early September 1999. Drilling operations were superintended by Gene Cobbs, USGS Eastern Earth Surface Processes Team (EESPT; Don Queen, Head Driller); Gene Cobbs III was the driller. The New Jersey Highway Authority provided space, water, and electricity at the Ocean View Service Area (Bharat Patel, Engineer). On 7 September, the USGS team arrived onsite and began rigging up, testing the water well onsite, and connecting electrical hookups. On 8 September, a Hecht field trailer was set up as a portable lab and S. Pekar (staff scientist) and B. Cramer moved equipment onsite. A Kodak DC260 digital zoom camera (38.4- to 115.2-mm lens; 1536 × 1024 megapixel resolution), Power Macintosh 7200, and photography stand were set up to photograph 2-ft (0.61 m) core segments; after testing, the camera's default settings (including flash) with wide-angle (38.4 mm) lens were used, yielding the truest colors and ensuring uniformity among photographs. Tests with the NIH Imaging 1.61 software program show a slight difference in lighting, with the greatest lighting in the center. Photographic analysis should be able to account for this effect.

All cores were measured in feet (all depths are given in feet below land surface with metric conversions provided). We continued to adopt the ODP convention of top-justifying depths for intervals with incomplete recovery for all field notes and photos. The first core was obtained on 9 September 1999 using a Christensen 94-mm (HQ) system, 4.5-in Long-year Amoeva/5 bit, and 2.5-in core diameter. For unconsolidated sands, an extended shoe was used to contact the sample 0.25–0.5 in ahead of the bit. Approximately 2 ft (0.61 m) of surface casing was set and coring began at 5 ft (1.52 m) below land's surface. Recovery was moderate in surface gravels. Run 3 (15–20 ft; 4.57–6.10 m) recovered only 0.3 ft (0.09 m) of caved gravels. Fine sands were encountered on the next run; we extended the shoe further and had good recovery on run 5 (25–30 ft; 7.62–9.14 m). Caving gravels inhibited recovery on the next run; we washed the hole and recovery improved. Core recovery from 25 to 60 ft (7.62 to 78.29 m) was good (recovery = 65%); actual recovery for this interval is higher due to squashing of sands. The day ended at 60 ft (18.29 m) with 28.0 ft (8.53 m) recovered (recovery =

50.1%). On 10 September, we shortened the runs to 3–4 ft (0.91–1.22 m) in aquifer sands and gravels; recovery was good (recovery = nearly 70% between 60 and 80 ft [18.29 and 24.38 m], not accounting for squashing of sands). Heavy rains, gravels, and caving sands slowed coring; at noon we shortened the shoe to 1.25 in and flushed the hole with mud. Sands flowed into the bottom of the rods and we pulled the rods to clear them. Rods were set and the water swivel blew. Coring did not resume for the rest of the day.

On 11 September, we lengthened the runs to 5 ft (1.52 m) because of the absence of gravels. Drilling runs were extended to 10 ft (3.05 m) as clayey sands were penetrated. Run 25 (120–130 ft; 38.10–39.62 m) was lost downhole and was flushed away by the drilling muds. On run 26, a sharp lithologic contact separating hard clays above from very coarse pebbly quartz sand below (141.9 ft; 43.25 m) resulted in ending the run at 144.5 ft (44.04 m). A strong water-pressure head was encountered at this level that pushed sand 6 ft (1.83 m) up the hole. The sands were flushed and the day ended with 42.9 ft (13.08 m) of recovery between 80 and 144.5 ft (24.38 and 44.04 m; recovery = 66.5%).

On 12 September, the hole was flushed until 0900. Because of abrupt changes in lithology, the first three runs were shortened once again to 5-ft (1.52 m) intervals. Run 31 was extended to 7.5 ft (2.29 m) (160–167.5 ft; 48.77–51.05 m), with run 32 completing the 10-ft (30.5 m) rod (167.5–170 ft; 51.05–51.82 m), both with 100% recovery. We tried to core 10 ft (3.05 m) on run 33 (170–180 ft; 51.82–54.86 m), but most of the core was lost. The hole was flushed, terminating drilling for the day with 20.3 ft (6.19 m) of recovery between 144.5 and 180 ft (44.04 and 54.86 m; recovery = 57.2%).

Caving sands continued to slow drilling operations on 13 September, requiring extensive washing between runs. Recovery was excellent with 10-ft (3.05 m) runs. Run 36 (200–208 ft; 60.96–63.40 m) was stopped at 8 ft (2.44 m), when the drill would not easily advance. Run 37 (208–210 ft; 63.40–64.01 m) recovered 2.97 ft (0.91 m) from 3 ft (0.91 m) drilled; the top 1.55 ft (0.47 m) is probably caved, as indicated by a coarse pebbly sand at this level. The next run (210–220 ft; 64.01–67.06 m) became blocked by pebbly sand at 213.5 ft (65.07 m). Silty clay immediately below the contact (213.5–213.6 ft; 65.07–65.11 m) was recovered, but the clays would not push the sands into the inner core barrel and the rest of the clays were lost (chewed up). The next run was stopped at 226.5 ft (69.04 m) with nearly full recovery; drilling marks on the upper clays (220–220.55 ft; 67.06–67.22 m) indicate that it is possible that they were sticking out of the bottom of the hole (BOH) and recored. Smooth coring began as we penetrated uniform sands of the Kirkwood Formation; virtually full recovery on the last two runs (226.5–240 ft; 69.04–73.15 m) resulted in 51.97 ft (15.84 m) of recovery between 180 and 240 ft (54.86 and 73.15 m; recovery = 86.6%).

On 14 September, silty clays of the Kirkwood Formation were penetrated at the base of the first 10-ft (3.05 m) run; we ran one more 10-ft (3.05 m) run into silty clay and decided to set casing. Recovery between 240 and 260 ft (73.15 and 79.25 m) was 20.05 ft (6.11 m; recovery = 100%). We pulled rods and began to ream the hole with a 7.875-in drag bit. On 15 September, we continued to ream the hole; we dropped the derrick in anticipation of Hurricane Floyd and suspended operations on 16 September. Wind and water damage were minimal from the hurricane (despite the eye passing over the site), and reaming operations were resumed and completed on 17 September. On 18 September, 365 ft (111.25 m) of 5-in polyvinyl chloride (PVC) casing was set without

grout to be removed on completion; coring resumed at 1400 hr. Smooth coring occurred between 260 and 290 ft (79.25 and 88.39 m), with 21.40 ft (6.52 m) recovered (recovery = 71.3%).

On 19 September, we drilled 80 ft (24.38 m; 290–370 ft; 88.39–112.78 m), recovering 69.75 ft (21.26 m; recovery = 87.2%). Coring was generally smooth and recovery excellent despite large lithologic changes. The only exception was run 53 (340–350 ft) (103.63–106.68 m), where 9 ft (2.74 m) slipped out of the core catcher and was lost. On run 51 (326.5–330 ft; 99.52–100.58 m), we recovered 7.6 ft (2.32 m) from a 6.5-ft (1.98 m) run; we believe that the extra foot (0.30 m) is from run 49 that was left sticking out of the BOH. Smooth coring continued on 20 September with excellent recovery (77.15 ft [23.52 m] from 90 ft [27.43 m] drilled; recovery = 85.7%). Rose Eppers of the USGS Water Resource Division (WRD) began sampling for pore-water studies, obtaining ~0.75-ft (0.23 m) whole-round core sections from silty clays at 387.45–388.0 ft (118.09–118.256 m), 393.1–393.95 ft (119.82–120.08 m), 403.25–404.0 ft (122.91–123.14 m), and 437.25–438.0 ft (133.27–133.50 m). Run 70 (410–420 ft; 124.97–128.02 m) had 2 ft (0.61 m) of slop at the top, probably due to caved material at the BOH. The drillers reported that pressure was high (200 lbs; 90 kg) for 6.5 ft (1.98 m) on this run then dropped off; we probably blew off sands below 6.5–7 ft (1.98–2.13 m) on the run. Sands from 410 to 423.5 ft (124.97 to 129.08 m) had a very heavy rind of mud; heavy washing revealed medium-coarse sands with gravel that is probably in situ. Recovery was very good-excellent in shelly, clayey fine sands (410–433.25 ft; 124.97–132.05 m) and tight silty clays (433.25–440 ft; 132.05–134.11 m). Run 64 (440–450 ft; 134.11–137.16 m) only recovered 1.5 ft (0.46 m) of shelly sand; the rest of the core slipped out of the core catcher back into the hole. The drillers were unable to recapture this core. The last coring run recovered 9.2 ft (2.80 m) of sand, ending the day at 460 ft (140.21 m) with 90 ft (27.43 m) drilled.

On 21 September, the first run was stopped at 465 ft (141.73 m) by a hard layer; we shortened the shoe from 1.5 to 1.25 in. Hard and dry sands slowed drilling, although recovery remained very good through run 68 (470–480 ft; 143.26–146.30 m). Run 69 (480–490 ft; 146.30–149.35 m) recovered only 2.3 ft (0.70 m) of silt that drilled like clay with moderate mud pressure; apparently, a hard layer blocked off the run. The next run (run 70) (490–500 ft; 149.35–152.40 m) had an increase in mud pressure as we passed from uniform silts into chocolate silty clays with 104% recovery. Shelly sands stopped the next run at 507.5 ft (154.69 m); the rod was finished to 510 ft (155.45 m) with total recovery. The last run of the day (510–520 ft; 155.45–158.50 m) recovered 7.55 ft (2.30 m), resulting in 45.90 ft (13.99 m) recovered from 60 ft (18.29 m) drilled (recovery = 76.5%).

On 22 September, 8.6 ft (2.62 m) was recovered from run 74 (520–530 ft; 158.50–161.54 m). A change from clayey silt to fine sands shortened the next run to 4 ft (1.22 m) (3.1 ft [0.94 m] recovered). The remaining 6 ft (1.83 m) was then cored, with 5.1 ft (1.55 m) recovered. Dominantly clay silts made coring easier, and 10.2 ft (3.11 m) was recovered from run 77 (540–550 ft; 164.59–167.64 m). On run 78 (550–560 ft; 167.64–170.69 m), only 4.9 ft (1.49 m) was recovered, as clays clogged the core barrel. On run 79 (560–570 ft; 170.69–173.74 m), 9.4 ft (2.87 m) of clay-silt was recovered, but the core was chattered. To try and remediate this, a longer shoe was used in the next run. This approach improved the recovery of silts and clays on the next two runs (570–590 ft; 173.74–179.83 m) (recovery = ~90% in this interval). The

day ended with 59.9 ft (18.26 m) recovered from 70 ft (21.34 m) drilled (recovery = 85.6%).

Smooth coring with excellent recovery through silty clays continued on 23 September until indurated zones slowed progress. Run 84 (610–619 ft; 185.93–188.67 m) was blocked by hard clays at 618.1 ft (188.40 m) and the bottom 0.9 ft (0.27 m) was lost. Run 85 (619–627 ft; 188.67–191.11 m) was blocked at 627 ft (191.11 m) at an indurated chalky ?porcellanitic claystone; we ran the next 3 ft (0.91 m) with the rock shoe, recovering 0.5 ft (0.15 m) of claystone, 2.4 ft (0.73 m) of clay, and 0.1 ft (0.03 m) of sand (recovery = 100%). Run 86 (630–636 ft; 192.02–193.85 m) was stopped short at 6 ft (1.83 m) into a 10-ft (3.05 m) run by an indurated zone; the rod was completed on the next run (636–640 ft; 193.85–195.07 m). Run 88 (640–650 ft; 195.07–198.12 m) culminated the day with only 2 ft (0.61 m) of recovery, as we penetrated loose sands. The day ended with 51.7 ft (15.76 m) recovered from 60 ft (18.29 m) drilled (recovery = 86.1%).

Very shelly sands and sandy shell beds proved difficult to recover on 24 September, with 7 ft (2.13 m) and 1.5 ft (0.46 m) recovered between 650 and 660 ft and 660 and 670 ft (198.12 and 201.17 m and 201.17 and 204.22 m), respectively. We shortened the runs to 5 ft (1.52 m) and enjoyed excellent recovery. We ended the day with 32.15 ft (9.80 m) recovered between 650 and 695 ft (198.12 and 211.84 m; recovery = 71.4%). Smooth coring with good recovery through silty clays and fine-medium quartz sand continued during the morning of 25 September. We limited coring to 5 ft (1.52 m) on runs 97 and 98 because of highly variable lithologies. Run 99 was shortened to 3 ft (0.91 m) after encountering a harder lithology. During this run, we recovered 3.9 ft (1.19 m) from a 3-ft (0.91 m) run; we believe that the extra foot (0.30 m) is from run 98. Run 100 was a 7-ft (2.13 m) run that recovered a spectacular shell bed near the base. However, run 101 (720–730 ft; 219.46–222.50 m), recovered only 2.3 ft (0.70 m) because of a malfunction of the automatic chuck jaw. The drillers decided to replace the jaw and returned to Reston, Virginia, suspending drilling operations until the morning of 27 September.

On 27 September, we ran 5 ft (1.52 m) (730–735 ft; 222.50–224.03 m) and recovered 1 ft (0.30 m) of caved material, resulting from the hole sitting for 2 days, and 4 ft (1.22 m) of solid medium-fine sand. Full recovery of interbedded sand and silty clay was obtained on run 103 (735–740 ft; 224.03–225.55 m). Run 104 (740–750 ft; 225.55–228.60 m) became blocked by pebbly sands 1.6 ft (0.49 m) into the run, and the bottom 8.4 ft (2.56 m) was blown away. Run 105 (750–760 ft; 228.60–231.64 m) had nearly full recovery; run 106 was stopped short at 765 ft (233.17 m) with 4.6 ft (1.40 m) recovered. Run 107 (765–775 ft; 233.17–236.22 m) recovered 10.05 ft (3.06 m). Total recovery for the day was 34.05 ft (10.38 m) from 45 ft (13.72 m) drilled (recovery = 75.7%). On 28 September, poorly consolidated sands hindered recovery on runs 108 and 109 (775–780 and 780–785 ft; 236.22–237.74 and 237.74–239.67 m). We shortened the shoe and had very good recovery of sands on runs 110 (785–790 ft; 239.27–240.79 m), 111 (790–800 ft; 240.79–243.84 m), and 112 (800–810 ft; 243.84–246.89 m) and excellent recovery of sandy silty clays on runs 113–115 (810–840 ft; 246.89–256.03 m). The day ended at 840 ft (256.03 m) with 54 ft (16.46 m) recovered (recovery = 83%).

On 29 September, drilling began with two 10-ft (3.05 m) runs, each with excellent recovery (10.65 and 9.65 ft; 3.25 and 2.94 m), as silty clays and silty fine sands were easily cored. The run from 860 to 870 ft

(262.13 to 265.18 m) recovered only 3.55 ft (1.08 m), as the shoe became clogged with silty clay. The next run (870–880 ft; 165.17–268.22 m) recovered 9.1 ft (2.77 m) of clayey silt-silty clay that was removed from the barrel using high pressure from the mud pump, fracturing parts of the core. The next run, 880–890 ft (268.22–271.27 m), was a silty clay and again recovery was excellent (9.6 ft; 2.93 m). The run from 890 to 900 ft (271.27 to 274.32 m) had excellent recovery (9.95 ft; 3.03 m) despite the fact that the shoe was ruined on a gravel bed. Coring ended with a 6-ft (1.83 m) run between 900 and 906 ft, (274.32 and 276.15 m) with 66.90 ft (20.39 m) recovered between 830 and 906 ft (252.98 and 276.15 m; recovery = 88.0%).

Heavy rain delayed the start of coring on 30 September and drilling was slow through gummy glauconitic sands. Run 123 (906–910 ft; 276.15–277.37 m) recovered 5.05 ft (1.54 m); part of this was probably from the previous runs, yielding 107.5% recovery for both runs. Recovery of run 124 (910–920 ft; 277.37–280.42 m) was excellent. On run 125 (920–930 ft; 280.42–283.46 m), mud pressures alternated between 200 and 600 lbs (90 and 270 kg), and only 7.65 ft (2.33 m) was drilled. Run 126 drilled 8 ft (2.44 m) and recovered 10 ft (3.05 m), including 2 ft (0.61 m) from the previous run. We decided to label figures and cores as 920–928 (280.42–282.85 m) and 928–938 ft (282.85–285.90 m) for runs 125 and 126, respectively. We finished the rod on run 127, ending at 940 ft (286.51 m), with 34.25 ft (10.44 m) recovered for the day (recovery = 95.1%).

Coring on 1 October began with excellent recovery on runs 128 and 129 (9.9 and 9.2 out of 10 ft [3.02 and 2.80 out of 3.05 m], respectively) in glauconitic medium-coarse quartz sand. The bottom 1.1 ft (0.34 m) of run 129 became softer and siltier, allowing for easier drilling. For the softer and siltier sediment, we switched to a longer shoe with a plastic core catcher on run 130 (960–970 ft; 292.61–295.66 m). Run 131 (970–975 ft; 295.66–297.18 m) (4.25 ft [1.30 m] recovered) was stopped at 5 ft (1.52 m) because of slow drilling in glauconite sands. The wider shoe was used on run 132 (975–980 ft; 297.18–298.70 m) (4.5 ft [1.37 m] recovered), but drilling remained extremely slow. We pulled two rods to wash and ream the hole on 2 October. The day ended at 980 ft (298.70 m) with 36.5 ft (11.13 m) recovered (recovery = 91.25%).

Coring on 2 October was faster after washing and reaming the bottom 30 ft (9.14 m) of the hole. Run 133 continued the good recovery (9.4 ft [2.87 m] out of 10 ft [3.05 m]). Drilling became even quicker on run 134 due to increasing clay. The lower 6 ft (1.83 m) of run 134 (990–1000 ft; 301.75–304.80 m) was lost but was recovered on run 135. We switched to the longer narrow shoe for run 135. On run 135 (1000–1005 ft; 304.80–306.32 m), the drill bit stopped advancing after drilling 5 ft (1.52 m) and we retrieved 10.65 ft (3.25 m), including 5.65 ft (1.72 m) from the previous run. We decided to top justify to 994 ft (302.97 m), labeling cores from run 135 as 994–1004.65 ft (302.97–306.22 m). Run 136 (1005–1007.5 ft; 306.32–307.9 m) (2.0 ft [0.61 m] recovered) was stopped at 2.5 ft (0.76 m) because the drill bit would not advance. This core was undercut by the drilling mud pressure and was only ~1.5 in (3.8 cm) in diameter with a 1-in (2.5 cm) rind. We switched back to the rock shoe for run 137. Run 137 (1007.5–1011.5 ft; 307.09–308.31 m) (3.55 ft [1.08 m] recovered) was stopped at 4 ft (1.22 m) due to extremely slow drilling. The day ended at 1011.5 ft (308.31 m) with 29.55 ft (9.01 m) recovered (recovery = 93.8%).

On 3 October, run 138 (1011.5–1020 ft; 308.31–310.90 m) (5.8 ft [1.77 m] recovered) drilled easily in the middle though the top and bot-

tom drilled slowly. From 1013.2 to 1015.5 ft (308.82 to 309.52 m), the mud pressure undercut the core; 1014.7–1015.4 ft (309.28–309.49 m) may be a mixture of drilling mud and core. Run 139 (1020–1030 ft; 310.90–313.94 m) drilled easily, but the core barrel became stuck. When the barrel was finally retrieved, only 0.85 ft (0.26 m) of "core" (likely mostly drilling mud) was in the barrel. Run 140 (1030–1033 ft; 313.94–314.86 m) (1.7 ft [0.52 m] recovered) was stopped at 3 ft (0.91 m) when the drill string quit advancing. Recovery improved on the final run (run 141) (1033–1040 ft; 314.86–316.99 m) with 5.6 ft (1.17 m) recovered out of 7 ft (2.13 m) drilled. The day ended at 1040 ft (316.99 m) with 48.3% recovery.

On 4 October, no water was available onsite. Problems in the service area required the shutting down of all water supplies until midafternoon. In the interim, we pulled rods, checked the bit, which was only slightly worn, cleaned all equipment, and reran the rods. The rods easily reentered the hole, encountering no bridges, boding well for logging. We finished lowering the rods on 5 October. The inner core barrel would not latch in because of sands in the outer core barrel; therefore, we washed the hole and cleared the barrel. We switched from a rock shoe to one extending slightly ahead of the bit. Run 142 (1040–1045 ft; 316.99–318.52 m) ran with high mud pressure for the first 3 ft (0.91 m); pressures dropped in the next 2 ft (0.61 m) in clayier sediments that were undercut. These sandy clays were protruding from the end of the core barrel on recovery, though nearly full recovery was obtained. Run 143 (1045–1050 ft; 318.52–320.04 m) recovered 2.9 ft (0.88 m) of sandy clays. Run 144 (1050–1053 ft; 320.04–320.95 m) stopped 3 ft (0.91 m) into the run, with full recovery. Run 145 was cut short at 1056.5 ft (322.02 m), ending the day with 13.5 ft (4.11 m) of recovery (recovery = 81.8%).

Hugh Scott of MPI Drilling (Picton, Ontario, Canada) arrived on site to demonstrate the Multi-Twin G-30 drill ("Sonic Metaprobe") for shallow (<125 ft; <38.1 m) holes. He drilled a 54-ft (16.46 m) hole on 5 October adjacent to the USGS B-61 drill rig. On 6 October, the Metaprobe hole was completed to 74 ft (22.56 m). We designated the Metaprobe hole the Ocean View B hole. The cores were described onsite, labeled in "B" boxes, and moved to permanent storage at the Rutgers core repository.

On 6 October, the first 3.5 ft (1.07 m) of run 146 (1056.5–1060 ft; 322.02–323.09 m) recovered 3 ft (0.91 m) and finished the rod. A perfect 10 ft (3.05 m) was recovered on the next run (1060–1070 ft; 323.09–326.14 m). Recovery remained excellent in the interval between 1070 and 1080 ft (326.14 and 329.18 m) (8.4 ft [2.56 m] recovered), although indurated zones slowed drilling. Recovery from 1080 to 1090 ft (329.18 to 332.23 m) was only 6.4 ft (1.95 m), and the core was mangled and covered with drilling mud in places, obscuring the true lithology. Recovery of run 150 (1090–1100 ft; 332.23–335.28 m) was 10.7 ft (3.26 m). We generally interpret small amounts of recovered core in excess of the amount of core drilled (such as the "extra" 0.7 ft [0.21 m] recovered from run 150) to be the result of core expansion. A total of 38.5 ft (11.73 m) of core was recovered for the day between 1056.5 and 1100 ft (322.02 and 335.28 m; recovery = 88.5%).

On 7 October, runs 151 (1100–1106.5 ft; 335.287–337.26 m) and 152 were short (1106.5–1113 ft; 337.26–339.24 m) (4.7 ft [1.43 m] recovered). Drilling was slow from 1113 to 1120 ft (339.24 to 341.38 m) in gummy glauconite sands, with 7.95 ft (2.42 m) recovered; the extra 0.95 ft (0.29 m) may be from the previous run sticking from the BOH.

The cores were labeled as 1112–1120 ft (338.94–341.38 m). Drilling rates increased on run 154 (1120–1126 ft; 341.38–343.20 m), but the run was stopped short to prepare for logging. The day ended at 1126 ft (343.20 m) with 25.05 ft (7.64 m) recovered (recovery = 96.3%). Total recovery for the HQ portion of Ocean View Hole A was 892.57 ft (272.06 m) from 1121.0 ft (341.68 m) cored (recovery = 79.6%).

We logged Ocean View Hole A on 8 October. Peter McLaughlin and Stefanie Baxter from the Delaware Geological Survey obtained a gamma log through the rods from land's surface to 1123.3 ft (342.38 m); sampling was at 0.1-ft (0.03 m) increments. Log quality was excellent as judged by the match between gamma ray–log kicks and lithologic changes (Figs. F2, F3, F4, F5, F6, F7). The rods were pulled, the hole stayed open, and a multitool run was obtained on formation from land's surface to 1123 ft (342.29 m); tools on the sonde include the natural gamma, 64-in (1.6 m) normal resistivity, 16-in (0.4 m) normal resistivity, fluid resistivity, lateral resistivity, spontaneous potential, single-point resistance, temperature, and delta temperature. A second run on the formation was made with the sonic tool to 1123 ft (342.29 m), and a third was made with the 3-armed caliper tool to 1123 ft (342.29 m). NQ rods were lowered to ~100 ft (30.48 m) above the BOH on 11 October in preparation for coring on 12 October. No problems were encountered while running the rods into the hole.

Coring resumed on 12 October using a Christensen CNWL (NQ) system, 3.162-in (8.03 cm) hole diameter, and 1.875-in (4.76 cm) core diameter with the rock shoe and 1.67 in (4.24 cm) with extended shoes. The first run, 155 (1126–1130 ft; 343.20–344.42 m), recovered 1.2 ft (0.37 m). A lithology change to glauconitic clay at the beginning of run 156 (1130–1135 ft; 344.42–345.95 m) clogged the barrel and prevented core from entering, limiting recovery to 0.4 ft (0.12 m). Similar results were obtained on run 157 (1135–1140 ft; 345.95–347.47 m), with 1.4 ft (0.43 m) recovered. The final run of the day recovered 4.1 ft (1.25 m) from 5 ft (1.52 m) cored (1140–1145 ft; 347.47–349.00 m). Despite the improved recovery for this run, the drillers decided to pull the rods. The drillers had varied the length of the shoe through the day in an attempt to improve recovery. Good recovery was finally achieved by running the shoe far out in front of the drill bit. This implied to the drillers that the drill bit was cracked and expanding under pressure; this created a core too large to fit inside the shoe. On 13 October, the rest of the drill string was removed from the hole. The bit had cracked in three places and was replaced with a new one. The drillers reran the NQ rods and coring resumed at 1600 hr with Run 159 (1145–1150 ft; 349.00–350.52 m) recovering 4.80 ft (1.46 m).

Drilling proceeded on 14 October using the 10-ft (3.05 m) inner core barrel. Run 160 (1150–1160 ft; 350.52–353.57 m) had good recovery (8.10 ft; 2.47 m), whereas run 161 (1160–1162.5 ft; 353.57–354.33 m) was stopped in a hard clay with 2.40 ft (0.73 m) recovered. Run 162 (1162.5–1170 ft; 354.33–356.62 m) became blocked in the rock shoe (0.5 ft [0.15 m] recovered). We switched back to the extended shoe in run 163 (1170–1180 ft; 356.62–359.66 m) and enjoyed perfect recovery across the Eocene/Oligocene boundary. Rapid, smooth drilling continued as we penetrated clays and silty clays (runs 164–165) (1180–1200 ft; 359.66–3365.76 m) with excellent recovery. The day ended at 1200 ft (365.76 m) with 45.95 ft (14.01 m) recovered between 1150 and 1200 ft (350.52 and 365.76 m; recovery = 91.9%). On 15 October, coring proceeded without incident and recovery was excellent. Recovery on several coring runs was >10 ft (3.05 m; recovery = >100%) (e.g., 1200–1210

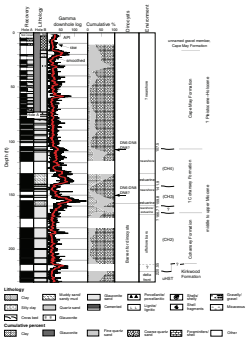

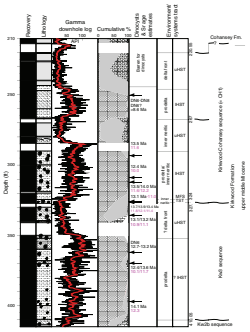

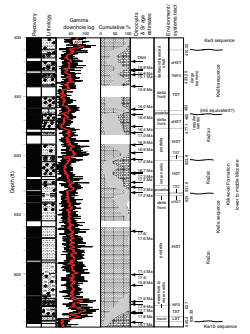

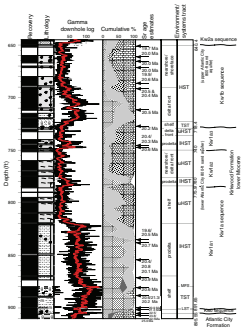

ft [365.76–368.81 m]; 1210–1220 ft [368.81–371.86 m]) due to clay expansion. Run 170 (1240–1250 ft; 377.95–381.00 m) was blocked off 3.75 ft (1.14 m) into the run, yielding 43.75 ft (13.34 m) recovered from 50 ft (15.24 m) penetrated for the day (recovery = 87.9%).

On 16 October, smooth coring on runs 171–175 (1250–1300 ft; 381.00–396.24 m) yielded good to excellent recovery (47.45 ft [14.46 m] from 50 ft [15.24 m] drilled; recovery = 94.9%). On 17 October, run 176 had good recovery (8.3 ft; 2.53 m). Run 177 was stopped by a hard layer, terminating this run after 3 ft (0.91 m) (2.95 ft [0.90 m] recovery). The top of run 178 contained 0.2 ft (0.06 m) of pyrite nodules and finished the 10-ft (3.05 m) section with 5.2 ft (1.58 m) recovery from a 7 ft (2.13 m) run. The last run of the day (run 179) contained perfect recovery (recovery = 104%), yielding 26.95 ft (8.21 m) from 30 ft (9.14 m) drilled. After a slight delay due to high winds associated with Hurricane Irene, smooth coring continued on 18 October. Run 180 (1330–1340 ft; 405.38–408.43 m) had full recovery, whereas the bottom of run 181 (1340–1350 ft; 408.43–411.48 m) would not break off, leaving 3 ft (0.91 m) in the BOH. The 3 ft (0.91 m) was not recovered and run 182 (1350–1360 ft; 411.48–414.53 m) recovered 10.5 ft (3.20 m). The day ended with run 183 (1360–1370 ft; 414.53–417.58 m), with 39.0 ft (11.89 m) recovered from 40 ft (12.19 m) drilled (recovery = 97.5%).

On 19 October, coring was slow on run 184 (1370–1390 ft; 417.58–423.67 m) as we penetrated variable clays and glauconitic clays. Coring rates improved as we penetrated the ash marls of the lower Shark River Formation below 1389.96 ft (423.66 m), with full recovery of runs 185 (1380–1390 ft; 420.62–423.67 m), 186 (1390–1400 ft; 423.67–426.72 m), and 187 (1400–1410 ft; 426.72–429.77 m). R. Eppers of the WRD sampled at 1370–1370.5 ft (417.58–417.73 m) and 1382–1382.8 ft (421.23–421.48 m); the 0.5-ft (0.15 m) sample was mandated by the large lithologic changes at 1370.5 and 1380 ft (417.73 and 420.62 m). The day ended with 40.85 ft (12.45 m) recovered between 1370 and 1410 ft (417.58 and 429.77 m; recovery = 102%). Drilling was suspended on 20 October because of heavy rains; the rods were rotated 60 ft (18.29 m) above the BOH, and the hole was reamed to 40 ft (12.19 m) above the BOH. The drillers had trouble getting to the BOH on 21 October due to expansion of the clays. Run 188 (1410–1420 ft; 429.77–432.82 m) was retrieved at 1330 hr, recovering 9.9 ft (3.02 m). Run 189 (1420–1430 ft; 432.82–435.86 m) retrieved only 3.7 ft (1.13 m) from 10 ft (3.05 m) drilled. We ran for the bottom 6.7 ft (2.04 m) on October 22 but only recovered 0.7 ft (0.21 m), 0.3 ft (0.09 m) of which was discarded as a mixture of drilling mud and chewed-up core. Run 190 (1430–1440 ft; 435.86–438.91 m) recovered 7.7 ft (2.35 m); 4 ft (1.22 m) of core was extending from the core catcher on recovery, indicating that 2.3 ft (0.70 m) had slipped out and was left in the hole. We ran 8 ft (2.44 m) on run 191 (1440–1448 ft; 438.91–441.35 m), recovering 10 ft (3.05 m), including the 2 ft (0.61 m) lost on the previous run; we top justified run 191 to 1438 ft (438.30 m). Run 192 (1448–1453 ft; 441.35–442.87 m) recovered 5.3 ft (1.62 m), ending the day with 23.0 ft (7.01 m) recovered between 1430 and 1458 ft (435.86 and 444.40 m; recovery = 100%).

Recovery was dismal on 23 October, as we attempted to drill heavily cemented clays. Run 193 (1453–1460 ft; 442.87–445.01 m) recovered 0.15 ft (0.05 m); run 194 (1460–1463 ft; 445.01–445.92 m) recovered 0.4 ft (0.12 m). We switched to the wider rock shoe for runs 195 (1463–1470 ft; 445.92–448.06 m) and 196 (1470–1480 ft; 448.06–451.10 m), recovering 2.2 and 0.4 ft (0.67 and 0.12 m), respectively. Throughout

F6. Atlantic City and Sewell Point Formations, p. 52.

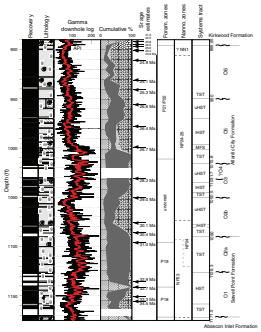

F7. Absecon Inlet and Shark River Formations, p. 53.

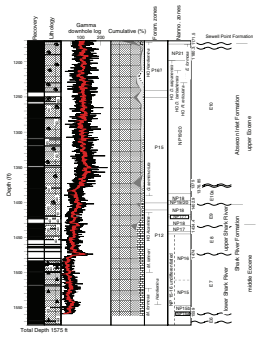

the day, mud pressures varied between high pressures typical of clays and low pressures typical of rock. Either the clays were too soft to push the indurated zones into the barrel or the clays plugged up the shoe and only the indurated zones were able to push through. The day ended with 11.7% recovery from 27 ft (8.23 m) drilled. On 24 October, run 197 (1480–1484 ft; 451.10–452.32 m) retrieved only 0.1 ft (0.03 m) of indurated sediment.

The core had not penetrated beyond the core barrel shoe and we ended coring for the day, yielding only 3.25 ft (0.99 m) recovered from 31 ft (9.45 m) drilled on 23 and 24 October (recovery = 10.5%). The drillers had not heard the inner core barrel latch into the outer core barrel since 22 October, although it must have latched in on run 195 in order to retrieve 2.2 ft (0.67 m). We lowered and retrieved the core barrel with a brand new extended shoe to ascertain if the barrel was locking into the drill bit. There were no gouge marks on the shoe, indicating that the shoe had not come into contact with the bit. We tried to pump out any obstructions without success and began pulling the rods at 1230 hr. We brought the rods above the NQ hole and repeatedly dropped the inner core barrel until we cleared an obstruction in the outer core barrel. A piece of core from the inner barrel must have broken off and lodged in the outer barrel, preventing the inner barrel from properly latching in. We began to re-run the rods to the BOH at 1484 ft (452.32 m) at 1930 hr. The rods were run to 20 ft (6.10 m) from the BOH on 25 October, recutting much of the NQ hole. Smooth but slow coring of porcellanitic clays resumed on 26 October. Runs 198 (1484–1487 ft; 452.32–453.24 m), 199 (1487–1490 ft; 453.24–454.15 m), and 200 (1490–1500 ft; 454.15–457.20 m) recovered 2.9, 3.5, and 8.5 ft (0.88, 1.07, and 2.59 m), respectively; run 201 (1500–1509 ft; 457.02–459.94 m) stopped 9 ft (2.74 m) into the run with 10.4 ft (3.17 m) recovered, including 1.4 ft (0.43 m) from the previous run. The day ended with 25.4 ft (7.74 m) recovered from 26 ft (7.9 m) drilled (recovery = 97.7%).

On 27 October, we drilled 10.3 ft (3.14 m) on run 202 (1509–1519.3 ft; 459.94–463.08 m), trying to jam the clays in so they would break off; we recovered 8 ft (2.44 m), leaving 2 ft (0.61 m) in the hole. Run 203 (1519.3–1527.5 ft; 463.08–465.82 m) recovered 0.37 ft (0.11 m) from the last run (logged as 1517.0–1517.37 ft; 462.38–462.49 m), 0.4 ft (0.12 m) of sloughed material that was discarded, and 6.8 ft (2.07 m) from the 8.2-ft (2.50 m) drilled interval. Run 204 was an 8.5-ft (2.59 m) run (1527.5–1536 ft; 465.58–468.17 m) that recovered 10.5 ft (3.20 m), with 2 ft (0.61 m) (logged as 1525.5–1527.5 ft; 464.97–465.58 m) from the previous run. The day ended with 25.7 ft (7.83 m) recovered from 27.0 ft (8.23 m) drilled (recovery = 95.1%).

On 28 October, drilling rates improved and 4.2, 9.6, and 10.4 ft (1.28, 2.93, and 3.17 m) were recovered from runs 205 (1536–1540 ft; 468.17–469.39 m), 206 (1540–1550 ft; 469.39–472.44 m), and 207 (1550–1560 ft; 472.44–475.49 m), respectively, for a total of 24.2 ft (7.38 m) recovered from 24.0 ft (7.32 m) drilled (recovery = 100%). Stefanie Baxter and Scott Strohmeier of the DGS arrived onsite and obtained a gamma log through the rods. On 29 October, runs 208 (1560–1570 ft; 475.49–478.54 m) and 209 (1570–1575 ft; 478.54–480.06 m) recovered 8.7 and 3.5 ft (2.65 and 1.07 m), respectively (recovery = 81.3% for the day), ending the hole with a total depth of 1575 ft (480.06 m). The hole was grouted with cement, plugged, and abandoned on 29–30 October.

At Ocean View, we recovered 1271.1 ft (387.43 m) from a TD of 1575 ft (480.06 m) (mean recovery = 80.7% for the 1570 ft [478.54 m] cored; median recovery = 91%). Lithologies were described onsite and subsequently at the Rutgers core facility; these descriptions form the basis for the preliminary lithologic descriptions. Samples were obtained at ~5-ft (1.52 m) intervals for planktonic foraminiferal, calcareous nannofossil, and diatom biostratigraphy and coarse-fraction lithologic studies. Cores were cut into 2-ft (0.61 m) sections, labeled at the top and bottom of each section, placed into split PVC pipe (3-in diameter), wrapped in plastic sheeting, and stored in 2-ft (0.61 m) wax boxes. One hundred and seventy-seven core boxes were moved to permanent storage at the Rutgers University core library for further study.

LITHOSTRATIGRAPHY AND SEQUENCE STRATIGRAPHY

Summary

The on-site scientific team provided preliminary descriptions of sedimentary texture, structure, color, fossil content, identification of lithostratigraphic units (NJGS Information Circular 1, 1990), and lithologic contacts (Table **T1;** Figs. **F2, F3, F4, F5, F6, F7, F8, F9**). Subsequent studies integrated preliminary descriptions with additional descriptions, biostratigraphy, biofacies studies, isotopic stratigraphy, and the downhole gamma-ray log. Unconformities were identified on the basis of physical stratigraphy, including irregular contacts, reworking, bioturbation, major facies changes, and gamma-ray peaks. Paraconformities were inferred from biostratigraphic breaks. Core photographs (Figs. **F10, F11, F12;** see also **"Visual Core Descriptions"**) illustrate sequence-bounding unconformities (Figs. **F10, F11**) and facies variation within sequences (Figs. **F10, F11, F12**).

For the nonmarine and nearshore sections (primarily the Miocene and younger section), lithofacies interpretations provide the primary means of recognizing unconformities and interpreting paleoenvironments and systems tracts. For the neritic sections (primarily the Paleogene), biostratigraphic and biofacies studies provide an additional means of recognizing unconformities and the primary means of interpreting paleoenvironments and systems tracts. Benthic foraminiferal biofacies were used to recognize inner (0–30 m), middle (30–100 m), and outer (100–200 m) neritic and upper bathyal (200–600 m) paleodepths. Cumulative percentages of the sediment grain size were computed from samples washed for paleontological analysis. Each sample was dried and weighed before washing and the dry weight was used to compute the percentage of sand. This differs from the method used in previous New Jersey coastal plain cores (Bass River, Island Beach, Atlantic City, and Cape May) in which the samples were not dried before washing.

Facies changes within onshore sequences generally follow repetitive transgressive-regressive patterns (Sugarman et al., 1993, 1995) that consist of (1) a basal transgressive glauconite (particularly Paleogene sections) or quartz sands (particularly Miocene sections) equivalent to the transgressive systems tract (TST) of Posamentier et al. (1988) and (2) a coarsening-upward succession of regressive medial silts and upper quartz sands equivalent to the highstand systems tracts (HST) of Posamentier et al. (1988). Lowstand systems tracts (LSTs) are usually absent

T1. Core descriptions, Ocean View borehole, p. 59.

F8. Age-depth plot for the Miocene sequences, p. 54.

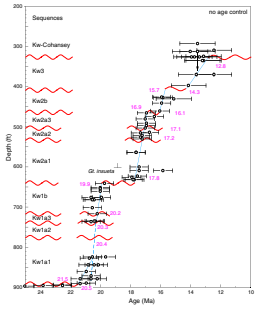

F9. Age-depth plot for the Oligocene sequences, p. 55.

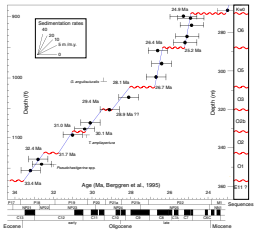

F10. Photographs showing a complete Kw0 sequence, p. 56.

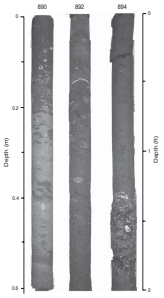

F11. Photographs of sequence boundaries, p. 57.

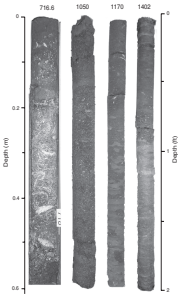

in the coastal plain and the TSTs are generally thin. Because the TSTs are thin, maximum flooding surfaces (MFSs) are difficult to differentiate from unconformities. Both can be marked by shell beds and gamma-ray peaks. Flooding surfaces, particularly MFSs, may be differentiated from sequence boundaries by the association of erosion and rip-up clasts at the latter, lithofacies successions, and benthic foraminiferal changes. The transgressive surface (TS) marking the top of the LST represents a change from generally regressive to transgressive facies; because LSTs are generally absent, these surfaces are generally merged with the sequence boundaries. Where present, LSTs are recognized as generally thin, regressive, fluvial-estuarine sediments underlying TSTs and overlying sequence-bounding unconformities.

F12. Photographs of facies changes within sequences, p. 58.

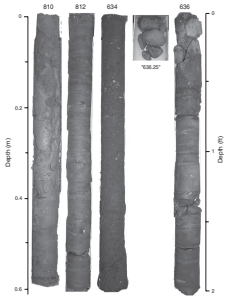

Cape May Formation

Age: middle-late Pleistocene
Interval: 5–107.5 ft (1.5–32.8 m)

The upper 16.1 ft (4.9 m) at Ocean View consists of sands and well-rounded pebbly gravels; the base of the gravels was recovered in Hole B, but not in Hole A (Fig. F2). The gravels represent reworked fluvial sediments deposited in nearshore environments and may constitute an unnamed member of the Cape May Formation. This gravel comprises the terrace on which the Garden State Parkway was built. Elsewhere, the terrace has been correlated with marine isotope Stage 5 (Ashley et al., 1991) and the Cape May Formation (Sheridan et al., 2000; W. Newell, pers. comm., 1999). Well-sorted yellow very fine to medium quartz sands underlie the gravels (16.1–35 ft; 4.9–10.7 m). A dark gray slightly sandy clay was missed in Hole A but recovered in Hole B (19.4–22.7 ft; 59–6.9 m); this clay is well expressed in the gamma log (Fig. F2). The sands bracketing the clay show several fining-upward patterns on the 1-ft scale (e.g., near 28 ft; 8.5 m). Alternating thin beds of gravelly sands, poorly sorted sands, and thin clay drapes (35–78.75 ft; 10.7–24.0 m) represent dynamic nearshore environments (?tidal delta/barrier complex). These sands and gravelly sands comprise an unconfined aquifer; the interval from 64 to 84 ft (19.5 to 25.6 m) was screened at the adjacent Ocean View Service Area #2 water well. The lower part of the Cape May Formation (78.5–107.5 ft; 24.0–32.8 m) (Fig. F2) is characterized by coarsening-upward successions (typically 0.2–1.0 ft [6–30 cm] thick) from fine quartz sands to very coarse sands with occasional reddish yellow gravels, iron-stained layers, and iron concretions. The contact between the Cape May and Cohansey Formations was placed at 107.5 ft (32.8 m) at a sharp, burrowed surface. This contact is probably a sequence boundary separating ?Pleistocene sediments above from ?upper Miocene (probably upper Miocene Zone DN6, although possibly middle Miocene Zone DN8) (see "Biostratigraphy," p. 33) sediments below. This lower part of the Cape May Formation was deposited in nearshore environments, interpreted as nearshore barrier island/tidal inlet complexes.

Cohansey Formation

Age: ?uppermost middle to late Miocene
Interval: 107.5–220.55 ft (32.8–67.2 m)

A sharp contact at 107.5 ft (32.8 m) separates reddish yellow medium to coarse quartz sand from underlying very dark gray, burrowed silty fine

quartz sand. This contact is interpreted as a sequence boundary (Fig. F2). We assign the section above 107.5 ft (32.8 m) to the Cape May Formation, in part because of the gravel contained throughout. Dark gray silty fine quartz sand characterizes the interval from 107.5 to 120 ft (32.8 to 36.6 m) (Fig. F2). Below an interval of no recovery (120–130 ft; 36.6–39.6 m), clayey fine sand to silty sandy clay (130–135.2 ft; 39.6–41.2 m) overlies a mottled clay containing granules (135.2–141.9 ft; 41.2–43.3 m). In the field, the clay surface was mottled with brown iron-stained oxidized patches; the clay weathered to a thick yellow Fe-oxidized rind with a strong sulfur odor. This granular clay facies is unusual for New Jersey Coastal Plain cores but could represent fluvial, estuarine, or possibly lagoonal/tidal deltaic environments. Given the marine sands above and below and the lack of a visible contact separating facies, we eliminate a fluvial interpretation. Given the bimodal grain size (clay and granules), we favor an estuarine interpretation.

A sharp contact (141.9 ft; 43.3 m) separates the clay from very coarse pebbly quartz sand below (141.9–146.2 ft; 43.3–44.6 m). We tentatively interpret this sharp facies change as a sequence boundary and the overlying succession as a classic Miocene sequence of lower HST clays and upper HST sands (Sugarman et al., 1993). However, due to the nearshore depositional setting, it is possible that this facies change merely reflects a lateral environmental shift.

A coarsening- (shoaling) upward succession is observed from 141.9 to 151.8 ft (43.3 to 46.3 m), consisting of very coarse quartz sand at the top fining downward to silty fine sand near the base (Fig. F2). This coarsening-upward succession constitutes the upper HST of a sequence; the sands were deposited in nearshore environments (i.e., the section contains dinoflagellates) (see **"Biostratigraphy,"** p. 33). Below an interval of no recovery (151.8–155.0 ft; 46.27–47.24 m), variegated clays with thin sand laminae and sand beds (155.0–159.8 ft; 47.2–48.71 m) comprising the lower HST were probably deposited in an estuarine environment (Fig. F2). A possible sequence boundary occurs at a burrowed contact at 159.8 ft (48.71 m), separating the clays above from clayey sand below (Fig. F2). Again, considering the nearshore/estuarine depositional setting, this change may only reflect a facies shift and not a sequence boundary. Burrowed, clayey silty quartz sand extends from 159.8 to 165.6 ft (48.71 to 50.47 m) (Fig. F2), although the section from 160 to 164 ft (48.77 to 49.99 m) suffers from coring disturbance. These clayey sands were probably deposited in nearshore or estuarine environments. There is a contact zone between 166.7 and 167.3 ft (50.81 and 50.99 m), with clayey sand burrowed into lighter gray massive sand. Massive medium quartz sand is found below the contact zone (167.3–172.5 ft; 50.99–52.58 m). We tentatively place a sequence boundary at the base of the burrowed clayey sands (166.7 ft; 50.81 m) (Fig. F2). Sands found from 166.7 to 220.55 ft (50.81 to 67.22 m) comprise the HST of a sequence (Fig. F2). Below an interval of no recovery (172.5–180 ft; 52.58–54.86 m), the sands are medium–coarse grained (180–213.5 ft; 54.86–65.07 m). They show several thin fining-upward successions (e.g., 191–191.2 ft [58.22–58.28 m], 191.2–192.0 ft [58.28–58.52 m]), faint cross beds, occasional pebbles, thin heavy mineral laminae, and mud chips (207.1–208 ft; 63.12–63.40 m). The sands were probably deposited in offshore bars. A sharp change to slightly sandy kaolinitic silty clay (213.5–213.6 ft; 65.07–65.11 m) could be interpreted as a sequence boundary; however, the absence of obvious erosion on this surface suggests that it is a facies change. Below an interval of no recovery (213.6–220 ft; 65.11–67.06 m) associated with a gamma-

log peak (Fig. F2), a massive sandy clayey silt extends to 220.55 ft (67.22 m), where there is a distinct irregular surface. The clayey silt is coarser and less kaolinitic than the clay above and differs from the underlying cross-bedded sands by the lack of common organic matter. The sequence stratigraphic placement of this silt is uncertain. We favor interpreting the surface at 220.55 ft (67.22 m) as a sequence boundary, based primarily on the gamma-log kick. Below the sequence boundary, cross-bedded organic-rich fine-medium dark sands deposited in delta-front environments are assigned to the Kirkwood Formation.

The formational assignment of the gray sands, yellow sands, and clays from 107.5 to 166 ft (32.77 to 50.60 m) is uncertain. We provisionally place them in the Cohansey Formation, although is it possible that they represent a distinct lithostratigraphic unit (even as unnamed sands and clays between 140 and 357 ft [42.67 and 108.81 m] at the Leg 150X Cape May borehole were not assignable to the Cohansey, Beaverdam, or Manokin Formations) (Miller et al., 1996a). The section from 166 to 220.55 ft (50.60 to 67.22 m) is similar in lithology and sedimentary structure to the Cohansey Sand found in outcrop, and we firmly assign this section to the Cohansey Formation. Initial correlation with the Cape May borehole suggests that the sequences bracketed by basal unconformities at 141.9, 159.8/166.7, and 220.55 ft (43.25, 48.71/50.81, and 67.22 m) may correspond with Sequences Ch4, Ch3, and Ch2 of de Verteuil (1997). The entire section from 107.5 to 220.55 ft (32.77 to 67.22 m) is upper middle to lower upper Miocene (dinocyst Zones DN6 or DN8) (see "Biostratigraphy," p. 33), consistent with the age of the Cohansey Formation elsewhere.

Kirkwood Formation

Age: early to middle Miocene
Interval: 220.55–1002.8 ft (67.22–305.65m)

Kw-Cohansey Sequence

Age: late middle Miocene
Interval: 220.55–327.1 ft (67.22–99.70 m)

Well-sorted fine-medium peaty, very dark gray quartz sands of the Kirkwood Formation underly the sequence boundary at 220.55 ft (67.22 m) (Fig. F3). The sands are heavily burrowed, are generally massive with occasional cross beds and laminae, were deposited on a marine shelf influenced by a delta, and comprise the upper HST of a sequence. Between 220.55 and 246.8 ft (67.22 and 75.22 m), the section alternates between very dark gray, laminated, very organic-rich sand (e.g., 220–224 and 231–233 ft; 67.01–68.28 and 70.41–71.02 m) and gray, cross-bedded to massive, moderately organic-rich to organic-poor sand. The gray beds became stained yellow during archiving as a result of Fe-rich pore waters. Below 246.8 ft (75.22 m), silts grade down to a silty clay with occasional cross beds of clayey silt (Fig. F3). The silty clays are occasionally lignitic and laminated and continue to just above an interval of no recovery (267–270 ft; 81.38–82.30 m); they were deposited in a prodelta environment of the lower HST. The basal 0.25 ft (0.08 m) of the sequence consists of clayey sands with rip-up clasts that appear to be a contact zone. This zone is associated with a gamma-log kick, and we infer that there is a sequence boundary at 267 ft (81.38 m) (Fig. F3). Sands from 270 to 284.8 ft (82.30 to 86.81 m) comprise the upper HST of the underlying

sequence (Fig. F3). From 270 to 280 ft (82.30 to 85.34 m), the section is predominantly silty, massive (extensively bioturbated), fine sand with some medium sand and traces of lignite. These sands were deposited on a shallow shelf. The section becomes siltier from 280 to 284.8 ft (85.34 to 86.81 m). Silty clays (290–327.1 ft; 88.39–99.70 m) comprising the lower HST appear below an interval of no recovery (284.8–290 ft; 86.81–88.39 m) associated with a gamma-log kick (Fig. F3). These silty clays are lignitic and shelly throughout, with shell hashes (including whole gastropod shells and pectinid fragments) at 308–308.8, 312–312.2, and 312.7–312.8 ft (93.88–94.12, 95.91–95.16, and 95.31–95.34 m). Silty clays grade downsection to TST silty fine sands (324.5–326.5 ft; 98.91–99.52 m) and an indurated shell bed (326.5 ft–327.1 ft; 99.52–99.70 m). A silty fine sand occurs (327.1–327.2 ft; 99.70–99.73 m) at the top of an interval of no recovery (327.2–330.0 ft; 99.70–100.58 m). We place a sequence boundary at the base of the shell bed (327.1 ft; 99.70 m). Age control for the two sequences between 220.55 and 327.1 ft (67.22 and 99.70 m) is equivocal. No Sr-isotopic age control is available for the sequence between 220.55 and 267 ft (67.22 and 81.3 m). Sr-isotopic ages from the sequence from 267 to 327.2 ft (81.38 to 99.70 m) appear to be reworked (Fig. F8), though an age of 12.4 Ma appears to be a maximum age (see **"Strontium Isotopic Stratigraphy,"** p. 40). Dinocysts tentatively assign both sequences to upper middle Miocene Zone DN6 or lower upper Miocene Zone DN8) (see **"Biostratigraphy,"** p. 33). We tentatively correlate both sequences with the Kw-Cohansey sequence of Miller et al. (1996a, 1997).

Kw3 Sequence

Age: late middle Miocene
Interval: 327.1–410.05 ft (99.70–124.98 m)

Shelly silty fine sand (327.1–352.2 ft; 99.70–107.35 m) occurs at the top of the underlying sequence (Fig. F3) with several thin shelly beds (331.5–331.8, 335.8, 337.9, 351.0, and 351.5 ft; 101.04–101.13, 102.35, 102.99, 106.98, and 107.14 m). The shelly sands are heavily bioturbated, finely micaceous, and contain sporadic clay laminae and finely disseminated lignite; we interpret the sands as the upper HST, probably deposited in a delta-front environment (Fig. F3). Toward the base of this interval, yellowish silty sands are interbedded with gray very silty sands as the section fines down. An irregular surface (352.2–352.5 ft; 107.35–107.44 m) marks the top of a fine-grained unit comprised of a laminated gray clay (352.5–360 ft; 107.44–109.73 m), greenish shelly silty clay (360–368.8 ft; 109.73–112.41 m), sandy silty clay (368.8–369.5 ft; 112.41–112.62 m), shell hash (369.5–369.6 ft; 112.62–112.65 m), and slightly silty clay (370–409.75 ft; 112.78–124.89 m). Shell debris increases below 398.6 ft (121.49 m) with several concentrations down to 409.75 ft (124.89 m). We interpret this fine-grained unit as the lower HST deposited in prodelta environments (Fig. F3). A subtle contact at 410.05 ft (124.98 m) separates clays above from poorly sorted, clayey, medium-coarse sand below. A gamma-ray peak and a change in Sr-isotopic ages (~15.9 Ma below; ~14.1 Ma above) (see **"Strontium Isotopic Stratigraphy,"** p. 40) mark this contact (Fig. F3). The sands immediately below the contact contain black phosphate, typical of sands in the upper Kw2b Sequence elsewhere in New Jersey (e.g., the ACGS #4 borehole) (Owens et al., 1988). Thus, we interpret the subtle contact at 410.05 ft (124.98 m) as a sequence boundary. Based on Sr-isotopic ages of ~12.4–14.1 Ma

(using the Oslick et al. [1994] age calibration) (see "Strontium Isotopic Stratigraphy," p. 40), we correlate the sequence above (327.1–410.05 ft; 99.07–124.98 m) with Sequence Kw3 of Sugarman et al. (1993) (Fig. F3).

Kw2b Sequence

Age: middle Miocene
Interval: 410.05–464.5 ft (124.98–141.58 m)

Below the unconformity, a poorly sorted clayey medium-coarse sand (410.05–413.4 ft; 124.98–126.00 m) overlies a slightly shelly silty fine sand (413.4–417.1 ft; 126.00–127.13 m) and shelly silty fine sand (420–433.25 ft; 128.02–132.05 m) with shell hashes (shell hashes occur at 421.6–421.7, 422.9, 425.7–426.1, 427.1, 427.65, 427.9–428.1, 431.2–431.6, and 431.9–432.1 ft; 128.50–128.53, 128.90, 129.75–129.88, 130.18, 130.35, 130.42–130.48, 131.43–131.55, and 131.64–131.70 m) (Fig. F4). An irregular heavily burrowed contact at 433.25 ft (132.05 m) separates shelly sands above from slightly shelly clayey silts below (Fig. F4). We interpret this surface as an MFS, with identical Sr-isotopic ages above and below (Fig. F4). The sands above are interpreted as an upper HST deposited on a muddy deltaic influenced shelf (Fig. F4). Slightly shelly clayey laminated silts (433.25–441.5 ft; 132.05–134.57 m) with thin sand laminae overlie massive fine sands (450–459.2 ft; 137.16–139.96 m) and interbedded clays and burrowed sands (460–464.5 ft; 140.21–141.58 m). These complex deposits indicate the influence of a delta (delta-front or proximal prodelta environments) on a shelf; the section from 462.1 to 464 ft (140.85 to 141.43 m) is predominantly silty clay with sand interbeds and is interpreted as prodelta (Fig. F4). A facies shift between prodelta silty clays above with medium to very coarse quartz delta-front sands below occurs at 464.0 ft (141.43 m), with a core break between 464.5 and 465.0 ft (141.58 and 141.73 m). We interpret the contact at 464.0 ft (141.43 m) as a sequence boundary. Phosphate pellets occur at 464.3–464.5 ft (141.52–141.58 m), consistent with placing of a sequence boundary at 464 ft (141.43 m). Sr-isotopes indicate that the sequence from 410.05 to 464.5 ft (124.98 to 141.58 m; 15.6–16.0 Ma) (Fig. F4) correlates with Sequence Kw2b of Sugarman et al. (1993), and a 0.9-m.y. hiatus occurs between this sequence and the sequence below (~16.9 Ma).

Kw2a Sequence

Age: early middle Miocene
Interval: 464.5–640.4 ft (141.43–195.19 m)

The entire section from 464.5 to 636.35 ft (141.43 to 193.96 m) correlates with the Kw2a Sequence of Sugarman et al. (1993), with Sr-isotopic ages of 16.9–17.9 Ma (Fig. F4) (cf. ages of 16.7–17.8 Ma at Atlantic City and 16.5–17.5 Ma at Cape May) (Miller et al., 1997). At Ocean View, this thick sequence can be subdivided into three distinct higher-order sequences, with basal unconformities (503.8, 531.6, and 636.35 ft; 153.56, 162.03, and 193.96 m), lower silty clays/clayey silts, and upper shelly sands (Fig. F4).

The first higher-order Kw2a sequence occurs from 464.5 to 503.8 ft (141.43 to 153.56 m); we term this the Kw2a3 sequence (Fig. F4). Shelly medium to very coarse quartz sand (465–477.1 ft; 141.73–145.39 m) displays several fining-upward successions consisting of basal very

coarse quartz sand with shelly concentrations grading up to medium sands. These sands are lignitic with occasional lignitic cross beds. Interbeds of clay occur from 470.4 to 472.1 ft (143.38 to 143.90 m) (Fig. F4). The sands sharply overlie a uniform cross-bedded shelly silt (477.1–495.0 ft; 145.42–150.88 m) and shelly silty clay (495.0–502.4 ft; 150.88–153.13 m) (Fig. F4). The silts and silty clays represent prodelta environments, whereas the sand above represents delta-front environments (Fig. F4). Shell beds (502.4–503.0 ft [153.13–153.31 m] and 503.6–503.8 ft [153.50–153.56 m]) are located between silty clay shell hashes and overlie a shelly clayey sand. These sediments are interpreted as a TST with a sequence boundary at 503.8 ft (153.56 m) (Fig. F4).

We interpret the sands (465–477.1 ft; 141.73–145.42 m) as the upper HST and the silts and clays as the lower HST (Fig. F4). However, it may be possible to interpret the sands as the LST, the sharp contact at 477.1 ft (145.42 m) as a sequence boundary and the contact at 465 ft (141.73 m) as a transgressive surface. Sr-isotopes are ambiguous on which interpretation is correct. The age of 16.9 Ma at 465.1 ft (141.76 m) is consistent with the interpretation of a sequence boundary 465 ft (141.73 m), although an age of 16.4 Ma at 475 ft (144.78 m) is consistent with 477.1 ft (145.42 m) as a sequence boundary. However, repetitions of sand/clay contacts continue below 477.1 ft (145.42 m) (e.g., 480.3 ft; 146.40 m), suggesting that the sharp contact at 477.1 ft (145.42 m) is a facies change.

The second higher-order Kw2a sequence occurs from 503.8 to 531.6 ft (153.56 to 162.03 m); we term this the Kw2a2 sequence (Fig. F4). The interval from 503.8 to 524.75 ft (153.56 to 159.94 m) is dominated by shelly medium sands, although the bottom few feet are clayey shelly sands (Fig. F4). These sands coarsen upsection, indicating a shallowing-upward HST; the shelly sands were deposited in inner neritic environments (Fig. F4). There is a facies contact at 524.75 ft (159.94 m), separating shelf facies above from prodelta facies below. From 524.75 to 531.1 ft (159.94 to 161.88 m), laminated clay-silt with few shell beds was deposited in prodelta environments (Fig. F4). The silts become shelly (531.3–531.6 ft; 161.94–162.03 m), interpreted as a thin TST. There is a sharp, though bioturbated contact (531.6 ft; 162.03 m) with silty fine sand below. This contact is interpreted as a sequence boundary (Fig. F4).

The third higher-order Kw2a sequence occurs from 531.6 to 636.35 ft (162.03 to 193.96 m); we term this the Kw2a1 sequence (Fig. F4). Fine-grained, slightly micaceous sands from 531.6 to 533.1 ft (162.03 to 162.49 m) with clayey silt interbeds comprise a thin upper HST deposited in delta-front or proximal prodelta environments (Fig. F4). Silts and sands deposited in proximal prodelta environments alternate from 533.1 to 538 ft (162.03 to 163.98 m): thin-bedded clay-silt (534–535 ft; 162.76–163.07 m), silts with thinner interbeds of silty fine-sand (535–536 ft; 163.07–163.37 m), laminated clayey silts (536–537.1 ft; 163.37–163.71 m), and thin-bedded fine micaceous sands with thinner silt laminae (537.1–538.0 ft; 163.71–163.98 m). Laminated slightly micaceous, slightly sandy, clayey silts dominate from 538.0 to 580 ft (163.98 to 176.78 m), representing deposition in prodelta environments (Fig. F4). Clay increases slightly downsection below 580 ft (176.78 m), with alternating beds of silty clays and clayey silts continuing to 620.65 ft (189.17 m). These alternating beds overlie a heavily burrowed silty sand (620.65–625.5 ft; 189.17–190.65 m) that becomes increasingly shelly toward the base and, in turn, overlies a spectacular shell bed (625.5–626.7 ft; 190.65–191.02 m). A tight clay with rip-up clasts (626.7–627.0

ft; 191.02–191.11 m) lies immediately above an indurated zone of calcareous claystone (627.0–627.45 ft; 191.11–191.25 m). The section from 625.5 to 627.45 ft (190.65 to 191.25 m) comprises the MFS, and the section from 533.1 to 625.5 ft (162.49 to 190.65 m) is interpreted as the lower HST (Fig. F4). Sandy shelly silty clay (627.45–631.2 ft; 191.25–192.39 m) and clayey fine sand (632.2–634.3 ft; 192.69–193.33 m) grade down to clayey medium to coarse to very coarse quartz sand (to 635.95 ft; 193.84 m), suggesting deepening upsection between 627.45 and 635.95 ft (191.25 and 193.84 m) (Fig. F12).

Placement of the sequence boundary is uncertain. An indurated calcarenite (635.95–636.35 ft; 193.84–193.96 m) (Fig. F12) could mark the sequence boundary, but we prefer the following interpretation. A deepening-upward section from 627.45 to 636.35 ft (191.25 to 193.96 m) is interpreted as the TST deposited in nearshore to inner-shelf environments (Figs. F4, F12). Below this (636.35–640.0 ft; 193.96–195.07 m), the facies consist of dark peaty, slightly micaceous silty clays (Fig. F12) with laminae and thin beds of fine sands showing decreasing sand downsection. These facies were deposited in lagoonal/estuarine/marsh environments (Fig. F4). The section from 640 to 640.4 ft (195.07 to 195.19 m) consists of medium to coarse sand deposited in shoreface setting. Thus, the section from 636.35 to 640.4 ft (193.96 to 195.19 m) shallows upsection, consistent with interpretation of this section as a prograding LST (Fig. F4). A sharp contact occurs at 640.4 ft (195.19 m), with shelly fine-medium shelf sand below (641.4–641.55 ft; 195.50–195.54 m); these sands are identical to shelly shelf sands found below an interval of no recovery (641.6–650 ft; 195.56–198.12 m). We interpret this sharp facies shift (640.4 ft; 195.19 m) as a sequence boundary. The bottom of the recovered interval consists of a return to shoreface sands (641.55–641.65 ft; 195.54–195.56 m) that we attribute to bioturbation of shoreface sands downsection below the sequence boundary. However, we cannot exclude the possibility that the shelly fine-medium shelf sand (641.4–641.55 ft; 195.50–195.54 m) was burrowed up and that the sequence boundary lies in the interval of no recovery (641.6–650 ft; 195.56–198.12 m).

Kw1b Sequence

Age: early Miocene
Interval: 640.4–718.4 ft (195.19–218.97 m)

Shelly fine-medium sands (650–670 ft; 198.12–204.22 m) grade down to shelly medium-coarse sands (670–675 ft; 204.22–205.74 m) and alternations of fine, medium, coarse–very coarse sand (675–680 ft; 205.74–207.26 m) with clay interbeds from 681.5 to 687.5 ft (207.72 to 209.55 m). We interpret the sands as reflecting nearshore/shoreface deposition and the clays as indicating the influence of a delta (delta-front sands and clays) (Fig. F5). The sands (650–680 ft; 198.12–207.26 m) comprise an aquifer unit that may correlate to the upper part of the Atlantic City 800-foot sand aquifer. The lithology gradually fines downcore as shown on the gamma-ray log (Fig. F5), alternating between fine to medium quartz sands and micaceous clays and silts (680–713 ft; 207.26–217.32 m). The clayey silts are laminated to burrowed and infilled with micaceous fine sands. These interbedded sands and clayey silts were deposited in a delta-front setting, though it appears that the delta front was prograding onto a storm-dominated shelf. Between 713 and 716.8 ft (217.32 and 218.48 m), the lithology consists of clayey micaceous fine sand with mi-

nor amounts of glauconite sand, representing deposition on a shelf. A major facies change occurs below 716.8 ft (218.48 m), with shells and pebbles within a sandy clay matrix (716.8–716.95 ft; 218.48–218.53 m), a massive shell bed (716.95–718.4 ft; 218.53–218.97 m), and a sequence boundary (718.4 ft; 218.97 m) (Fig. F11).

The interval between 640.4 and 718.4 ft (195.19 and 218.97 m) is interpreted as a sequence: the shell bed is the transgressive lag (716.8–718.4 ft; 218.53–218.97 m), the glauconitic unit is the thin TST (713–716.95 ft; 217.32–218.53 m), and the coarsening-upward succession is the HST (636.35–713 ft; 193.96–217.32 m) (Fig. F5). Based on Sr-isotopic ages of ~19.9–20.6 Ma, this sequence correlates with Sequence Kw1b of Sugarman et al. (1993). The spectacular sequence boundary at 718.4 ft (218.97 m) (Fig. F11) thus correlates with a sequence boundary at 666 ft (203.00 m) at the Leg 150X Atlantic City borehole (Fig. F5). The Kw1c sequence found downdip at Cape May (Miller et al., 1997) apparently has been cut out at both Ocean View and Atlantic City (Miller et al., 1997).

Kw1a Sequence

Age: early Miocene
Interval: 718.4–891.65 ft (218.97–271.88 m)

The entire section from ~718.4 to 891.65 ft (~218.97 to 271.88 m), with Sr-isotopic ages ranging between 20.4 and 21.5 Ma (Fig. F8), correlates with the Kw1a sequence of Sugarman et al. (1993) (Fig. F5). Like the Kw2a sequence above, it is possible to subdivide this thick sequence into several higher-order sequences (Fig. F5), with basal unconformities at ?740, 775.9/780, and 891.65 ft (?225.55, 236.49/237.74, and 271.88 m). From the top down, we term these higher-order sequences as Kw1a3, Kw1a2, and Kw1a1 (Fig. F5).

Lignitic medium to coarse quartz sands with occasional shell fragments (720–730 ft; 219.46–222.50 m) appear at 718.4–720 ft (218.97–219.46 m). These sands represent the upper HST of a sequence (Fig. F5); the environment of deposition of these organic-rich shelly sands may have been delta front. The sands grade down to interbeds of shelly fine-medium sand and silty clay (730–738.2 ft; 222.50–225.00 m), with predominantly peaty silty clay at 738.8–740 ft (225.19–225.55 m). These clays are lower HST deposits from a prodelta or delta-front environment (Fig. F5). There is a facies boundary between shelly sands and clays (delta-front/prodelta interface) and cross-bedded medium-coarse sands below ~740 ft (~225.55 m) (nearshore environments, though with a deltaic influence). This facies shift from lower HST silts and clays above to upper HST sands below could be interpreted as a higher-order sequence or facies shift due to autocyclical processes (e.g., lobe switching). We tentatively interpret the section from 718.4 to 740 ft (218.97 to 225.55 m) as a sequence and term it Sequence Kw1a3 (Fig. F5).

Organic-rich micaceous fine-medium-coarse sands return from 740 to 766.2 ft (225.55 to 233.54 m), comprising the upper HST of a sequence deposited in nearshore/delta-front environments (Fig. F5). Occasional silty drapes appear at 750 ft (228.60 m) and are interbedded with the sands to 766.2 ft (233.54 m). Interbeds of micaceous silty clay appear at 770.2–770.4, 770.7–771.0, and 774.3–775.2 ft (234.76–234.82, 234.91–235.00, and 236.01–236.28 m); although the section is predominantly sand, the gamma log shows an interval of high radiation from 770 to 777 ft (234.70 to 236.83 m) (Fig. F5). These interbedded silty

clays and sands probably mark delta-front/prodelta environments and the lower HST of a sequence (Fig. F5); the sequence boundary may be in an interval of no recovery between 775.9 and 780.0 ft (236.49 and 237.74 m). We term the tentative sequence between 740 and 775.9/780 ft (225.55 and 236.49/237.74 m) as Sequence Kw1a2 (Fig. F5). The strong deltaic influence on Sequences Kw1a3 and Kw1a2 explains the great thickness of the Kw1a sequence(s) at this site. The greater thickness of this section is consistent either with autocyclical shifts or the preservation of two higher-order sequences due to higher sediment supply and accommodation space provided by loading.

Cross-bedded to massive micaceous fine-medium sands with common opaque minerals are found from 780 to 810 ft (237.74 to 246.89 m), marking an upper HST (Figs. F5, F12). Occasional silty clay laminae differentiate these sands from their temporal Kw1a equivalents at Cape May and Atlantic City (Miller et al., 1997); at those boreholes, the Kw1a sands were deposited in neritic environments. At Ocean View, there is a clear deltaic influence on these sands, although extensive bioturbation and dominance of burrowed sands still suggest deposition on a storm-dominated shelf. The sands from 718.4 to 810.0 ft (218.97 to 246.89 m) comprise an aquifer that correlates with the lower part of the Atlantic City 800-foot sand aquifer (Fig. F5), with the section from 780 to 810 ft (237.74 to 246.89 m) providing the best potential aquifer based on the lithology.

Laminated micaceous silty fine sands with interbedded darker laminated silty clays and thin sand laminae characterize the sediments from 810 to 863.8 ft (246.89 to 263.29 m). These proximal prodelta/distal delta-front deposits represent the lower HST (Figs. F5, F12). The silty clays contain more sand than is typical of prodelta deposits in the Kw1 sequence(s) elsewhere in New Jersey, reflecting closer proximity to source. The section from 862 to 863.8 ft (262.74 to 263.29 m) is a more uniform silty clay. A facies change to a fine sandy glauconitic silt containing abundant shells (870–872.1 ft; 265.18–265.82 m) marks the transition to deeper water facies of the TST; this level is associated with a distinct gamma-ray peak that we interpret as the MFS (Fig. F5). These deeper-water (shelf) deposits continue downsection with a shelly silty clay (872.1 ft–879.1 ft; 265.82–267395 m) and massive silty micaceous shelly clay (880–889.6 ft; 268.22–271.15 m). These sediments are either very distal prodelta or very muddy shelf deposits (Fig. F5). Below the shelly sands, there is a spectacular bioturbated gray clay from 890.7 to 892.3 ft (271.49 to 271.97 m) (Fig. F5). The top of the clay is a sharp though heavily bioturbated contact with sand burrowed down into the clay. This contact (890.7 ft; 271.49 m) lacks evidence for erosion (e.g., rip-up clasts or an irregular contact), and we interpret it as a transgressive surface and the section from 890.7 to 891.65 ft (271.49 to 271.77 m) as an LST (Fig. F5). A sequence boundary marked by a minor gamma-ray peak (Fig. F5) at 891.65 ft (271.77 m) separates clay from clayey sands below. We correlate the sequence between 718.4 and 891.65 ft (218.97 and 271.88 m) with the Kw1a sequence of Sugarman et al. (1993) and Miller et al. (1997) and the sequence below this with Sequence Kw0 of Miller et al. (1997).

Kw0 Sequence

Age: early Miocene
Interval: 891.65–895.55 ft (271.77–272.96 m)

A clayey, slightly glauconitic, slightly micaceous fine sand between 891.65 and 895.3 ft (271.77 and 272.89 m) gradually becomes clayier near its base, as evinced by a minor gamma-log peak (Fig. F5). A sequence boundary occurs at the base of a contact zone between 895.3 and 895.55 ft (272.89 and 272.96 m). The contact zone consists of reworked sandy glauconitic clay with shells and pebbles. It is slightly cemented and has common phosphorite pellets in the contact zone that are burrowed upsection. Sr-isotopic age estimates available for this thin sequence indicate ages of 21.3–23.8 Ma, thus correlating with the Kw0 sequence. This entire sequence is illustrated in Figure F10.

Atlantic City Formation

Age: Oligocene
Interval: 895.55–1086.4/1090 ft (272.96–331.13/332.23 m)

O6 Sequence

Age: late Oligocene
Interval: 895.55–950 ft (272.96–289.56 m)

Below the contact at 895.55 ft (272.96 m) is a dark greenish gray, slightly silty, heavily bioturbated, glauconitic, medium quartz sand (895.55–950 ft; 272.96–289.56 m) (Fig. F6). Scattered shells are found from 895.8 to 905.7 ft (273.04 to 276.06 m). Shells are rare in these sands from 906 to 920 ft (276.15 to 280.42 m) and become notable again below 920 ft (280.42 m). These sands were deposited on the shelf in inner-middle neritic environments. Sr-isotopes indicate that these sands are uppermost Oligocene (24.9–25.3 Ma), correlating with Sequence O6 of Pekar et al. (1997a) (Fig. F6). Green sands above 950 ft (289.56 m) are distinct from clayey brown sands below; we interpret the brown sands below as an HST and the green sands above as a TST (Fig. F6). Thus, a sequence boundary should occur near 950 ft (289.56 m). Sr-isotopes indicate that the brown sands are clearly older (26.4–26.7 Ma) than the green sands above (25.3 Ma). The green sands between 895.55 and 950 ft (272.96 and 289.56 m) correlate with Sequence O6 of Pekar et al. (1997a), and the brown sands below 950 ft (289.56 m) correlate with Sequence O5 of Pekar et al. (1997a). However, there is no physical surface indicative of a sequence boundary near 950 ft (289.56 m), unless is it in a coring gap (949.9–950.0 ft; 289.53–289.56 m).

O5 Sequence

Age: late Oligocene
Interval: 950–1015.8 ft (289.56–309.62 m)

The interval from 950 to 960 ft (289.56 to 292.61 m) contains a silty medium-to-coarse quartz-glauconite sand interbedded with brown fine-sandy clay layers and thin indurated zones (Fig. F6). From 960 to 970 ft (292.61 to 295.66 m), the sediments are slightly clayey (~25% clay), massive (bioturbated), quartzose medium-to-coarse glauconite sands that are lithologically distinct from the interbedded clayey sands above (950–960 ft; 289.56–292.61 m). The section from 950 to 970 ft (289.56 to 292.61 m) is interpreted as an upper HST deposited on a shelf (Fig. F6). From 970 to 980 ft (295.66 to 298.70 m), the section generally coarsens downsection with clay and silt content decreasing and the sand-sized

fraction becoming coarser and very glauconite rich (<20% quartz). Below this coarse interval, clay increases and coarse sand decreases downsection (980–1000 ft; 298.70–304.8 m) (Fig. F6). Shells appear at ~992 ft (~302.36 m) and increase in abundance to a maximum between 1000 and 1002 ft (304.8 and 305.41 m). The section from ~970 to 996 ft (~295.66 to 303.58 m) is interpreted as the lower HST; the shelly interval (996–1002 ft; 303.58–305.41 m) is interpreted as the MFS, based on the highest abundance of shells (Fig. F6). Below 1002.8 ft (305.65 m), shells are absent and very coarse glauconite and goethite predominate. The goethite component consists of brown pellets of weathered glauconite interpreted as reworked from older strata. The peak in glauconite/goethite abundance at 1005 ft (306.32 m) is associated with a gamma-log kick that could be interpreted as the MFS, although common reworked glauconite (goethite) at this level suggests that the MFS is slightly higher. The sediments become slightly clayey with minor coarse quartz sand between 1005 and 1014 ft (306.32 and 309.07 m). An indurated interval between 1015.3 and 1015.8 ft (309.46 and 309.62 m) separates clayey coarse glauconite/goethite (~50% glauconite, ~50% ?goethite) with interbedded glauconitic clay (1014.5–1015.4 ft; 309.22–309.49 m) above from very coarse glauconite sand with very little clay and minor goethite below. This indurated interval marks a sequence boundary at 1015.8 ft (309.62 m), separating Sequence O5 (based on a Sr-isotopic age of 26.7 Ma) (Fig. F6) of Pekar et al. (1997a) above from Sequence O3/4 below (based on a Sr-isotopic age of 28.3 Ma) (Fig. F6).

O3/4 Sequence

Age: late Oligocene
Interval: 1015.8–1050.5 ft (309.62–320.19 m)

Very coarse glauconite sand with very little clay and minor goethite (1015.8–1035 ft; 309.62–315.47 m) encompasses an interval of poor recovery (Fig. F6), probably due to alternation of indurated zones (which clog the core catcher) and friable glauconite sands. These very coarse sands comprise the upper HST of the sequence. Shells become abundant in the interval from 1033 to 1040 ft (314.86 to 316.99 m), with a concentration of shells at 1035.6–1035.7 ft (315.65–315.68 m) (Fig. F6). The sands become gravelly with little shell debris (1040–1043.3 ft; 316.99–318.00 m) and give way to glauconitic sandy clay (1045–1050.5 ft; 318.52–320.19 m), indicative of the contact of the lower HST with the TST (Fig. F6). A surface at 1050.5 ft (320.19 m) (Fig. F11) separates glauconitic sandy clay above from pebbly, slightly clayey coarse glauconitic quartz sand below. We interpret this surface as a sequence boundary and the underling glauconitic quartz sand as the HST of the underlying sequence (Fig. F6). Only one Sr-isotopic age estimate (28.1 Ma at 1031.0 ft [314.25 m]) is available for the sequence between 1015.8 and 1050.5 ft (309.62 and 320.19 m), correlating it with Sequence O3 of Pekar et al. (1997a). Sequence O4 may be cut out at Ocean View. Alternatively, a thin cemented zone at 1031.7–1031.75 ft (314.46–314.48 m) overlain by a thin clay (1031.4–1031.7 ft; 314.37–314.46 m) may be a sequence boundary separating Sequence O3 from O4 below. If so, the interval between 1015.8 and 1031.7 ft (309.62 and 314.46 m) could be assigned to Sequence O4. Note that this interpretation requires the Sr age estimate at 1031.00 ft (314.25 m) to be from a reworked shell.

O2b Sequence

Age: early Oligocene
Interval: 1050.5–1086.4/1090 ft (320.19–331.13/332.23 m)

Sands from 1050.5 to 1077.6 ft (320.19 to 328.45 m) are massive silty glauconitic medium-to-coarse quartz sand (Fig. F6). This unit was deposited as the upper HST and was deposited on a marine shelf (Fig. F6). The glauconite is rounded to ovoid and dominated by brown reworked grains (goethite). The sediments from 1060 to 1070 ft (323.09 to 326.14 m) contain granules to pebbles in the sand fraction. Interspersed very weathered thin shells occur in the lower part of the section, with occasional thin highly weathered shell concentrations (e.g., 1064.8–1064.9 ft; 324.55–324.58 m). The interval from 1077.6 to 1080 ft (328.45 to 329.18 m) consists of slightly quartzose, slightly glauconitic silty clay deposited as the lower HST on a marine shelf (Fig. F6). Sediments from 1080.0 to 1086.4 ft (329.18 to 331.13 m) consist of slightly quartzose clayey glauconite sands interbedded with glauconitic clay. Glauconite in this interval consists of black, primarily unweathered grains, representing the TST and basal part of the sequence (Fig. F6). A sequence boundary occurs in an unrecovered interval between 1086.4 and 1090 ft (311.13 and 332.23 m), probably at the level of a sharp gamma-log spike at 1090 ft (332.23 m) (Fig. F6). An indurated zone at 1090.4 ft (332.35 m) may mark the boundary (Fig. F6), although the major facies change occurs within the coring gap. Based on Sr-isotope ages of 30.1 and 30.4 Ma at 1076 and 1080.6 ft (327.96 and 329.18 m), respectively, we correlate the sequence between 1050.5 and 1090 ft (320.19 and 332.23 m) with Sequence O2 of Pekar et al. (1997a).

We assign the glauconitic quartz and quartzose glauconite sands (895.55–1086.4/1090 ft; 272.96–331.13/332.23 m) to the Oligocene Atlantic City Formation of Pekar et al. (1997b) (Fig. F6). It might be possible to place the formational boundary at 1000 ft (304.80 m) at the base of consistent quartzose sands or at 1086.4/1090 ft (331.13/332.23 m) at the base of quartzose sands. We favor the lower placement, because brown weathered glauconite, typical of the Atlantic City Formation, is common above 1090 ft (332.23 m).

Sewell Point Formation

Age: early Oligocene
Interval: 1086.4/1090–1171.5 ft (331.13/332.23–357.07 m)

O2a Sequence

Age: early Oligocene
Interval: 1086.4/1090–1126.3 ft (331.13/332.23–343.30 m)

Clayey, slightly quartzose fine-grained glauconite sand is found throughout the interval from 1090 to 1126.3 ft (332.23 to 343.30 m) (Fig. F6). The entire section from 1090 to 1126.3 ft (332.23 to 343.30 m) was deposited on an inner to middle neritic shelf. The upper part of this interval (1090–1110 ft; 332.23–338.33 m) consists primarily of green unweathered glauconite that is typical of TSTs in New Jersey. From 1110 to 1126.3 ft (338.33 to 343.30 m), brown, weathered, abraded glauconite is common to predominant in clayey glauconite sands. This facies succession is unusual because such brown weathered glauconite is typical of

upper HSTs. These weathered glauconite sands have a sharp contact with a brown clay at 1126.3 ft (343.30 m). The section below 1126 ft was drilled with smaller-diameter NQ rods (see "Operations," p. 6) and the Oligocene NQ cores were covered in a thick rind of drilling mud and formational sands that obscures structures and lithologies. Only by cutting the cores in half could the original lithology be determined, although in some sections is was not clear if clay interbeds represent drilling disturbance or original strata. Clays with interbedded quartzose glauconite sands continue to 1140.2 ft (347.53 m) (Fig. F6). The sequence stratigraphy of the entire section from 1090 to 1140.2 ft (332.23 to 347.53 m) is enigmatic. Gamma-ray logs show a large increase from 1124 to 1127 ft (342.60 to 343.51 m) (Fig. F6), whereas Sr-isotopes suggest a break between 1096.0 and 1135.7 ft (334.06 and 346.16 m; 31.0 and 32.9 Ma). We reconcile these observations as follows: the section below 1140.2 ft (347.53 m) was deposited as nearshore sands, with the clays (1126.3–1140.2 ft; 343.30–347.53 m) also deposited in nearshore setting. A sequence boundary occurs at 1126.3 ft (343.30 m) in association with a gamma-ray peak; Sr-isotopes indicate that the sequence below correlates with Sequence O1 and the sequence above with Sequence O2 of Pekar et al. (1997a). The facies successions from brown, primarily transported glauconite (1110–1126.3 ft; 338.33–343.30 m) to in situ glauconite (1090–1110 ft; 332.23–338.33 m) represents a transgressive deposit, with the HST missing due to truncation.

O1 Sequence

Age: early Oligocene
Interval: 1126.3–1171.5 ft (343.30–357.07 m)

Clays with interbedded quartzose glauconite sands (1126.3–1140.2 ft; 347.53–343.30 m) overlie heavily bioturbated (?*Ophiomorpha* burrows), slightly clayey ("gummy") quartzose glauconite sands with thin clay interbeds/laminae (1140.1–1151.1 ft; 347.50–350.86 m) (Fig. F6). The glauconite is primarily brown, weathered, and cracked, degrading easily to clay and was reworked in shallow shelf/nearshore environments. Green glauconite increases downsection from trace amounts at 1141 ft (347.78 m) to >5% at 1149 ft (350.22 m). The section becomes slightly shelly (1150–1551.1 ft; 350.6–472.9 m) and then grades down from clayey sand (1151.1–1152 ft; 350.9–351.2 m) to shelly sandy clay (1152–1155 ft; 351.2–352.1 m). The section above this is clearly regressive, shallowing upsection from middle-?outer neritic glauconite clays to nearshore reworked glauconite sands. Sandy interbeds generally increase downsection beginning at 1155–1158 ft (352.04–352.96 m) to an indurated sandstone at 1158–1158.2 ft (352.96–353.02 m). This sandstone may mark the MFS; alternatively, the MFS may occur within the shelliest of the glauconitic clays (1153 ft; 351.52 m). Below 1158 ft (352.96 m), the section is clearly transgressive and is assigned to the TST (Fig. F6). Quartzose clayey glauconite sand (1160–1163.0 ft; 353.57–354.48 m) with green unweathered glauconite becomes shelly at the base of the sequence (1170–1171.5 ft; 356.62–357.07 m). Coring gaps (1158.2–1160 ft [353.02–353.57 m] and 1163–1170 ft [354.48–356.62 m]) otherwise limit interpretation of this section (Fig. F6). We recovered a spectacular sequence boundary at 1171.5 ft (356.98 m), separating Oligocene from Eocene strata.

Based on Sr-isotopic ages, we correlate the section from 1126.0 to 1171.5 ft (343.20 to 357.07 m) to the O1 sequence of Pekar et al.

(1997a) (Fig. F6). However, one Sr-isotopic age of 33.3 Ma at 1151 ft (350.82 m) suggests that perhaps the Mays Landing (ML) basal Oligocene sequence is represented at Ocean View (Fig. F6). If this is true, then a sequence boundary separating O1 from ML may occur at a contact between slightly shelly clayey glauconite sand (1150–1151.1 ft; 350.52–350.89 m) and a clayey sand (1151.1–1152 ft; 350.86–351.13 m). However, the contact appears gradual and we prefer interpretation of one lowermost Oligocene (1126.0–1171.5 ft; 343.20–357.07 m) sequence correlated with Sequence O1 of Pekar et al. (1997a).

Absecon Inlet Formation

Age: late Eocene
Interval: 1171.5–1402.9 ft (357.07–427.60 m)

Laminated micaceous greenish gray clays to slightly silty clays appear below a spectacular sequence boundary at 1171.5 ft (357.07 m) (Figs. F7, F11). The sequence boundary consists of basal shelly quartzose glauconite clay (1170.0–1170.9 ft; 356.62–356.89 m), an interval with pods of reworked greenish clay within a matrix of glauconite sands (1170.9–1171.5 ft; 356.89–357.07 m), and a sharp contact at 1171.5 ft (357.07 m). Glauconite (1%–2%) is found in the sequence below, starting at 1176.2 ft (358.51 m) and continuing downsection to a possible sequence boundary at 1180.3 ft (359.76 m) (Fig. F7). The 1180.3-ft (359.76 m) contact is burrowed with lighter green clays below burrowed up into brown clays above. The uniform silty clay lithology below 1171.5 ft (357.07 m) is assigned to the Absecon Inlet Formation of Browning et al. (1997a), which is upper Eocene where previously dated. Benthic foraminiferal assemblages at Ocean View are similar to those in the Absecon Inlet Formation at Cape May and Atlantic City: *Siphonina tenuicarinata, Siphonina claibornensis, Melonis barleeanum, Hanzawaia blanpiedi, Cibicidoides* ?*speciousus, Uvigerina multistriata, Ceratobulimina* sp., *Spiroplectammina mississippiensis, Osangularia* sp., *Fursenkoina*, and common dentilinids. These assemblages indicate deposition in middle to outer neritic paleodepths (probably the *Siphonina* or *Cibicidoides* biofacies of Browning et al., 1997a) (~75- to 100-m paleodepth). Planktonic foraminifers indicate that the section below 1172.1 ft (357.26 m) is upper Eocene, based on the highest occurrence (HO) of *Hantkenina alabamensis* at this level (Fig. F7). Nannofossils indicate that the section from 1174.2 to 1198 ft (358.01 to 365.27 m) belongs to Zone NP21, which spans the Eocene/Oligocene boundary, consistent with previous correlations of the upper Absecon Inlet Formation (Browning et al., 1997a). Thus, the sequence from 1171.7 to 1180.3 ft (357.13 to 359.76 m) is uppermost Eocene (i.e., the portion of Zone NP21 within the range of *Hantkenina*) and corresponds to Sequence E11 of Browning et al. (1997a).

Clays and silty clays below the 1180.3-ft (359.76 m) sequence boundary become slightly siltier below 1190 ft (362.71 m) (Fig. F7). Below 1210 ft (368.81 m), the sediments become clayier with slightly glauconitic burrows and thin shell layers. Glauconite increases (usually in burrows) from 1220 to 1242.25 ft (371.86 to 381.30 m), and occasional pyrite nodules are found. A very slightly sandy (~15% quartz sand) section at 1231–1255.8 ft (375.21–382.77 m) may mark the top of a shallowing-upward succession with a minor flooding at ~1231 ft (375.21 m) (Fig. F7). An increase in the abundance of planktonic foraminifers and benthic foraminiferal assemblages between 1241 and 1251 ft (378.26 and 381.30 m) may mark a minor flooding event (see **"Biostratigra-**

phy," p. 33); alternatively, it may be possible to interpret a sequence boundary at ~1241–1251 ft (~378.26–381.30 m) (see "Biostratigraphy," p. 33). However, physical evidence for a sequence boundary is minimal. The similarity in size and abundance of glauconite and quartz sand components through this interval (1231–1255.8 ft; 375.21–381.30 m) is evidence that the glauconite is reworked and the faunal change near 1251 ft (381.30 m) represents a change from an upper HST to a lower HST (Fig. F7). From 1260 ft to 1330 ft (384.05 to 405.38 m), the lithology consists of slightly glauconitic shelly pyritic clay (Fig. F7). Shells become common below 1272 ft (387.71 m). Glauconitic burrows increase from 1329.6 to 1338.65 ft (405.26 to 408.02 m). Glauconite is rare, and the clay alternates with silty clay from 1340 to 1371.4 ft (408.43 to 418.00 m); these alternations of silty clay and clay have a typical thickness of ~2 cm. Some "clays" noted from ~1358 to 1370 ft (413.92 to 417.58 m) may represent intrusion of drilling mud into fractures of silty clay–clay, though most appear to be in situ silty clay–clay couplets. The cause of the cyclicity is unclear, although it is certainly on the centennial-millennial scale.

Glauconite appears in trace abundance at ~1370 ft (417.58 m), becoming slightly glauconitic silty clay at 1370.75 ft (417.80 m) with glauconite lenses (Fig. F7). A change occurs at 1371.4 ft (418.00 m) from brownish silty clay above to greenish glauconitic clay to silty clay that continues down to 1373.2 ft (418.55 m). From 1373.2 to 1374.4 ft (418.55 to 418.92 m), there is a glauconitic silty clay with dispersed shell fragments. A clayey, heavily burrowed glauconite sand occurs from 1374.4 to 1374.8 ft (418.92 to 419.04 m). Glauconite increases to an irregular bioturbated surface at 1375.0 ft (419.10 m), which represents a major sequence boundary (Fig. F7). The facies shifts from transgressive glauconitic clays to regressive silty clays (i.e., changes at 1371.4 and 1374.4 ft [418.00 and 418.92 m] may represent flooding surfaces associated with parasequences.

The sequence from 1180.3 to 1375.0 ft (359.76 to 419.10 m) correlates with Sequence E10 of Browning et al. (1997a). Sediments between 1375.0 and 1376.85 ft (419.10 and 419.66 m) appear to represent a very thin sequence. A surface at 1376.85 ft (419.66 m) is erosional with clay rip-up clasts from the section below; above this, the sequence fines upsection from clayey glauconite sand to slightly glauconitic silty clay. Below the sequence boundary at 1376.85 ft (419.66 m), slightly glauconitic olive gray, slightly shelly silty clay (1376.85–1379.62 ft; 419.66–420.51 m) overlies heavily burrowed very light green clay to silty clay (1379.62–1400 ft; 420.51–426.72 m). A facies change at 1393.5 ft (424.74 m) from dark brown clays above to light green clays below may mark the MFS, with the brown clays above representing the HST. Glauconite and shells increase downward to a sequence boundary at 1402.9 ft (427.60 m) (Fig. F11). We tentatively correlate the sequence from 1376.85 to 1402.9 ft (419.66 to 427.60 m) with sediments between 770.7 and 840.1 ft (234.91 and 256.06 m) at Bass River and between ~1330 and 1352 ft (~405.38 and 412.09 m) at Atlantic City. This previously unnamed sequence is here termed Sequence E10a. The lithologic assignment of the section between 1374.4 and 1402.9 ft (418.92 and 427.60 m) is equivocal (Fig. F7). The section contains variable facies that have aspects both of the silty clays of the Absecon Inlet Formation and the glauconitic clays and yellow clays of the underlying Shark River Formation. Coarse-grained facies (fine-to-medium quartz sands) that mark the upper Shark River Formation elsewhere in New Jersey are absent at Ocean View because of its downdip position, further complicat-

ing placement of the Absecon Inlet/Shark River Formational boundary. We tentatively place the formational boundary at the top of slightly coarser-grained (slightly sandy) yellow clays at 1402.9 ft (427.60 m) (Fig. F11). This is consistent with sequence stratigraphic and biostratigraphic correlations among boreholes.

Shark River Formation

Age: middle Eocene
Interval: 1402.9–1575 ft (427.60–480.06 m)

Upper Shark River Formation

Below the 1402.9-ft (427.60 m) sequence boundary (Fig. F11), extremely dry, green, slightly glauconitic shelly silty clays (upper HST?) grade down to green clays (lower HST?) (Fig. F7). Glauconite increases downsection below 1422.3 ft (433.52 m) from slightly glauconitic clay to clayey glauconite sand from 1434.1 to 1434.4 ft (437.11 to 437.21 m); this section is interpreted as a TST (Fig. F7). A distinct sequence boundary at 1434.4 ft (437.21 m) separates clayey glauconite sand above from slightly glauconitic clay below. We tentatively correlate the sequence from 1402.9 to 1434.4 ft (427.60 to 437.21 m) with Sequence E9 of Browning et al. (1997b). In other boreholes on the coastal plain, Sequence E9 contains a mix of middle Eocene foraminifers and upper Eocene calcareous nannoplankton. This sequence contains *Acarinina,* indicative of the middle Eocene and upper Eocene calcareous nannoplankton indicative of Zone NP18 (Fig. F7), requiring reworking of the middle Eocene foraminifers. This sequence is much finer grained at this site than it is in updip boreholes.

Below the 1434.4-ft (437.21 m) sequence boundary, slightly glauconitic (typically 2%), foraminifer-rich (typically 20%–25%), slightly clayey silt grades down to foraminiferal silty clay at 1465 ft (446.53 m) (Fig. F7). No core was recovered between 1465 and 1484 ft (446.53 and 452.32 m). A sharp gamma ray–log peak occurs at 1473.8 ft (449.21 m), suggesting a sequence boundary (Fig. F7). Porcellanitic Eocene clays ("ash colored marls") of the lower Shark River Formation are found below the gamma-log kick at 1474 ft (449.28 m) (Fig. F7). The clays above 1474 ft (449.28 m) contain more glauconite and are distinctly browner in color than clays below 1474 ft (449.28 m). Because of poor recovery, it is not possible to be certain that a sequence boundary was penetrated. Nevertheless, the character of the clay between 1434.4 and ~1474 ft (437.21 and ~449.28 m) suggest that it is equivalent to Sequence E8 of Browning et al. (1997b) and the section below 1474 ft (449.28 m) is assigned to Sequence E7 of Browning et al. (1997b) (Fig. F7). The inferred sequence between 1434.4 and 1473.8 ft (437.21 and 449.21 m) is assigned to planktonic foraminiferal Zone P12 and the upper part to Zone NP17 (see "Biostratigraphy," p. 33), indicating that it correlates with Sequence E8 of Browning et al. (1997b).

Lower Shark River Formation

The clays below 1474 ft (449.28 m) contain alternations of slightly glauconitic porcellanitic foraminiferal clay with beds of clayey porcellanite at 1487.2–1487.9 and 1488.9–1489.8 ft (453.30–453.51 and 453.82–454.09 m) (Fig. F7). A strong petroleum odor was noted on the cores from 1484 to 1486 ft (452.32 to 452.93 m). From 1490 to 1543.3 ft

(454.15 to 470.40 m), the clays display large- (centimeter) and small-scale (millimeter) burrows that break up laminations; these distinctive burrows are reminiscent of the lower middle Eocene section at the ACGS #4 borehole and deep-water bioturbation (Miller et al., 1990). Field samples from 1488 and 1490 ft (453.54 and 454.15 m) contain common *Cibicidoides subspiratus* and *Cibicidoides eocanus* and occasional *Alabamina wilcoxensis, Anomalinoides acuta, Cibicidoides praemundulus, Gyroidinoides* sp., and sparse plankton; this benthic fauna appears similar to biofacies G of Browning et al. (1997b), which is found in the lower Shark River Formation at Allaire, Island Beach, ACGS #4, and Atlantic City. Planktonic foraminifers are sparse and poorly preserved and include primarily *Acarinina* spp.; tentative identification of *Acarinina primitiva* and *Acarinina soldadoensis* are consistent with an uppermost lower to lowermost middle Eocene assignment. The section between 1501 and 1521 ft (457.50 and 463.60 m) is largely indurated and foraminifers were difficult to process. There is a small percentage (1%–2%) of glauconite throughout this section, with the amount becoming greater (2%–3%) between 1515 and 1517 ft (461.77 and 462.38 m) (Fig. **F7**). The section from 1521 ft (463.60 m) and below contains an interesting mix of lower Eocene planktonic foraminifers (Zones P6b/P7) (*Morozovella formosa, Morozovella gracilis,* and various acarininids) and middle Eocene nannofossils (Zone NP15) and planktonic foraminifers (Zone P10 or younger) (*Globigerinatheka subconglobata, Subbotina frontosa,* and *Hantkenina nuttalli*). This biostratigraphic discrepancy engendered considerable debate as to the assignment of this section to the middle or lower Eocene. Based on the following criteria, we interpret the section from 1521 ft (463.60 m) to TD as middle Eocene.

1. Nannofossils clearly indicate assignment of the section below 1521 ft (463.60 m) to middle Eocene Zone NP15.
2. Benthic foraminifers in the sequence between 1517 and 1559 ft (462.38 and 475.18 m) are predominantly of biofacies G of Browning et al. (1997b), a biofacies restricted to the lower middle Eocene portion of the Shark River Formation elsewhere.
3. The lower/middle Eocene boundary generally has a diagnostic double or triple gamma-log peak throughout the New Jersey Coastal Plain and is associated with two or more thin sequences; at Ocean View, this distinctive gamma and sequence stratigraphic signature is not present (Fig. **F7**).
4. The evidence for possible closely spaced sequences at the base of the hole (1571–1573 ft; 478.84–479.60 m) suggests that we were close to the lower/middle Eocene boundary at TD but that we did not penetrate the lower Eocene.
5. We checked for laboratory contamination by carefully resampling and rewashing the samples but still found a mixture of lower and middle Eocene planktonic foraminifer taxa. Planktonic foraminifers indicative of the middle Eocene could be caved downhole, though based on nannofossil, benthic foraminifer, and sequence stratigraphic analyses, we regard it as more likely that the lower Eocene planktonic foraminifers are reworked. Even though we favor this hypothesis, we note that such pervasive reworking is generally uncommon in New Jersey Coastal Plain subsurface boreholes.

Uniform porcellanitic foraminiferal clays continue from 1521 to 1543.3 ft (463.60 to 470.40 m), where glauconite increases from trace

(<2%) above to up to 7% at 1550 ft (472.44 m) (Fig. F7). Glauconite increases to a sequence boundary at 1559.0 ft (475.18 m) (Fig. F7). Based on assignment of this sequence to nannofossil Subzone NP15b, we correlate the sequence between 1474 and 1559.0 ft (449.28 and 475.18 m) with Sequence E7 of Browning et al. (1997b).

Uniform indurated, porcellanitic, slightly glauconitic foraminiferal clay returns from 1559 ft (475.18 m) to the bottom of the hole (Fig. F7). A slightly glauconitic interval with rip-up clasts occurs at ~1571 ft (478.84 m), wheras the shoe at 1573.3–1573.5 ft (479.54–479.60 m) (i.e., the lowest sample recovered) contains common glauconite and mud chips, perhaps indicating that a sequence boundary was penetrated at the BOH (i.e., 1571–1573.5 ft; 479–479.7 m). Based on assignment to Subzone NP15a, we tentatively correlate the sequence between 1559.0 ft (475.18 m) and TD with Sequence E6 of Browning et al. (1997b) (lower Eocene) (Fig. F7). If one or more sequence boundaries are located at 1571–1573 ft (478.84–479.60 m), then it would predict that the BOH correlates with Sequence E5 of Browning et al. (1997b), which is assigned to Subzone NP14a at other locations. Further nannofossil studies will test this correlation.

BIOSTRATIGRAPHY

Palynomorphs

Lower Miocene through Pleistocene sediments were sampled at coarse and irregular intervals for palynological analysis (dinoflagellate cysts and pollen) (Table T2), concentrating around sequence boundaries identified in field studies. Unfortunately, few dinocysts were found in the highly terrigenous Pleistocene succession and none of these were useful for biostratigraphy. Dinocysts are useful for dating Miocene sediments at Ocean View using the zonation of de Verteuil and Norris (1996) (Fig. F1).

T2. Dinocyst occurrences, Ocean View borehole, p. 66.

No biostratigraphically useful dinocysts were found in sediments above 108 ft (32.92 m). Dinocyst abundance and diversity are low from 108 to 150 ft (32.92 to 45.72 m). *Palaeocystodinium golzowense* (HO = top of Zone DN8) is found together with *Trinovantedinium glorianum* (lowest occurrence [LO] = DN6) in samples from 107.6 and 115 ft (32.80 and 35.05 m), suggesting an age of 8.6–13.2 Ma (DN6–DN8). A sample from 150 ft (45.72 m) can be assigned an age range of 7.5–13.2 Ma, based on the presence of *Heteraulacacysta campanula* (HO = DN9) and *Selenopemphix dionaeacysta* (LO = base of DN6); the age of the overlying samples constrains this level to >8.6 Ma. We can restrict the age of these sediments to either middle middle Miocene Zone DN6 (12.8–13.2 Ma) or to early late Miocene Zone DN8 (8.6–11.2 Ma). Zone DN7 appears to be missing (unless represented by the barren interval) because *Cannosphaeropsis passio,* the dinocyst that characterizes Zone DN7 (de Verteuil and Norris, 1996), was not found at Ocean View.

Eight samples examined from 156 to 243 ft (47.55 to 74.07 m) were barren of palynomorphs. We interpret that sea levels were very low for a prolonged interval during the late middle or early late Miocene, allowing nearly 100 ft (30.48 m) of sediment to be oxidized. Dinocyst abundance and diversity are relatively high from 250 to 629 ft (76.20 to 191.72 m). The presence of *P. golzowense* (HO = top of Zone DN8) in a dinocyst-rich sample at 250 ft (76.20 m) provides a minimum age of 8.6 Ma for this sample. There are no biostratigraphically useful dinocysts in

sparse samples at 258 or 273 ft (78.64 or 83.21 m). The presence of *P. golzowense,* together with common *S. dionaeacysta* (LO = base of DN6), in a sample from 291 ft (88.70 m) provides an age range of 8.6–13.2 Ma. A sample from 362 ft (110.34 m) can be assigned to Zone DN6 based on the first appearance of *T. glorianum*, whose LO was revised to DN6 by de Verteuil (1997). This gives a maximum age of 13.2 Ma for these sediments. The presence of *Cousteaudinium aubryae* (HO = top of DN4) in this sample is attributed to reworking.

The presence of *Apteodinium spiridoides* and *C. aubryae* (HO = the top of Zone DN4) at 420 ft (128.02 m) supports an assignment of no younger than DN4 for this sample (>15.1 Ma). The first appearance of *Labyrinthodinium truncatum truncatum* at 450 ft (137.16 m) also suggests a middle Miocene age for this sample, because the LO of this dinocyst occurs near the base of Zone DN4 (de Verteuil and Norris, 1996). Samples at 490 ft and 523 ft (149.35 and 159.41 m) are no younger than ~15.1 Ma, based on the presence of *A. spiridoides,* whose HO occurs at the top of Zone DN4.

Samples at 534, 596, 621, and 629 ft (162.76, 181.66, 189.28, and 191.72 m) are lower Miocene, based on the presence of *Sumatradinium hamulatum* and *Lingulodinium multivirgatum*, whose HOs occur at the top of Zone DN3 (de Verteuil and Norris, 1996). The presence of *Cribroperidinium tenuitabulatum,* which was not found in sediments younger than upper Zone DN3 at Cape May and Atlantic City (de Verteuil, 1997), lends further support to an early Miocene age (dinocyst Zone DN2 or DN3; ~22.2–16.7 Ma).

Palynofacies analysis provides a means of evaluating the character of stratal surfaces in sections. Palynomorphs are too scarce in the section above 156 ft (47.55 m) to aid in detailed palynofacies analysis, although their scarcity suggests high clastic input and/or a high degree of sediment oxidation in a very nearshore environment. The interval from 156 to 243 ft (47.55 to 74.07 m) was entirely barren of palynomorphs. Whereas this precludes palynofacies analysis to support lithologically proposed sequence boundaries within the interval, the absence of the palynomorphs indicates extreme oxidation (exposure) of almost 100 ft (30.48 m) of sediment. It is therefore likely that there are several sequence boundaries located within the barren interval, although they cannot be placed by palynofacies analysis. A sample from 250 ft (76.4 m) contains aquatic pollen, lending support to a prodelta/delta-front depositional environment at this level.

The sample at 273 ft (83.2 m), underlying the sequence boundary at 267 ft (81.4 m), is virtually barren of palynomorphs, containing only two pollen grains and two dinocysts, reflecting the extreme oxidation of the sediments at this level. The increase in dinocyst concentration and decrease in palynomorphs:dinocysts (P:D) from 258 to 250 ft (78.9 to 76.4 m) indicates an increase in the distance to the shoreline resulting from transgression due to rising sea level.

The highest dinocyst concentrations and one of the lowest P:D ratios in the sampled material is found at 291 ft (88.70 m). The diversity of dinocysts at this depth is moderate to high, whereas the diversity of pollen is relatively low, with high proportions of bisaccate pollen. These variables indicate deep-water and low sediment accumulation, and more specifically, to a condensed section.

The sequence boundary at 533 ft (162.03 m) is consistent with the palynofacies analysis. The sample from 534 ft (162.76 m) contains a palynomorph assemblage characteristic of the upper HST suggested in the lithology. The sample at 534 ft (162.76 m) has rather low dinocyst con-

centration, low dinocyst diversity, and very high pollen concentrations and diversity. This palynofacies is characteristic of upper HST deposits where the shoreline is regressing and environments are becoming increasingly shallow. The very high P:D ratio and the presence of aquatic pollen are further evidence that water levels were low and the Ocean View site was near the shoreline. Above the sequence boundary at 523 ft (159.6 m), we find the palynological signature of the TST with a lower P:D, lower pollen concentrations, and a reduction in pollen diversity, reflecting the increased distance to the shoreline. The sample at 490 ft (149.5 m) has remarkably similar pollen and dinocyst concentrations and proportions of bisaccate pollen to the sample at 523 ft (159.6 m), which was also taken from TST sediments deposited immediately above a sequence boundary.

The lithologically proposed MFS at 627 ft (191.11 m) is supported by the palynofacies found in the samples at 621 and 629 ft (189.28 and 191.72 m). In the lower sample, we see the characteristic TST palynofacies—a low P:D and a high abundance and diversity of dinocysts. Above the surface at 621 ft (189.28 m), the P:D ratio is higher, indicating deeper water at 629 ft (191.72 m) than at 621 ft (189.28 m). P:D ratios continue to increase up to the sequence boundary at 533 ft (162.03 m).

Planktonic Foraminifers

Summary

Like other Leg 150X and 174AX Oligocene–Miocene sections, planktonic foraminiferal assemblages at Ocean View suffer from low abundance, low diversity, rare occurrence of marker species, and the dominance of nonage-diagnostic planktonic taxa. However, the downdip location of Ocean View allows better Oligocene–Miocene foraminiferal biostratigraphic control vs. more updip locations (e.g., Ancora, Bass River, Island Beach, or Atlantic City). Eocene planktonic foraminiferal assemblages at Ocean View are common to abundant and contain marker taxa for several zones (Table T3). However, an admixture of lower Eocene and middle Eocene taxa below 521 ft (463.60 m), along with silica diagenesis of the section below 1480 ft (451.10 m), precludes a detailed zonation.

T3. Eocene planktonic foraminiferal occurrences, Ocean View borehole, p. 67.

Miocene

Miocene foraminifers are only sporadically abundant. Specimens are much more common at the base of the Miocene section (Sequence Kw1a) than in overlying sequences. Samples higher in the section, especially in Sequence Kw3, show signs of dissolution. Planktonic foraminifers are generally rare, and few age diagnostic specimens were found. A single planktonic specimen assigned to *Globigerina bulloides* was found in a sample at 401 ft (122.22 m). A sample at 601 ft (183.18 m) contained *Globigerinitella insueta, Globigerinoides diminutus,* and *Globigerina labiacrassata*. The first occurrence (FO) of *G. insueta* marks the base of Zone M3 (18.8 Ma) (Berggren et al., 1995); its last occurrence in Zone N9 indicates an age older than ~14.8 Ma. Common planktonic foraminifers were found in samples from 876 to 886 ft (267.00 to 270.05 m), near the base of the Kw1a sequence. *Globigerinoides trilobus* dominates the planktonic assemblage that also includes *Dentoglobigerina globularis, Dentoglobigerina altispira, Catapsydrax unicavus, Globigerina*

praebulloides, Globigerina angustiumbilicata, and *Globorotalia mayeri*. The common occurrence of *Globigerinoides* may indicate that these samples should be assigned to Subzone M1b (Berggren et al., 1995). The sample at 891 ft (271.58 m) in Sequence Kw0 contains *G. praebulloides* and *G. ciperoensis;* the latter indicates assignment to Zone N4 or older (Zone M1 of Berggren et al., 1995).

Benthic foraminifers were found more commonly than planktonic foraminifers and are generally restricted to the TSTs. Most samples are dominated by *Nonionellina pizarensis* and can be assigned to the *Nonionellina* biofacies of Miller et al. (1997), indicating paleodepths of 25–50 m. However, elements of the *Hanzawaia* (10–25 m) and *Uvigerina* (>75 m) biofacies were also present:

Sequence Kw-Ch: samples from 296 to 301 ft (90.22 to 91.74 m) in the middle of the sequence are dominated by *N. pizarensis* with abundant *Hanzawaia,* indicating ~25 m paleodepth.

Sequence Kw2b: samples from 401 to 406 ft (122.22 to 123.75 m) contain *N. pizarensis* with abundant *Uvigerina* sp., indicating ~50 m water depth.

Sequence Kw2b: a single sample (431.0 ft; 131.37 m) contains rare *Elphidium, Nonionellina, Buliminella,* and *Hanzawaia.*

Sequence Kw2a: samples from 601 to 631 ft (183.18 to 192.33 m) generally contain abundant *N. pizarensis* with *Hanzawaia* being more important in samples from 601 and 611 ft (183.18 and 186.23 m) and *Uvigerina* being more important in the sample at 631 ft, perhaps indicating shallowing upward.

Sequence Kw1b: a single sample (716 ft; 218.24 m) at the base of the sequence contained a broken and pyritized textularid, pointing to dissolution.

Sequence Kw1a: the samples at the base (876–886 ft; 267.00–270.05 m) of the sequence contain the most abundant and diverse benthic foraminiferal assemblage in the Ocean View Miocene section. The following genera and species were noted: *N. pizarensis, Buliminella elegantissima, Pyrgo, Quinqueloculina, Spiroloculina, Uvigerina, Lenticulina, Spiroplectammina,* and *Guttulina*. The fauna at 876 ft (267.00 m) is dominated by *N. pizarensis*, whereas the sample at 886 ft (270.05 m) is dominated by *Uvigerina*, indicating shallowing upwards.

Sequence Kw0: the sample at 891 ft (271.58 m) in the Kw0 sequence is dominated by *N. pizarensis* and *Uvigerina,* perhaps indicating middle neritic (>75 m) paleodepths.

Oligocene

Low abundance, low diversity, rare occurrences of marker species, and the dominance of nonage-diagnostic planktonic taxa characterize Oligocene planktonic foraminiferal assemblages. Benthic foraminifers dominate over planktonic foraminifers at Ocean View, representing inner to outer neritic faunas (e.g., *Uvigerina* spp., *Trifarina* spp., *Cibicides* spp., *Bulimina gracilis, Epistominella pontoni,* and *Bolivina paula*).

Planktonic foraminiferal Zone P18 extends from the base of the Oligocene (1171.5 ft; 357.1 m) to 1141.0 ft (347.8 m), based on the occurrence of *Pseudohastigerina* spp. at 1151 and 1141 ft (350.8 and 347.8 m). Planktonic foraminiferal Zone P19 possibly extends up to 1096.0 ft (334.1 m), based on the single occurrence of *Turborotalia ampliapertura* at 1096.0 ft (334.1 m). *Chiloguembelina cubensis* also occurs infrequently

along with other nonage-diagnostic planktonic forms (*Globigerina euapertura, Dentoglobigerina venezuelana, Subbotina* spp., and *Tenuitella* spp.) from 1171 to 1096 ft (357.1 to 334.1 m). Samples from 1091 to 1011 ft (332.5 to 308.2 m) were either barren of planktonic foraminifers or contained undiagnostic marker species. The first occurrence of *Globigerina angulisuturalis,* at 1006.0 ft (306.6 m), marks the base of planktonic foraminiferal Zone P21. *Paraglobigerina opima opima* was not observed at Ocean View; thus, Zones P21 and P22 are undivided and extend up to the top of the Oligocene unit at 895.5 ft (272.9 m).

Eocene

Samples between 1172.1 and 1401 ft (357.26 and 427.02 m) are placed in the upper Eocene, and samples between 1411 (430.07 m) and TD are placed in the middle Eocene. The HO of *Hantkenina alabamensis* is at 1172.1 ft (357.3 m) (Fig. **F7;** Table **T3**), and the HOs of *Turborotalia cerroazulensis* and *Turborotalia cocoaensis* are at 1181 ft (359.97 m). A sharp change in benthic and planktonic assemblages takes place between 1401 and 1411 ft (427.02 and 430.07 m). Planktonic foraminifers are very abundant through this section but are represented by diagnostic middle Eocene species (*Acarinina bullbrooki, Acarinina pentacamerata, Acarinina rohri, Acarinina topilensis, Globigerinatheka kugleri, Morozovella lehneri, Morozovella spinulosa, Subbotina frontosa,* and *Turborotalia possagnoensis*) below and upper Eocene species (*Dentoglobigerina galavisi* and *Globigerinatheka semiinvoluta*) above. The middle Eocene species place the section below 1141 ft (430.07 m) in Zone P12 (*M. lehneri* Zone), whereas the upper Eocene species identify Zone P15 (*Globigerinatheka semiinvoluta* Zone) above. Zones P13 and P14 are not represented, suggesting that an unconformity and hiatus of ~2 m.y. separates the middle and upper Eocene. Species of the genera *Bolivina, Cibicides, Cibicidoides, Gyroidinoides,* and *Uvigerina* suggest an outer-neritic environment of deposition for this middle Eocene transgressive systems tract (Table **T4**). The upper Eocene environment of deposition ranges from outer neritic in the basal part to inner-mid neritic in the upper part. However, it is probable that two systems tracts and possibly more parasequences are present in the upper Eocene, based on the distribution of benthic and planktonic species. A rather sharp change in benthic assemblages occurs between 1241 and 1251 ft (378.26 and 381.30 m). Planktonic foraminifers are rare in the upper interval, whereas below, planktonic foraminifers are common to abundant, suggesting that a hiatus or flooding surface may be present between these two samples. Above 1251 ft (381.30 m), the planktonic assemblage, although sparse, contains species more common in the upper part of the upper Eocene (*Globigerina officinalis, Globoturborotalia ouachitatensis, Paragloborotalia nana*) in addition to *Turborotalia pseudoampliapertura,* which appears in Zone P16 (*Turborotalia cunialensis–Cribrohantkenina inflata* Zone). Although the zonal species are absent at Ocean View, the section above 1241 ft (378.35 m) is placed in Zone P16 based on the presence of *T. pseudoampliapertura* and *Turborotalia pomeroli.* The last occurrence of *T. pomeroli* is at the base of Zone P16 according to Berggren et al. (1995). This species is quite common in the section below 1241 ft (378.35 m) but is absent above. The section from 1401 to 1251 ft (427.02 to 381.30 m) is placed in Zone P15 (*G. semiinvoluta* Zone), although the occurrence of this species is sporadic. It is not present in samples between 1251 and 1281 ft (381.30 and 390.45 m).

T4. Eocene benthic foraminiferal occurrences, Ocean View borehole, p. 69.

Recovery of foraminifers was poor in samples at 1502.5 and 1512.5 ft (457.96 and 461.01 m) because of difficulty in disaggregating the samples. The planktonic species *Subbotina eocaena, S. frontosa,* and *Pseudohastigerina micra* indicate either upper lower Eocene or lower middle Eocene. Abundant early Eocene planktonic foraminifers are in samples from 1522 to 1542 ft (463.91 to 442.57 m): *Acarinina quetra, M. gracilis, M. formosa, M. subbotina, S. frontosa,* and *S. senni.* These taxa would normally place this section in Zones P6b/P7 of Berggren et al. (1995). The sample at 1552 ft (473.05 m), the lowermost sample in the section, contained poorly preserved lower Eocene foraminifers including *Acarinina soldadoensis.* However, middle Eocene planktonic foraminifers found in this section suggest assignment to Zone P10 or younger: *Globigerinatheka subconglobata, S. frontosa,* and *Hantkenina nuttalli* (LO = 1545.6 ft; 471.10 m). As discussed above, nannofossil biostratigraphy, benthic foraminiferal biostratigraphy, and sequence and log stratigraphic correlations suggest that the borehole bottomed at the base of the middle Eocene and that the lower Eocene planktonic foraminifers are reworked. Species of the benthic genera *Cibicidoides, Melonis, Alabamina,* and *Gyroidinoides* and the abundance of planktonic foraminifers suggest a middle to outer-shelf environment of deposition for this section.

Calcareous Nannofossils

Summary

Calcareous nannofossil analyses were performed on samples taken at ~3-ft (0.91 m) intervals from the lowermost part of the Kirkwood Formation (basal Kw1a sequence) through the Shark River Formation (890.4 ft–1574 ft; 271.39–479.9 m). The abundance, preservation, and diversity of coccoliths and nannoliths (particularly discoasters) vary considerably through the section, resulting in uneven success at establishing biostratigraphic subdivisions for the successive lithostratigraphic units.

Three biostratigraphic intervals are exceptionally well represented in the Ocean View Borehole. The NP23–NP25 zonal interval, although poorly differentiated, is at least 264.2 ft (79.98 m) thick and corresponds to the Atlantic City and Sewell Point Formations. As elsewhere on the New Jersey margin, the NP19–NP20 zonal interval is thick (202 ft; 61.59 m) from ~1388 to ~1403 ft (~423.20 to ~427.77 m) and its base (between 1388 and 1403 ft; 423.20 and 427.77 m) is characterized by abnormal intercalations of layers assignable to Zone NP18, a likely signature of the Chesapeake Bay impact. The greater part of the Absecon Inlet Formation belongs to this zone. The NP15–NP16 zonal interval is 139 ft (42.38 m) thick and constitutes the lower part of the upper Shark River Formation and the lower Shark River Formation (1445–1575 ft; 440.58–480.22 m). In contrast, all other biozonal intervals (Zones NP22, NP21, NP18, and NP17) identified in the Ocean View borehole are extremely thin, ranging from <5 ft (1.52 m) (Zone NP22) to <30 ft (9.15 m) (Zone NP18).

Four outstanding features concern the calcareous nannofossil assemblages preserved in the Paleogene section recovered at Ocean View. First, the occurrence of *Braarudosphaera*-rich horizons in the NP23–NP25 zonal interval is reminiscent of the Oligocene deep sea *Braarudosphaera*-rich oozes reported from the North Atlantic Ocean (e.g., Parker et al., 1985). Second, calcareous nannofossil assemblages pre-

served in the Absecon Inlet Formation (Zone NP19) are rich and well preserved. Third, and in stark contrast with above, the calcareous nannofossil assemblages are generally scarce and extremely poorly preserved in the Shark River Formation. And fourth, we note that tiny placoliths (2–5 µm) are abundant, particularly in NP15–NP16 and NP23–NP25 zonal intervals. This may be indicative of high productivity.

Biostratigraphic Subdivision

The zonal scheme used below is that of Martini (1971) and Martini and Müller (1976). Determination of the zones is based on the recognition of the zonal markers. The age estimates are from Berggren et al. (1995).

Kirkwood Formation, Kw1a Sequence (718.4–891.65 ft; 218.97–271.88 m) and Kw0 Sequence (891.65–895.55 ft; 271.77–272.96 m)

Only three samples (890.4, 893.0, and 895.9 ft; 271.48, 272.27, and 273.16 m) were examined from the Kirkwood Formation. No zonal markers were found, but a Miocene age is attested by the co-occurrence of *Coccolithus miopelagicus, Discoaster deflandrei, Helicosphaera carteri,* and *Reticulofenestra floridana*.

Atlantic City Formation (895.55–1086.4/1090 ft; 272.96–331.13/332.23 m)

This formation strictly belongs to Zones NP23–NP25 undifferentiated. However, the occurrence of *Reticulofenestra abisecta* between 1086 and 967 ft (331.12 and 294.84 m) allows a restricted assignment to Zones NP24–NP25. In addition, a single well-preserved typical specimen of *Sphenolithus distentus* indicates that level 1074.01 ft (327.46 m) cannot be younger than the NP24/NP25 zonal boundary (~27.5 Ma).

Two datum levels that are used to approximate the Oligocene/Miocene boundary were recorded at 906.1 ft (276.27 m) (HO of *Reticulofenestra bisecta*) and 909 ft (277.15 m) (HO of *Zygrhablithus bijugatus*). The upper bounding surface of the Atlantic City Formation may thus be slightly younger than the NP25/NN1 chronal boundary (~23.9 Ma).

Calcareous nannofossils are common at most levels, but preservation is moderate to poor (dissolution) and a few levels were barren. We note the (minor) reworking of late Eocene–early Oligocene species (e.g., *Reticulofenestra reticulata* and *Isthmolithus recurvus*) at 920.1 and 980.1 ft (280.54 and 298.83 m). *Braarudosphaera*-rich assemblages occur at 938.1, 950.1, and 959.0 ft (286.03, 289.69, and 292.40 m).

Sewell Point Formation (1086.4/1090–1171.5 ft; 331.13/332.23–357.07 m)

This formation is assigned to Zones NP24–NP23 at Ocean View. The LO of *R. abisecta* at an indefinite level between 1093 and 1120 ft (333.26 and 341.49 m) can be taken to approximate the Zone NP23/NP24 boundary. The imprecision in this determination reflects the scarcity of the coccoliths in the uncertainty interval. The (unexplained) common occurrence of *I. recurvus* in samples from 1140.0 and 1143.0 ft (347.59 and 348.50 m) is noteworthy. A striking change in composition of the calcareous nannofossil assemblages occurs between 1162.0 and 1174.2 ft (354.29 and 358.01 m) (a sample taken at 1170.3 ft [356.82 m] was essentially barren).

Absecon Inlet Formation (1171.5–1402.9 ft; 357.07–427.60 m)

This formation encompasses Zones NP21, NP19–NP20, and NP18 at Ocean View, but its major thickness belongs to Zones NP19–NP20. Zone NP21 extends from 1174.2 to 1198 ft (358.01 to 365.27 m). As in other complete upper Eocene sequences, we observe the sequential HOs of *Discoaster saipanensis* (1201.0 ft; 366.16 m), *Discoaster barbadiensis* (1213.0 ft; 369.84 m) and *R. reticulata* (1235.0 ft; 376.55 m). Zones NP19–NP20 extend down to 1403 ft (427.77 m). The intercalation of an interval (1388–1397 ft; 423.20–425.95 m) assignable to Zone NP18 (toward the base of the zone) reflects impact-related displacement of sediments at the beginning of Biochron NP19–NP20 (Poag and Aubry, 1995).

Shark River Formation (1402.9–1575 ft; 427.60–480.06 m)

This formation comprises Zones NP18, NP17, an undifferentiated NP15–NP16 zonal interval, and Subzones NP15a and NP15b. Calcareous nannofossil assemblages are common to abundant in the upper part (1403 and 1470 ft; 427.77 and 488.20 m) of the formation, and preservation varies between moderate and good. Below 1470 ft (488.20 m), preservation deteriorates rapidly and assemblages, scarce at many levels, are dominated by diagenesis-resistant placoliths. Discoasters are few and strongly overgrown; they are not identifiable at the species level. Curiously, many levels yield abundant tiny placoliths.

Zone NP18 is well characterized between 1406 and 1418 ft (428.69 and 432.35), but its lower boundary is ambiguous. *Chiasmolithus oamaruensis* does not occur at 1421 ft (433.26 m) but occurs at 1430 (typical) and 1433 ft (436.01 and 436.92 m), whereas *Chiasmolithus grandis* (with an HO just slightly older than the LO of *C. oamaruensis*) occurs at 1421 ft (433.26 m). Zone NP17, bracketed by the LO of *C. oamaruensis* and the HO of *Chiasmolithus solitus,* constitutes a thin sliver extending from 1436 to 1442 ft (437.84 to 439.67 m). The undifferentiated NP15–NP16 zonal interval is delineated between the HO of *C. solitus* (1445 ft; 440.58 m) and the LO of *Nannotetrina quadrata* at 1571 ft (479.00 m). A sample at 1574.5 ft (480.07 m) was barren. In this interval we note (1) the occurrence of *Cruciplacolithus staurion* at 1559 ft (475.34 m), suggestive of Subzone NP15a; (2) the HO and LO of *Chiasmolithus gigas* (at, respectively, 1547 and 1556 ft; 471.68 and 474.42 m), indicative of Subzone NP15b; (3) the LO of large morphotypes of *Reticulofenestra umbilicus* at 1511 ft (460.70 m), used by some authors to delineate the NP15/NP16 zonal boundary; (4) the presence of *R. reticulata* at 1470 ft (448.20 m), indicative of a level in the upper part of Zone NP16; and (5) the LO of *R. bisecta* at 1445 ft (440.58 m), indicative of a level close to the NP16/NP17 zonal boundary.

STRONTIUM ISOTOPIC STRATIGRAPHY

Sr-isotopic age estimates were obtained from mollusk shells (~4–6 mg) at the Ocean View borehole (Table **T1;** Figs. **F2, F3, F4, F5, F6, F8, F9**). Shells and foraminiferal tests were cleaned ultrasonically and dissolved in 1.5-N HCl. Sr was separated using standard ion-exchange techniques (Hart and Brooks, 1974) and analyzed on a VG Sector mass spectrometer at Rutgers University. Internal precision on the Sector for the data set averaged 0.000007; external precision is approximately ±0.000020 (Oslick et al., 1994). National Bureau of Standards Reference Material 987 is measured routinely at Rutgers at 0.710255 normalized

to $^{88}Sr/^{86}Sr$ of 0.1194 (Oslick et al., 1994). Sr-isotopic ages were assigned using the Cande and Kent (1992) time scale (Table T5) using the early Miocene and middle Miocene regressions of Oslick et al. (1994) with age errors of ±0.61 and ±1.17 m.y. at the 95% confidence interval for one analysis, respectively. The Oligocene–Miocene portion of the Cande and Kent (1992) scale is identical to the Berggren et al. (1995) time scale, which is used to assign calcareous and planktonic foraminiferal ages. The regressions of Martin et al. (1999) were also computed for the middle to late Miocene. A significant age discrepancy exists between ages derived using the regressions of Oslick et al. (1994) vs. Martin et al. (1999) that must be resolved in future work.

The Miocene section drilled at Ocean View contained more shells than previous Leg 150X and 174AX boreholes, thereby allowing a detailed Sr-isotope age chronology. No shells were found above 293 ft (89.33 m). Six shell beds between 293.3 and 327 ft (89.42 and 99.69 m) (Fig. F3) within the Kw-Cohansey sequence yielded ages ranging from 12.4 to 14.0 Ma (regression of Oslick et al., 1994) or 10.0 to 11.8 Ma (regression of Martin et al., 1999). The variable and stratigraphically inverted ages obtained for this sequence vs. the underlying sequence (Fig. F8) suggest reworking of older shell material upsection or diagenetic alternation or original Sr-isotopic ratios. As a result, the Sr-isotopic ages for this sequence do not reflect the true ages, though the youngest ages obtained (12.4 Ma using Oslick et al. [1994] at 309.4 ft [94.31 m]) may provide a maximum age for the Kw-Cohansey sequence at Ocean View (i.e., at Cape May, the Kw-Cohansey sequence is dated as 12.1–11.5 Ma) (Miller et al., 1997).

Five Sr-isotope age estimates obtained between 335.8 and 397.12 ft (102.4 and 121.04 m) (Fig. F3) range from 12.4 to 14.1 Ma (regression of Oslick et al., 1994) or 10.1 to 12.3 Ma (regression of Martin et al., 1999) and show a more continuous age progression than the sequence above. These ages suggest correlation of the sequence between 327.1 and 410.05 ft (99.70 and 124.98m) with the Kw3 sequence of Sugarman et al. (1993, 1997) and Miller et al. (1997). A definitive age break of 1.8 m.y. occurs between the Kw3 sequence and the underlying sequence (Fig. F3).

The section from 427.1 to 460.65 ft (130.18 to 140.41 m) records ages of 15.6–16.0 Ma (Fig. F4). This correlates the sequence from 410.05 to 464.5 ft (124.98 to 141.58 m) to the Kw2b sequence of Sugarman et al. (1993, 1997) and Miller et al. (1997).

The Kw2a sequence (464.5–640.4 ft; 141.43–195.19 m) contains 18 Sr-isotopic age estimates from different shell-bearing horizons (Fig. F4). Sr-isotopic age estimates clearly separate Sequence Kw2a from Sequence Kw2b with a 16.0- to 16.9-Ma age break between 460.65 and 465.1 ft (140.41 and 141.76 m), although there is one younger age of 16.4 Ma at 475 ft (144.78 m) (Fig. F4).

A detailed lithostratigraphic and sequence stratigraphic analysis of the thick Kw2a sequence (see "Lithostratigraphy," p. 15) allows subdivision of this thick sequence into three higher-order sequences (Fig. F4). The age differences among the three higher-order sequences, Kw2a3, Kw2a2, and Kw2a1, are distinguishable by Sr-isotopic age constraints, although hiatuses between the sequences are within the errors.

1. Sequence Kw2a3 was dated by five Sr-isotopic age estimates of 16.9–17.0 Ma (Fig. F4). An ~0.2-m.y. break separating Sequence Kw2a3 from Sequence Kw2a2 is well within Sr-isotopic error estimates (Fig. F4).

T5. Sr-isotopic data, Ocean View borehole, p. 71.

2. Four Sr-isotopic age estimates obtained within the Kw2a2 sequence between 515 and 531.6 ft (156.97 and 162.03 m) cluster at 17.2–17.3 Ma (Fig. F4). A fifth age estimate at 514.5 ft (156.82 m) yielded a slightly younger age of 16.7 Ma that is within age errors of ±0.6 m.y. for a single analysis. A 17.2-Ma Sr-isotopic age was obtained at 531.6 ft (162.03 m), just above the basal Kw2a2 sequence unconformity (Fig. F4).
3. Seven different shell-bearing units between 563.75 and 633.06 ft (171.83 and 171.84 m) give an Sr-isotopic age estimate from 17.4 to 17.9 Ma for the third higher-order Sequence Kw2a1 (Fig. F4). An older age of 19.7 Ma at 641 ft (195.38 m), just above the Kw2a1 sequence boundary at 641.55 ft (195.54 m) is probably reworked from the older sequence below.

The Kw1b sequence (640.4–718.4 ft; 195.19–218.97 m) underlies the Kw2 sequence complex (Fig. F5). Seven Sr-isotopic age estimates obtained between 651.5 and 717.13 ft (198.58 and 218.58 m) range from 19.9 to 20.6 Ma. These ages correlate the sequence (640.4–718.4 ft; 195.19–218.97 m) with the Kw1b sequence of Sugarman et al. (1993) and Miller et al. (1997) and establish an ~2-m.y. age break separating it from the younger Kw2a sequences.

Nine different Sr-isotopic age estimates ranging from 19.6 to 21.3 Ma correlate the sequence from 718.4 to 891.65 ft (218.97 to 271.88 m) with the Kw1a sequence of Sugarman et al. (1993, 1997) and Miller et al. (1997) (Fig. F5). The best estimate for the ages of this sequence is 20.4 to either 20.5 or 21.5 Ma (Fig. F8).

Like Sequence Kw2a, Sequence Kw1a can be further subdivided into three higher-order sequences termed, youngest to oldest, Sequences Kw1a3, Kw1a2, and Kw1a1 (Fig. F5). Sr-isotopic age estimates have only been found from shell-bearing beds in Sequences Kw1a3 and Kw1a1; the thick sand beds of Sequence Kw1a2 have yet to yield any dateable material. Two different shell-bearing units (735.5 and 737.35 ft; 224.09 and 224.74 m) within the Kw1a3 sequence yielded ages from 20.3 to 20.6 Ma (Fig. F5) (an age of 19.6 Ma at 825.25 ft [252.54 m] is considered an outlier, as indicated by a duplicate age of 20.5 Ma at this level). Seven Sr-isotopic age estimates from within the Kw1a1 sequence (825.25–890 ft; 251.54–271.27 m) yielded ages between 20.4 and 21.3 Ma (Fig. F5).

The oldest Miocene sequence, Kw0, encountered along the New Jersey margin occurs at Ocean View between 891.65 and 895.55 ft (271.77 and 272.96 m) (Fig. F5). Four shells within this sequence yielded Sr-isotopic age estimates from 21.3 to 23.8 Ma (Fig. F5). Just beneath the Kw0 sequence boundary identified by lithostratigraphic data, a shell bed at 897 ft (273.41 m) gave an Sr-isotopic age estimate of 25.0 Ma (Fig. F5).

Sr-isotopic age estimates provided the chronostratigraphic framework for correlating the Oligocene strata at Ocean View to Oligocene sequences previously defined in New Jersey (Pekar et al., 1997a, 2000).

1. Five Sr-isotope age estimates between 897 and 941 ft (273.41 and 286.82 m) range from 24.9 to 25.3 Ma and correlate the sequence from 895.55 to 950 ft (272.96 to 289.56 m) with Sequence O6 (Pekar et al., 1997a).
2. Three Sr-isotope age estimates between 956.4 and 999.0 ft (291.5 and 304.5 m) range from 26.4 to 26.7 Ma and correlate the sequence between 950 and 1015.8 ft (289.56 and 309.62 m) with Sequence O5 of Pekar et al. (1997a).

3. A single Sr-isotope age estimate of 28.3 Ma at 1031.0 (314.2 m) correlates the sequence between 1015.8 and 1050.5 ft (309.62 and 320.19 m) to Sequence O3 of Pekar et al. (1997a).
4. Three Sr-isotope age estimates between 1050.5 and 1086.0 ft (320.27 and 331.09 m) range from 29.0 to 30.4 Ma and correlate the sequence between 1050.5 and 1090 ft (320.19 and 332.23 m) to Sequence O2b of Pekar et al. (2000). Although 30.4 Ma is slightly older than the previously defined age for Sequence O2b (30.1–29.0 Ma), the age error for a single Sr-isotope analysis for the lower Oligocene is ±0.7 m.y., well within the range of uncertainty for this type of age estimate.
5. A single isotope age estimate of 31.0 Ma at 1096.0 ft (334.1 m) correlates the sequence between 1090 and1126.3 ft (332.23 and 343.30 m) with Sequence O2a of Pekar et al. (2000).
6. Three Sr-isotope age estimates between 1135.7 and 1155.5 ft (346.25 and 352.29 m) range in age from 32.7 to 34.5 Ma and correlate to Sequences O1 and ML of Pekar et al. (1997a).

The Ocean View borehole contains an exceptional record of Oligocene stratigraphy. For example, Ocean View contains the thickest Oligocene section recovered in New Jersey (275.95 ft; 84.13 m) and the best representation of Oligocene sequences (only Sequence O4 is not definitively recognized at this site).

SUMMARY AND CONCLUSIONS

At the Ocean View Leg 174AX borehole, 1575 ft (480.06 m) of middle Eocene to Holocene strata was continuously cored with very good recovery (81% total) and a full suite of downhole logs. Ocean View provided a record of middle to upper Miocene sequences that compliments Legs 150X and 174AX drilling at Cape May, and Atlantic City, New Jersey, and Bethany Beach, Delaware. More importantly, in comparison to other Legs 150X or 174AX boreholes, drilling at Ocean View provides the thickest and stratigraphically most complete record of

1. Lower Miocene Sequences Kw2a and Kw1a, which may each be subdivided into three higher-order sequences at Ocean View;
2. Oligocene sequences, where six to eight sequences are resolvable in one borehole for the first time;
3. Upper Eocene deposition, including three to four thick sequences and an apparent record of the Chesapeake Bay impact event; and
4. Middle Eocene sequences, revealed in a downdip location.

Several thick sandy aquifers and silty clay-confining units were recovered at Ocean View, including the Atlantic City 800-foot sand aquifer. By relating these aquifer-confining unit couplets to sequence stratigraphy, we should improve the hydrostratigraphic framework of the region.

REFERENCES

Ashley, G.M., Wellner, R.W., Esker, D., and Sheridan, R.E., 1991. Depositional model for valley fills on a passive continental margin. *Spec. Publ.—Soc. Econ. Paleontol. Mineral.,* 51:285–301.

Austin, J.A., Jr., Christie-Blick, N., Malone, M.J., et al., 1998. *Proc. ODP, Init. Repts.,* 174A: College Station, TX (Ocean Drilling Program).

Benson, R.N., 1994. Mid-Oligocene unconformity and faulting in the Atlantic coastal plain of Delaware correlated with uplift history of Appalachian-Labrador and Bermuda Rises. *Geol. Soc. Am. Abstr. Progr.,* 26:A-91. (Abstract)

Berggren, W.A., Kent, D.V., Swisher, C.C., III, and Aubry, M.-P., 1995. A revised Cenozoic geochronology and chronostratigraphy. *In* Berggren, W.A., Kent, D.V., Aubry, M.-P., and Hardenbol, J. (Eds.), *Geochronology, Time Scales and Global Stratigraphic Correlation*. Spec. Publ.—Soc. Econ. Paleontol. Mineral. (Soc. Sediment. Geol.), 54:129–212.

Browning, J.V., Miller, K.G., and Bybell, L.M., 1997a. Upper Eocene sequence stratigraphy and the Absecon Inlet Formation, New Jersey coastal plain. *In* Miller, K.G., Newell, W., and Snyder, S.W. (Eds.), *Proc. ODP, Sci. Results,* 150X: College Station, TX (Ocean Drilling Program), 243–266.

Browning, J.V., Miller, K.G., and Olsson, R.K., 1997b. Lower to middle Eocene benthic foraminiferal biofacies and lithostratigraphic units and their relationship to sequences, the New Jersey coastal plain. *In* Miller, K.G., Newell, W., and Snyder, S.W. (Eds.), *Proc. ODP, Sci. Results,* 150X: College Station, TX (Ocean Drilling Program), 207–228.

Cande, S.C., and Kent, D.V., 1992. A new geomagnetic polarity time scale for the Late Cretaceous and Cenozoic. *J. Geophys. Res.,* 97:13917–13951.

de Verteuil, L. 1997. Palynological delineation and regional correlation of lower through upper Miocene sequences in the Cape May and Atlantic City boreholes, New Jersey coastal plain. *In* Miller, K.G., Newell, W., and Snyder, S.W. (Eds.), *Proc. ODP, Sci. Results,* 150X: College Station, TX (Ocean Drilling Program), 129–145.

de Verteuil, L., and Norris, G., 1996. Miocene dinoflagellate stratigraphy and systematics of Maryland and Virginia. *Micropaleontology,* 42 (Suppl.):1–172.

Hart, S.R., and Brooks, C., 1974. Clinopyroxene-matrix partitioning of K, Rb, Cs, and Ba. *Geochim. Cosmochim. Acta,* 38:1799–1806.

Martin, E.E., Shackleton, N.J., Zachos, J.C., and Flower, B.P., 1999. Orbitally-tuned Sr isotope chemostratigraphy for the late middle to late Miocene. *Paleoceanography,* 14:74–83.

Martini, E., 1971. Standard Tertiary and Quaternary calcareous nannoplankton zonation. *In* Farinacci, A. (Ed.), *Proc. 2nd Int. Conf. Planktonic Microfossils Roma:* Rome (Ed. Tecnosci.), 2:739–785.

Martini, E., and Müller, C., 1976. Current Tertiary and Quaternary calcareous nannoplankton stratigraphy and correlations. *Newsl. Stratigr.,* 16:99–112.

Miller, K.G., Barrera, E., Olsson, R.K., Sugarman, P.J., and Savin, S.M., 1999a. Does ice drive early Maastrichtian eustacy? *Geology,* 27:783–786.

Miller, K.G., et al., 1994a. Atlantic City site report. *In* Miller, K.G., et al., *Proc. ODP, Init. Repts.,* 150X: College Station, TX (Ocean Drilling Program), 35–58.

————, 1994b. Island Beach site report. *In* Miller, K.G., et al., *Proc. ODP, Init. Repts.,* 150X: College Station, TX (Ocean Drilling Program), 5–33.

Miller, K.G., Kent, D.V., Brower, A.N., Bybell, L.M., Feigenson, M.D., Olsson, R.K., and Poore, R.Z., 1990. Eocene-Oligocene sea-level changes on the New Jersey coastal plain linked to the deep-sea record. *Geol. Soc. Am. Bull.,* 102:331–339.

Miller, K.G., Liu, C., Browning, J.V., Pekar, S.F., Sugarman, P.J., Van Fossen, M.C., Mullikin, L., Queen, D., Feigenson, M.D., Aubry, M.-P., Burckle, L.D., Powars, D., and Heibel, T., 1996a. Cape May site report. *Proc. ODP, Init. Repts.,* 150X (Suppl.): College Station, TX (Ocean Drilling Program).

Miller, K.G., and Mountain, G.S., 1994. Global sea-level change and the New Jersey margin. *In* Mountain, G.S., Miller, K.G., Blum, P., et al., *Proc. ODP, Init. Repts.,* 150: College Station, TX (Ocean Drilling Program), 11–20.

Miller, K.G., Mountain, G.S., Browning, J.V., Kominz, M., Sugarman, P.J., Christie-Blick, N., Katz, M.B., and Wright, J.D., 1998. Cenozoic global sea level, sequences, and the New Jersey transect: results from coastal plain and continental slope drilling. *Rev. Geophys.,* 36:569–601.

Miller, K.G., Mountain, G.S., and Leg 150 Shipboard Party and Members of the New Jersey Coastal Plain Drilling Project, 1996b. Drilling and dating New Jersey Oligocene-Miocene sequences: ice volume, global sea level and Exxon records. *Science,* 271:1092–1995.

Miller, K.G., Rufolo, S., Sugarman, P.J., Pekar, S.F., Browning, J.V., and Gwynn, D.W., 1997. Early to middle Miocene sequences, systems tracts, and benthic foraminiferal biofacies, New Jersey coastal plain. *In* Miller, K.G., Newell, W., and Snyder, S.W. (Eds.), *Proc. ODP, Sci. Results,* 150X: College Station, TX (Ocean Drilling Program), 361–373.

Miller, K.G., Sugarman, P.J., Browning, J.V., Cramer, B.S., Olsson, R.K., de Romero, L., Aubry, M.-P., Pekar, S.F., Georgescu, M.D., Metzger, K.T., Monteverde, D.H., Skinner, E.S., Uptegrove, J., Mullikin, L.G., Muller, F.L., Feigenson, M.D., Reilly, T.J., Brenner, G.J., and Queen, D., 1999b. Ancora Site. In Miller, K.G., Sugarman, P.J., Browning, J.V., et al., *Proc. ODP, Init. Repts.,* 174AX (Suppl.), 1–65 [Online]. Available from World Wide Web: <http://www-odp.tamu.edu/publications/174AXSIR/VOLUME/CHAPTERS/174AXS_1.PDF>.

Miller, K.G., Sugarman, P.J., Browning, J.V., Olsson, R.K., Pekar, S.F., Reilly, T.J., Cramer, B.S., Aubry, M.-P., Lawrence, R.P., Curran, J., Stewart, M., Metzger, J.M., Uptegrove, J., Bukry, D., Burckle, L.H., Wright, J.D., Feigenson, M.D., Brenner, G.J., and Dalton, R.F., 1998. Bass River Site. *In* Miller, K.G., Sugarman, P.J., Browning, J.V., et al., *Proc. ODP, Init. Repts.,* 174AX: College Station, TX (Ocean Drilling Program), 5–43.

Monteverde, D.H., Miller, K.G., and Mountain, G.S., 2000. Correlation of offshore seismic profiles with onshore New Jersey Miocene sections. *Sediment. Geol.,* 134:111–127.

Mountain, G.S., Miller, K.G., Blum, P., et al., 1994. *Proc. ODP, Init. Repts.,* 150: College Station, TX (Ocean Drilling Program).

NJGS Information Circular 1, 1990. Generalized stratigraphic table for New Jersey. *New Jersey Geol. Surv.*

Oslick, J.S., Miller, K.G., and Feigenson, M.D., 1994. Oligocene-Miocene strontium isotopes: stratigraphic revisions and correlations to an inferred glacioeustatic record. *Paleoceanography,* 9:427–423.

Owens, J.P., Bybell, L.M., Paulachok, G., Ager, T.A., Gonzalez, V.M., and Sugarman, P.J., 1988. Stratigraphy of the Tertiary sediments in a 945-foot-deep core hole near Mays Landing in the southeastern New Jersey Coastal Plain. *Geol. Surv. Prof. Pap. U.S.,* 1484.

Owens, J.P., Miller, K.G., and Sugarman, P.J., 1997. Lithostratigraphy and paleoenvironments of the Island Beach borehole, New Jersey Coastal Plain. *In* Miller, K.G., Newell, W., and Snyder, S.W. (Eds.), *Proc. ODP, Sci. Results,* 150X: College Station, TX (Ocean Drilling Program), 15–24.

Owens, J.P., and Sohl, N.F., 1969. Shelf and deltaic paleoenvironments in the Cretaceous-Tertiary formations of the New Jersey Coastal Plain. *In* Subitzky, S. (Ed.), *Geology of Selected Areas in New Jersey and Eastern Pennsylvania and Guidebook of Excursions:* New Brunswick, NJ (Rutgers Univ. Press), 235–278.

Parker, M.E., Clark, M., and Wise, Jr., S.W., 1985. Calcareous nannofossils of Deep Sea Drilling Project Sites 558 and 563, North Atlantic Ocean: biostratigraphy and the distribution of Oligocene Braarudosphaerids. *In* Bougault, H., Cande, S.C., et al., *Init. Repts. DSDP,* 82: Washington (U.S. Govt. Printing Office), 559–589.

Pekar, S., Miller, K.G., and Browning, J.V., 1997a. New Jersey Coastal Plain Oligocene sequences, ODP Leg 150X. *In* Miller, K.G., Newell, W., and Snyder, S.W. (Eds.), *Proc. ODP, Sci. Results,* 150X: College Station, TX (Ocean Drilling Program), 187–206.

Pekar, S.F., Miller, K.G., and Kominz, M.A., 2000. Reconstructing the stratal geometry of latest Eocene to Oligocene sequences in New Jersey: resolving a patchwork distribution into a clear pattern of progradation. *Sediment. Geol.,* 134:93–109.

Pekar, S.F., Miller, K.G., and Olsson, R.K., 1997b. *Data report:* The Oligocene Sewell Point and Atlantic City formations, New Jersey Coastal Plain. *In* Miller, K.G., Newell, W., and Snyder, S.W. (Eds.), *Proc. ODP, Sci. Results,* 150X: College Station, TX (Ocean Drilling Program), 81–87.

Poag, C.W., and Aubry, M.-P., 1995. Upper Eocene impactites of the U.S. east coast: depositional origins, biostratigraphic framework, and correlation. *Palaios,* 10:16–43.

Posamentier, H.W., Jervey, M.T., and Vail, P.R., 1988. Eustatic controls on clastic deposition, I. Conceptual framework. *In* Wilgus, C.K., Hastings, B.S., Kendall, C.G.St.C., Posamentier, H.W., Ross, C.A., and Van Wagoner, J. (Eds.), *Sea-Level Changes: An Integrated Approach.* Spec. Publ.—Soc. Econ. Paleontol. Mineral., 42:109–124.

Sea-Level Working Group Report, 1992. *JOIDES J.,* 18:28–36.

Sheridan, R.E., Ashley, G.M., Miller, K.G., Waldner, J.S., Hall, D.W., and Uptegrove, J., 2000. Onshore-offshore correlation of upper Pleistocene strata, New Jersey coastal plain to continental shelf and slope. *Sediment. Geol.,* 134:197–207.

Sugarman, P.J., and Miller, K.G., 1997. Correlation of Miocene sequences and hydrogeologic units, New Jersey Coastal Plain. *In* Segall, M.P., Colquhoun, D.J., and Siron, D.L. (Eds.), *Evolution of the Atlantic Coastal Plain-Sedimentology, Stratigraphy, and Hydrogeology.* Sediment. Geol., 108:3–18.

Sugarman, P.J., Miller, K.G., Bukry, D., and Feigenson, M.D., 1995. Uppermost Campanian-Maestrichtian strontium isotopic, biostratigraphic, and sequence stratigraphic framework of the New Jersey Coastal Plain. *Geol. Soc. Am. Bull.,* 107:19–37.

Sugarman, P.J., Miller, K.G., Owens, J.P., and Feigenson, M.D., 1993. Strontium isotope and sequence stratigraphy of the Miocene Kirkwood Formation, Southern New Jersey. *Geol. Soc. Am. Bull.,* 105:423–436.

Zapecza, O.S., 1989. Hydrogeologic framework of the New Jersey coastal plain. *Geol. Surv. Prof. Pap. U.S.,* 1404-B.

Figure F1. Location map showing existing ODP boreholes analyzed as a part of the New Jersey transect. Also shown are multichannel seismic data (MCS) from Ew9009, Oc270, and CH0698.

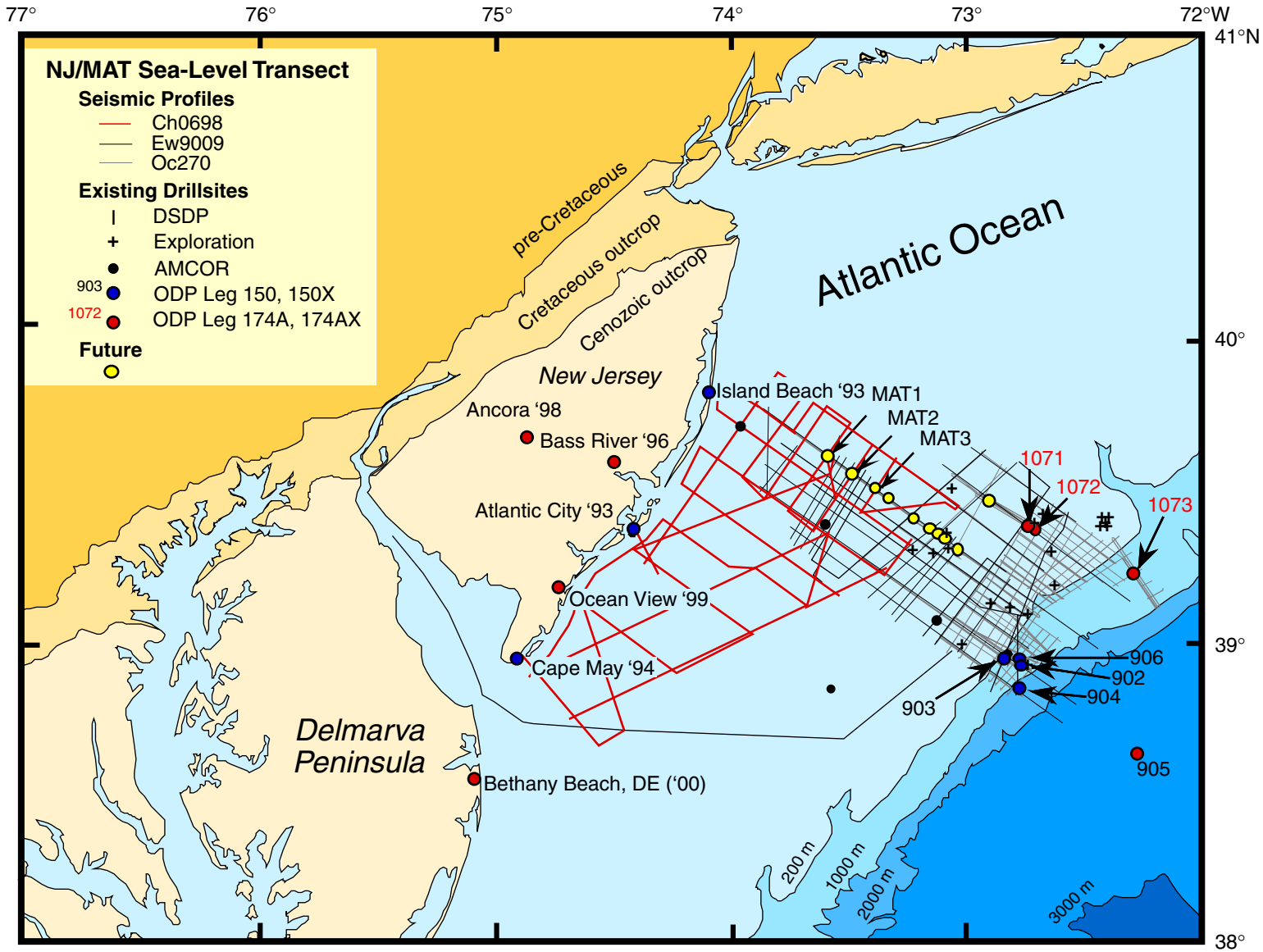

Figure F2. Surficial (?Pleistocene–Holocene), ?Cohansey Formation (?upper and/or ?middle Miocene), and Cohansey Formation (?upper and/or ?middle Miocene) from the Ocean View borehole. uHST = upper highstand systems tract. CH2, CH3, and CH4 = Kirkwood-Cohansey sequences.

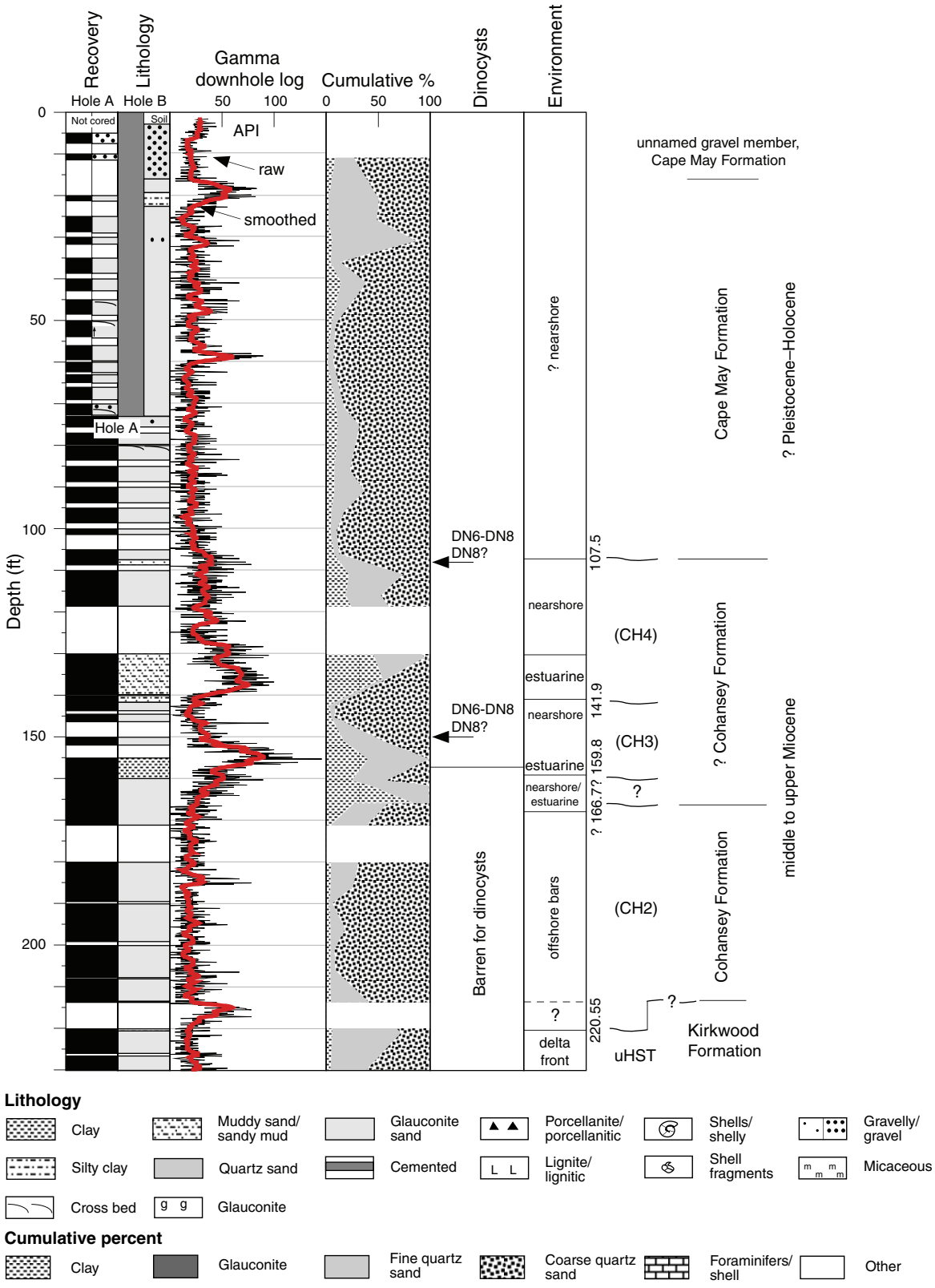

Figure F3. Kirkwood-Cohansey (middle to upper Miocene) and Kw3 (middle Miocene) sequences from the Kirkwood Formation at the Ocean View borehole. Kirkwood-Cohansey and Kw3 are sequences defined by Miller et al. (1997) and Sugarman et al. (1993). uHST = upper highstand systems tract, lHST = lower highstand systems tract, MFS = maximum flooding surface, TST = transgressive systems tract. The key to lithologic symbols is given in Figure F2, p. 48.

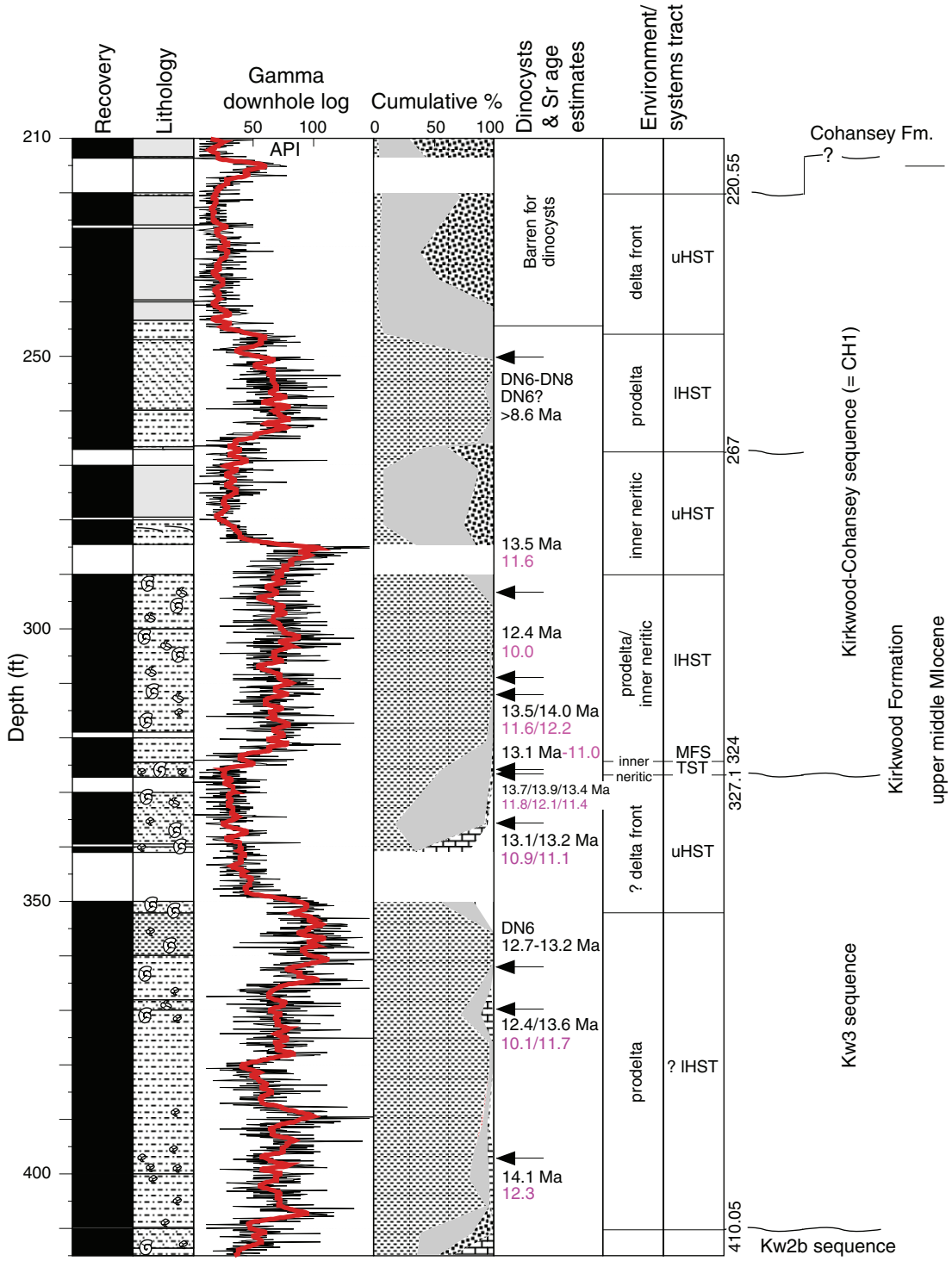

Figure F4. Kw2 sequences (lower to middle Miocene) from the Kirkwood Formation at the Ocean View borehole. Kw2a and Kw2b are sequences defined by Miller et al. (1997) and Sugarman et al. (1993). Subdivision of Sequence Kw2a into three higher-order sequences is new. uHST = upper highstand systems tract, lHST = lower highstand systems tract, MFS = maximum flooding surface, TST = transgressive systems tract, LST = lowstand systems tract. The key to lithologic symbols is given in Figure F2, p. 48.

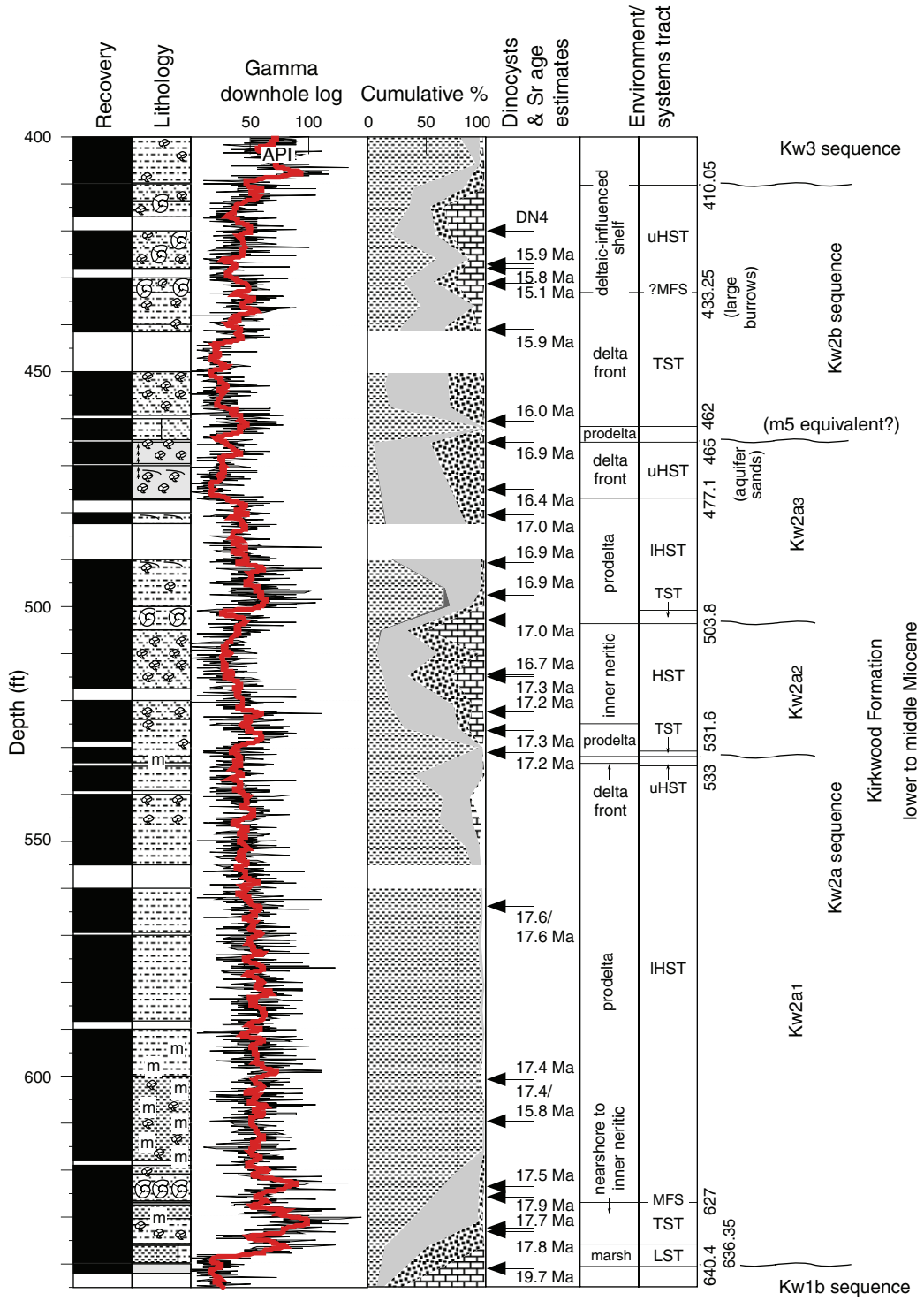

Figure F5. Kw1 and Kw0 sequences (lower Miocene) from the Kirkwood Formation at the Ocean View borehole. Kw1a, Kw1b, and Kw0 are sequences defined by Miller et al. (1997) and Sugarman et al. (1993). uHST = upper highstand systems tract, lHST = lower highstand systems tract, MFS = maximum flooding surface, TST = transgressive systems tract, LST = lowstand systems tract. The key to lithologic symbols is given in Figure F2, p. 48.

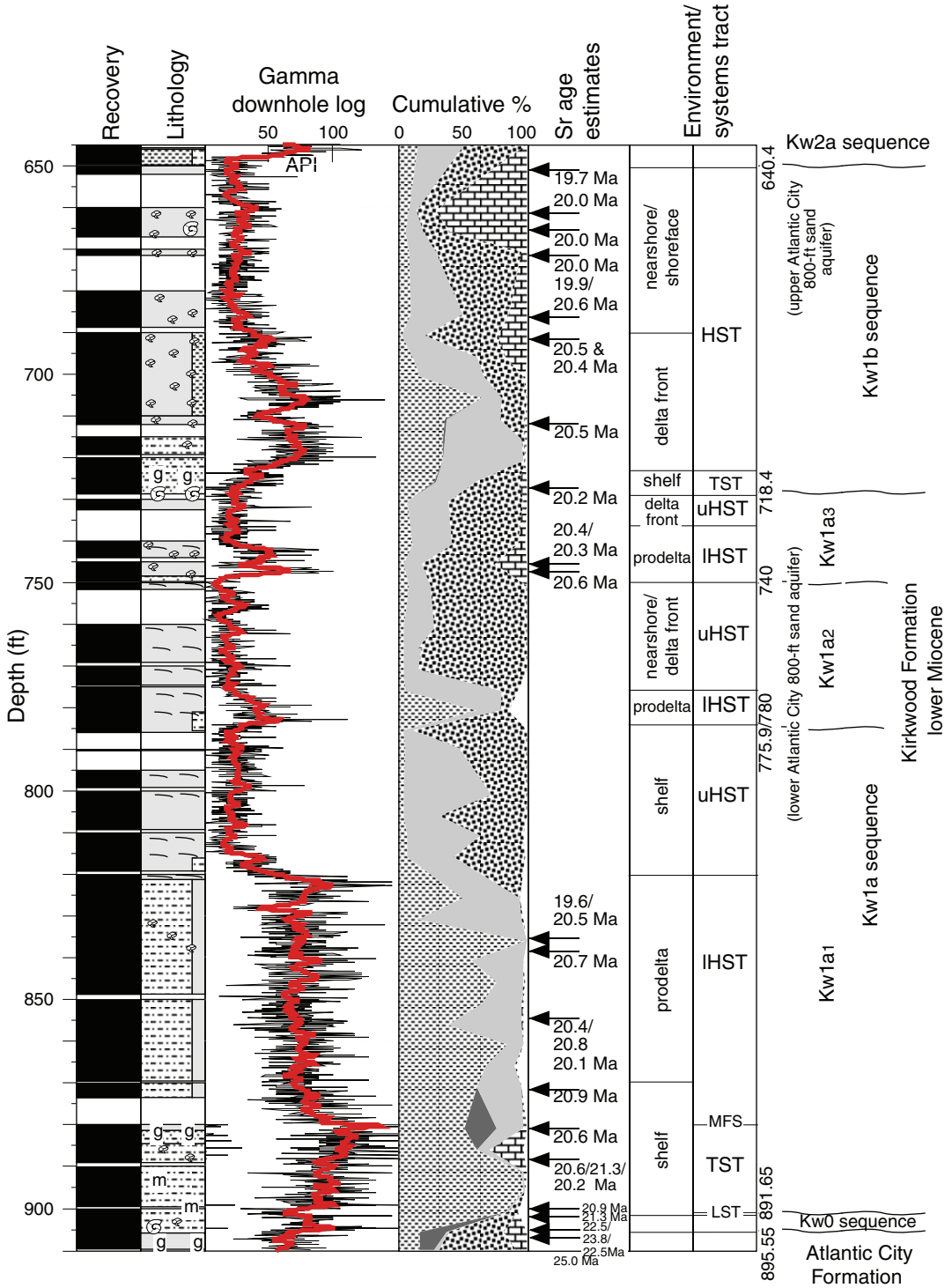

Figure F6. Atlantic City Formation (Oligocene) and Sewell Point Formation (Oligocene) from the Ocean View borehole. O1 to O6 are sequences defined by Pekar et al. (1997a). uHST = upper highstand systems tract, lHST = lower highstand systems tract, MFS = maximum flooding surface, TST = transgressive systems tract. The key to lithologic symbols is given in Figure F2, p. 48.

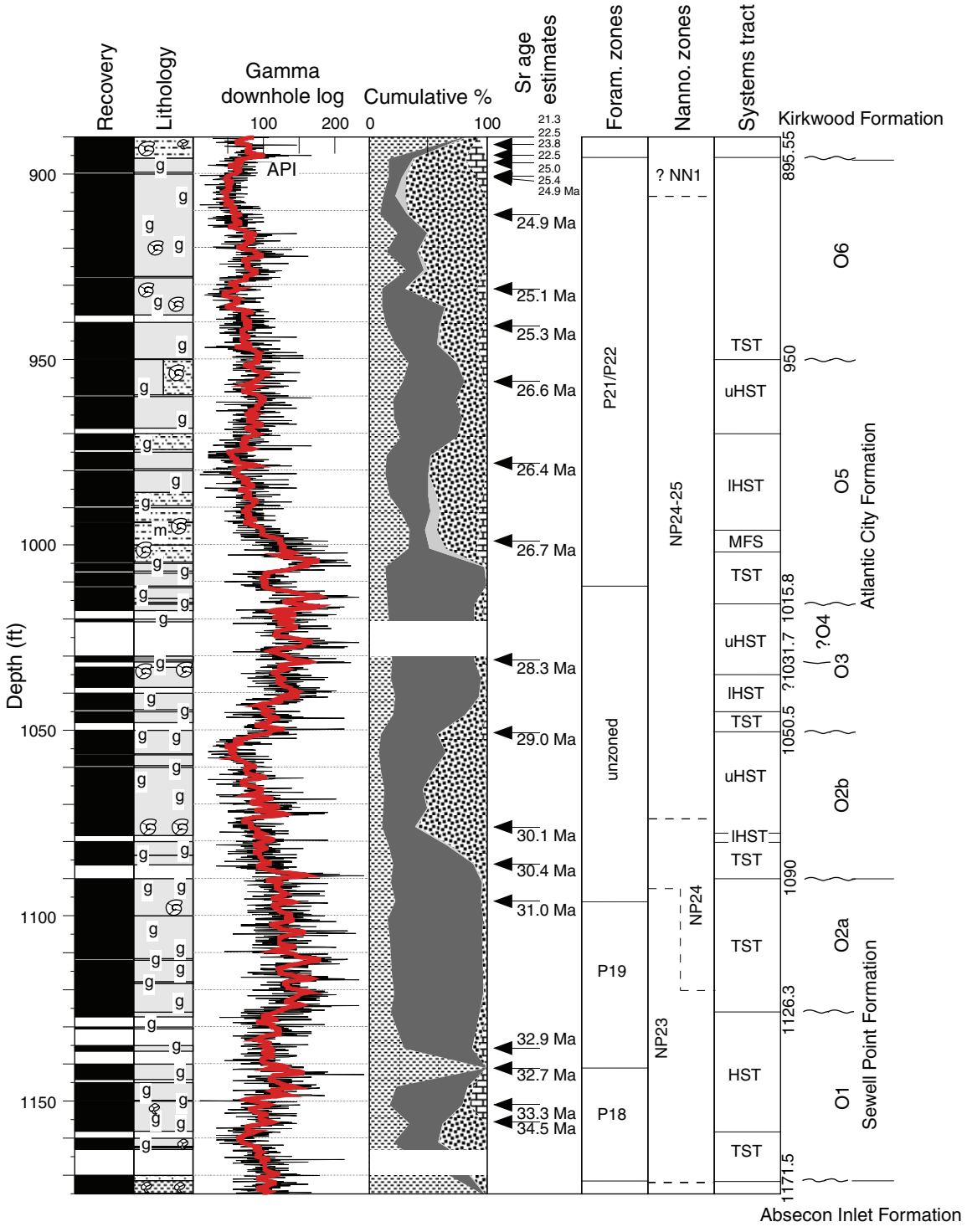

Figure F7. Absecon Inlet (upper Eocene) and Shark River Formations (middle Eocene) from the Ocean View borehole. E6 to E10 are sequences defined by Browning et al. (1997a, 1997b). HO = highest occurrence. The key to lithologic symbols is given in Figure F2, p. 48.

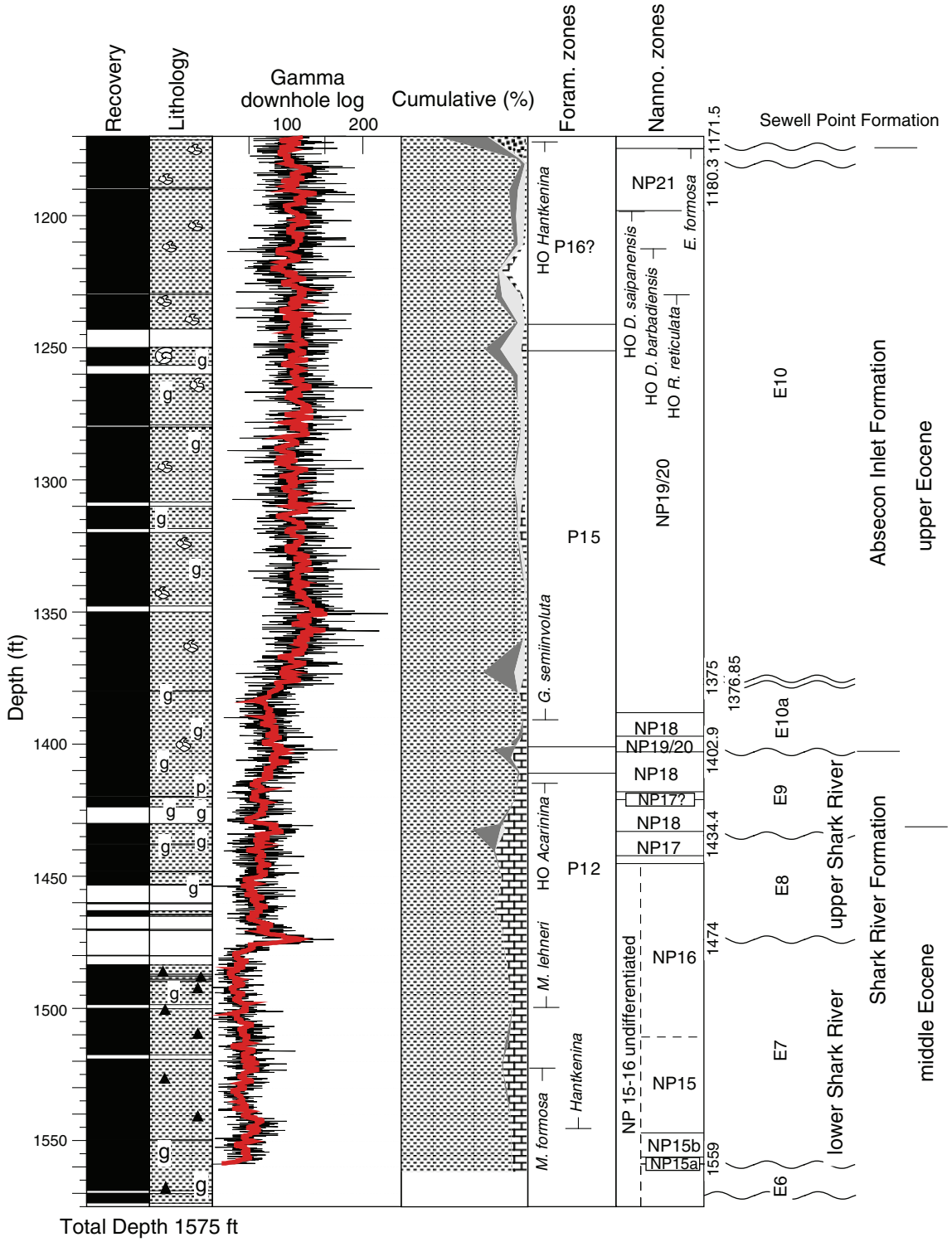

Figure F8. Age-depth plot for the Miocene sequences from the Ocean View borehole. Open circles = Sr age estimates. Error bars = 2σ for one analysis (Oslick et al., 1994).

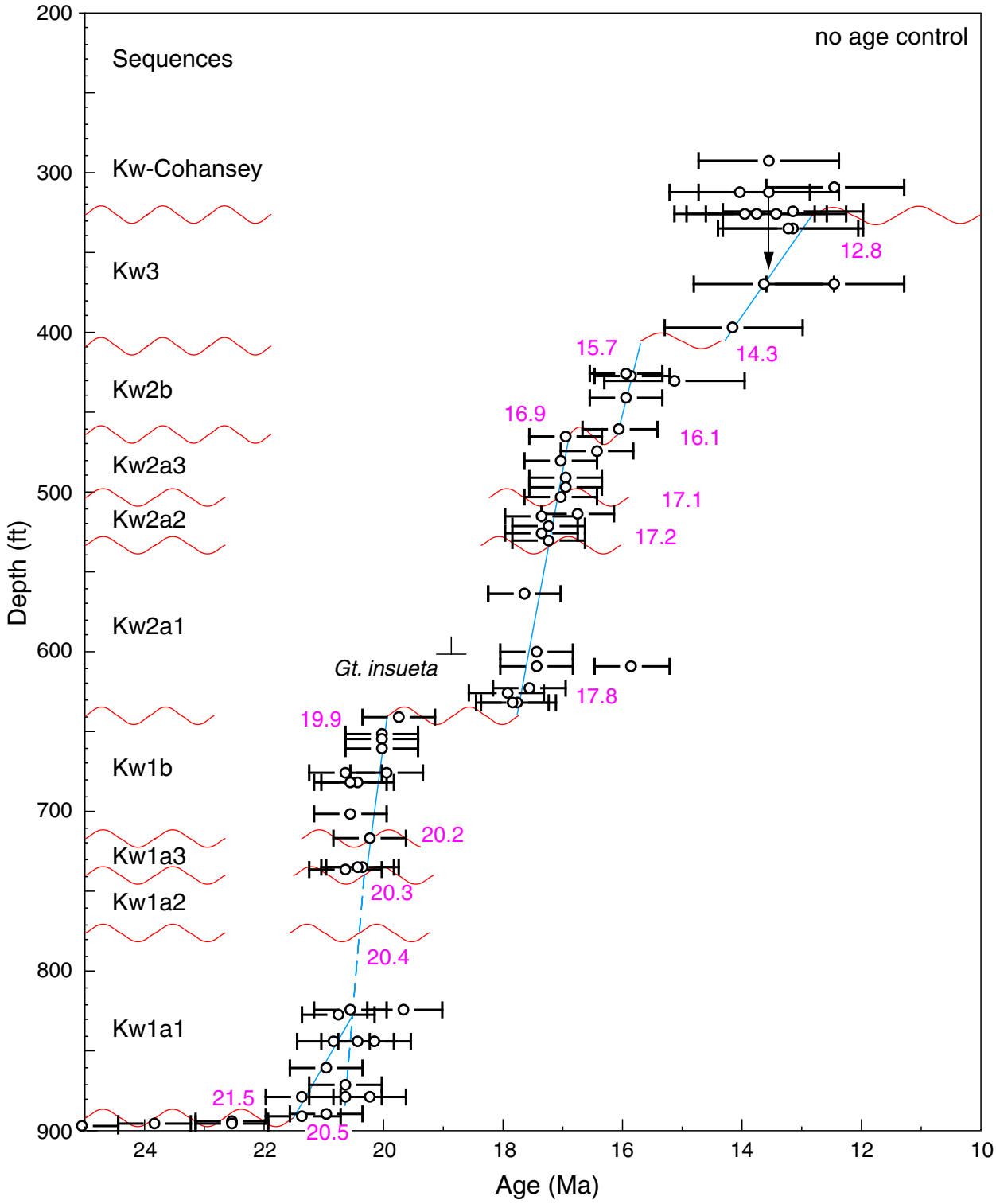

Figure F9. Age-depth plot for the Oligocene sequences from the Ocean View borehole. Solid circles = Sr age estimates. Error bars = 2σ for one analysis (Oslick et al., 1994).

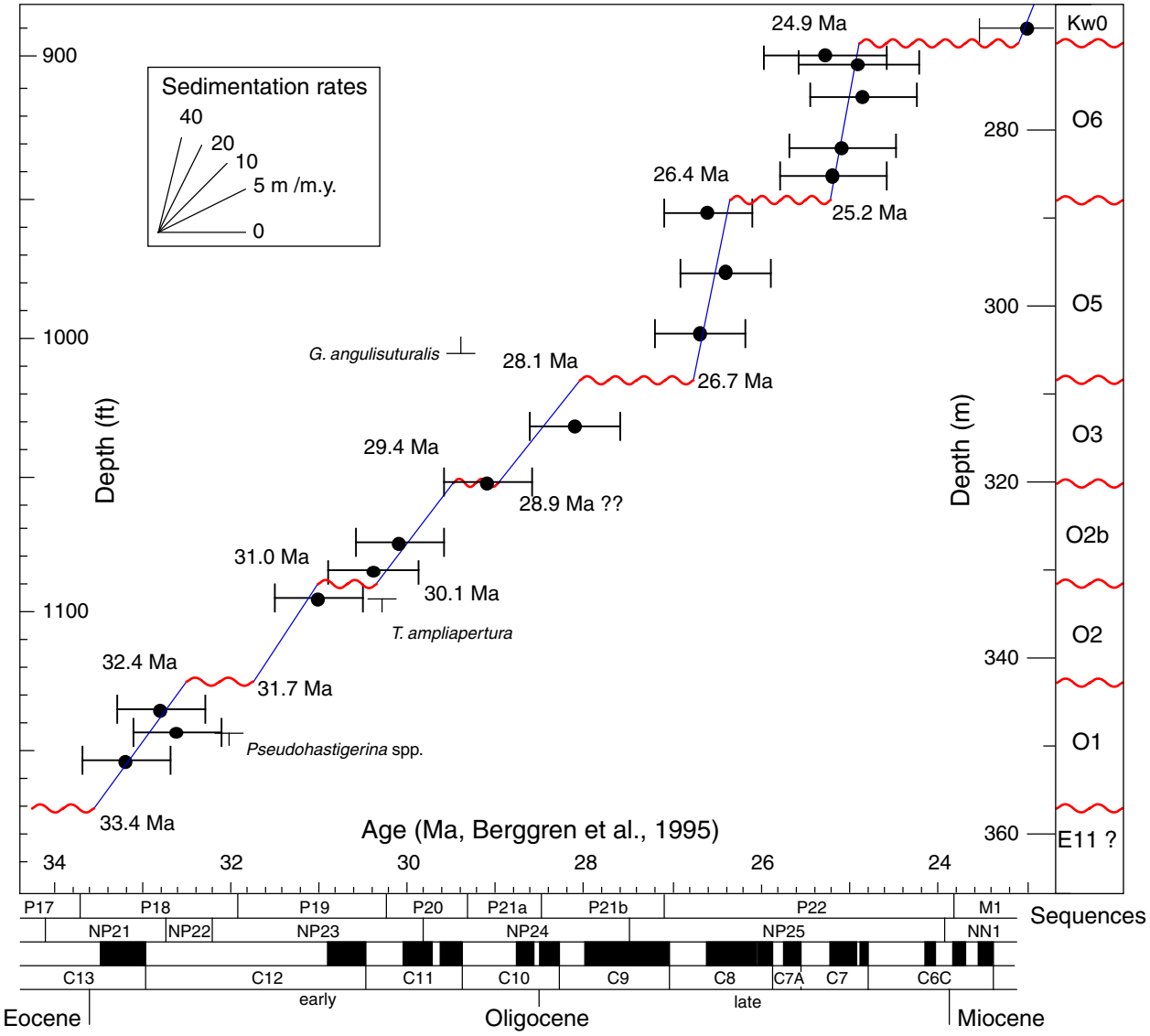

Figure F10. Photographs showing a complete Kw0 sequence from the New Jersey coastal plain. Sequence boundaries are at 891.65 and 895.55 ft (271.77 and 272.96 m). The sequence consists of a TST and a MFS with a truncated HST. A pebble and shell lag mark the base of the sequence. The TST contains burrowed glauconitic sandy clay. Note that the sequence boundary at 891.65 ft (271.77 m) is extensively burrowed.

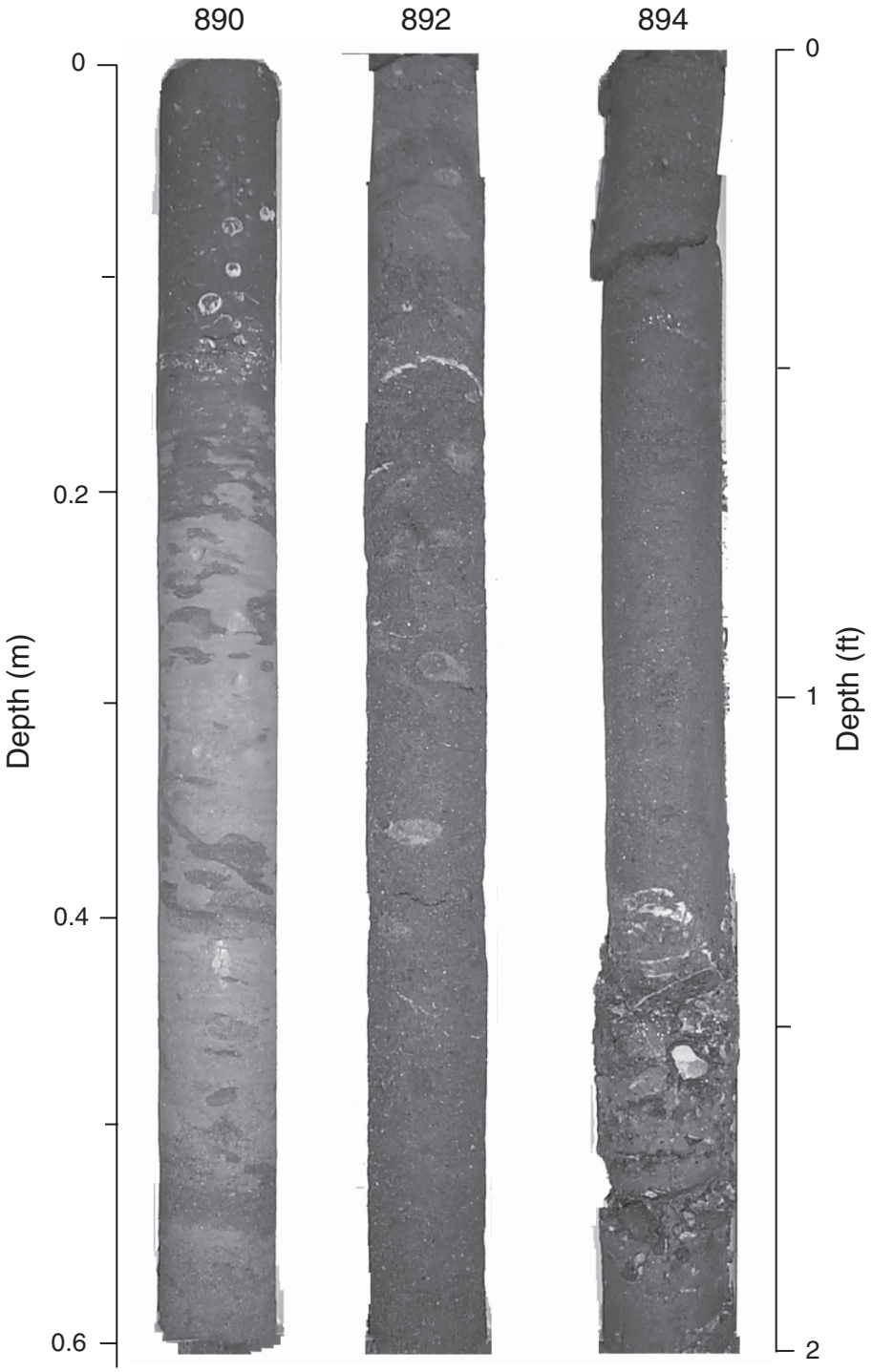

Figure F11. Photographs of sequence boundaries from the Miocene (718.4 ft; 218.97 m), Oligocene (1050.5 ft; 320.19 m), Eocene/Oligocene boundary (1171.5 ft; 357.07 m), and Eocene (1402.9 ft; 427.60 m). Miocene sequence boundaries tend to feature large shifts in facies with clays or highstand quartz sands below and sandy shell beds above. Oligocene sequence boundaries are often subtle with clayey glauconite sands below and glauconitic sandy clay above. The Eocene/Oligocene boundary features large facies changes from outer neritic clays below to inner neritic glauconite sandy clays above. Note the extensive burrowing that has taken place across the sequence boundary. Eocene sequence boundaries generally consist of clays on top of clays with a thin glauconite-rich layer at the base of the sequence.

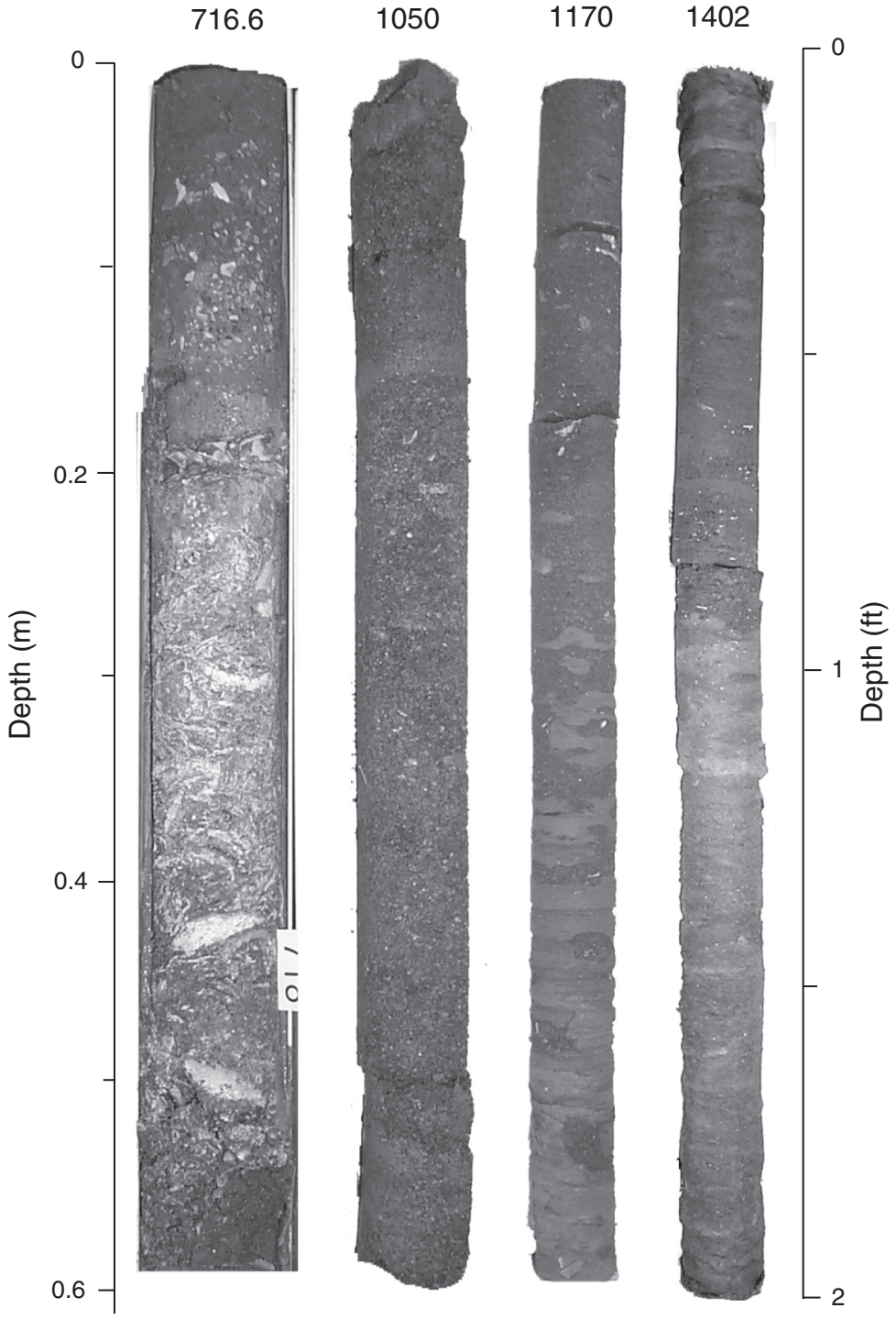

Figure F12. Photographs of facies changes within sequences. The interval from 810 to 814 ft (246.89 to 248.11 m) illustrates the change from lower HST prodelta clays to upper HST shelf sands. Note the laminations in the clays below 812 ft (247.50 m). The interval from 634 to 638 ft (193.24 to 194.46 m) illustrates the change from LST marsh sediments below to neritic sands above.

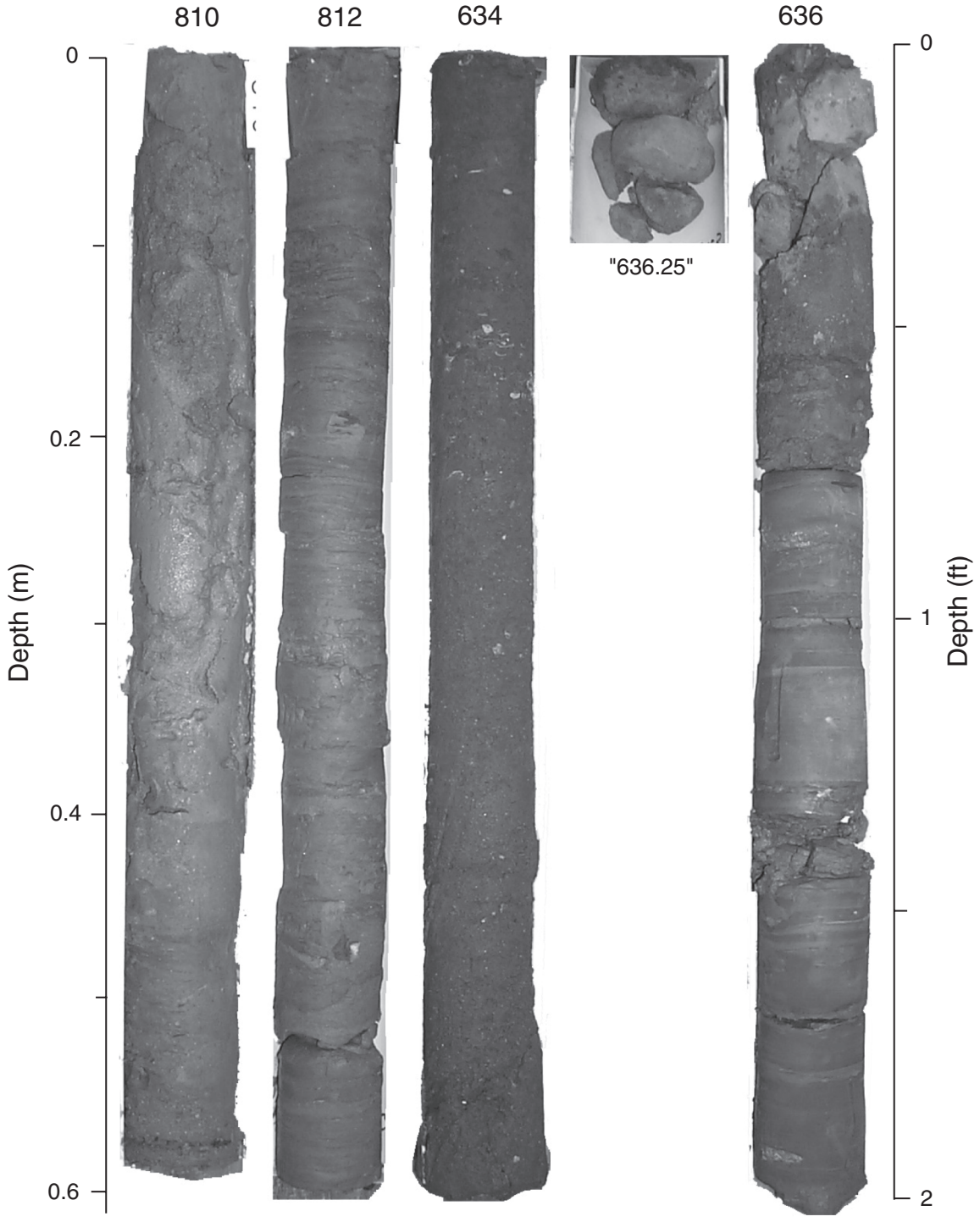

Table T1. Core descriptions, Ocean View borehole, Leg 174AX. (See table note. Continued on next seven pages.)

Core	Interval (ft)	Recovery (ft)	Recovery (%)	Primary lithology	Color (Munsell)	Formation
Hole A						
1	5-10	2.45	49	Sand and pebble gravel	10YR 4/6 yellowish brown	Unnamed gravel member; Cape May
2	10-15	1.35	27	Sandy gravel	10YR 4/6 yellowish brown	Unnamed gravel member; Cape May
3	15-20	0.3	6	Gravel (caved)	Not recorded	Caved
4	20-25	1.2	24	Fine-very fine sand	10YR 5/6 yellowish brown	Cape May
5	25-30	3.85	77	Fine-medium sand	10YR 5/4 yellowish brown	Cape May
6	30-35	1.65	33	Very fine sand	2.5Y 6/3 light yellowish brown	Cape May
7	35-40	3.4	68	Poorly sorted fine-medium sand	2.5Y 6/3 light yellowish brown	Cape May
8	40-45	2.7	54	Clayey fine-very coarse sand	10YR 7/2 light gray	Cape May
9	45-50	3.5	70	Fine sand with clay-bedded clay drapes	2.5Y 6/2 light yellowish brown	Cape May
10	50-56	4	67	Cross-bedded sand/fining-upward sand	10YR 6/6 brownish yellow	Cape May
11	56-60	3.6	90	Poorly sorted fine-coarse sand	10YR 6/2 light yellowish brown	Cape May
12	60-63	2.25	75	Clay and medium-coarse sand	7.5YR 6/8 reddish yellow	Cape May
13	63-66	1.9	63	Fine-very coarse sand	10YR 6/6 brownish yellow	Cape May
14	66-70	2.75	69	Fine-very coarse sand	10YR 6/4 light brownish yellow	Cape May
15	70-73	1.7	57	Gravel (0-0.9 ft) and silty fine-coarse cross-bedded sand	10YR 6/4 light yellowish brown; 10YR 7/3 very pale brown	Cape May
16	73-77	2.55	64	Slightly silty, slightly gravelly medium sand	2.5Y 7/3 pale yellow	Cape May
17	77-80	2.6	87	Medium-coarse sand; possible contact (color change)	7.5YR 6/6 reddish yellow with 10YR 7/2 light gray	Cape May
18	80-85	3.7	74	Medium to coarse quartz sand	2.5Y 8/4 pale yellow to 2.5Y 7/6 yellow	Cape May
19	85-90	3.5	70	Fine to medium to occasional coarse quartz sand; occasional bedding	2.5Y 7/5 yellow to 2.5Y 6/6 olive yellow to 5YR 5/8 yellowish red	Cape May
20	90-95	3.9	78	Medium to very coarse quartz sand	2.5Y 7/4 pale yellow	Cape May
21	95-100	3.3	66	Medium to coarse quartz sand	2.5Y 7/5 yellow to 2.5Y 6/6 olive yellow to 5YR 5/8 yellowish red	Cape May
22	100-105	1.6	32	Medium to very coarse quartz sand with pebbles	2.5Y 7/5 yellow to 5YR 3/4 dark reddish brown	Cape May
23	105-110	3.7	74	Medium to coarse quartz sand; silty fine sand; contact at 107.5 ft	10YR 6/6 brownish yellow to 7.5YR 6/6 reddish yellow with 7.5YR 2.5/3 very dark brown; 2.Y5 5/6 light olive brown; 2.5Y 6/6 olive yellow; 5Y 3/1 very dark gray	Cape May/?Cohansey
24	110-120	8.4	84	Silty fine sand	5Y 3/1 dark gray to 5Y 4/1 very dark gray	?Cohansey
25	120-130	0	0	No recovery		?Cohansey
26	130-140	9.8	98	Clayey fine sand to silty sandy clay; clay	Dark gray to very dark gray 5Y 4/1 to 5Y 3/1 above 5Y 5/3 olive	?Cohansey
27	140-144.5	3.3	73	Mottled clay to 141.9 ft; medium to pebbly quartz sand below	5Y 5/3 olive to 2.5Y 4/1 dark gray	?Cohansey
28	144.5-150	1.7	31	Coarse quartz sand	2.5Y 5/1 gray	?Cohansey
29	150-155	1.8	36	Silty fine quartz sand, fining downward to clayey fine quartz sand at base; occasional lignite in upper portion	N 3/ to N 4/ dark gray-very dark gray	?Cohansey
30	155-160	5.6	112	Interbedded clays and clayey silty very fine quartz sand; ?sequence boundary at 159.8 ft; silty clayey fine quartz sand	10YR 4/3 brown, 5YR 5/2 reddish brown, 5GY 6/1 greenish gray; 7.5YR 5/1 gray	?Cohansey
31	160-167.5	7.5	100	Clayey silty quartz sand; massive medium sand below; contact at 66.7 ft	5YR 5/2 reddish gray; 5Y 3/1 very dark gray; 5Y 5/1 gray; 7.5YR 5/1 gray; 5G 5/2 grayish green; 5B 4/1 dark bluish gray	?Cohansey/Cohansey
32	167.5-170	2.5	100	Fine-medium quartz sand	N6/ gray	Cohansey
33	170-180	1.2	12	Medium quartz sand	N6/ gray	Cohansey
34	180-190	9.4	94	Fine-medium quartz sands; poorly sorted slightly gravelly fine-coarse sand	10YR 6/2 light brownish gray; 10YR 6/4 light yellowish brown	Cohansey
35	190-200	9	90	Slightly pebbly fine-coarse sand	10YR 6/4 light yellowish brown	Cohansey

Table T1 (continued).

Core	Interval (ft)	Recovery (ft)	Recovery (%)	Primary lithology	Color (Munsell)	Formation
36	200-208	7.8	98	Medium-coarse quartz sand	10YR 6/2 light brownish gray; 10YR 6/6 brownish yellow	Cohansey
37	208-210	2.97	149	Medium-coarse quartz sand	2.5Y 6/3 light yellowish brown	Cohansey
38	210-220	3.6	36	Gravelly medium-coarse quartz sand/sandy silty clay	10YR 6/2 light brownish gray; 10YR 6/6 brownish yellow	Cohansey
39	220-226.5	5.9	91	Sandy silty clay; organic medium-coarse sands; contact at 220.55 ft	5GY 5/1 greenish gray; 10YR 3/1; very dark gray; 10YR 3/1 very dark gray	Cohansey/Kirkwood (Kw-C)
40	226.5-230	3.6	103	Fine and medium quartz sand	2.5Y 4/1 dark gray	Kirkwood (Kw-C)
41	230-240	9.7	97	Medium quartz sand	2.5Y 4/1 dark gray; 2.5Y 3/1 very dark gray (subordinate)	Kirkwood (Kw-C)
42	240-250	9.7	97	Fine-medium quartz sand/silty clays; lithology change at 246.9 ft	2.5Y 4/1 dark gray; 5Y 4/1 dark gray; 5Y 4/2 olive gray	Kirkwood (Kw-C)
43	250-260	10.35	104	Silty clay (dominant) and clayey silt	5GY 5/1 to 5GY 4/1; greenish gray-dark greenish gray	Kirkwood (Kw-C)
44	260-270	7	70	Finely laminated silty clay; sand with silt and clay; sequence boundary at 267 ft	5Y 3/2 dark olive gray; 5Y 3/1 very dark gray	Kirkwood (Kw-C)
45	270-280	9.6	96	Silty fine sand	5GY 4/1; dark greenish gray	Kirkwood (Kw-C)
46	280-290	4.8	48	Silty fine sand, cross bedding	5GY 4/1; dark greenish gray	Kirkwood (Kw-C)
47	290-300	10.4	104	Slightly sandy silty clay, shelly throughout, light and dark lenses	5GY 4/1 dark greenish gray; 5Y 5/2 olive gray; 5Y 2.5/1 black	Kirkwood (Kw-C)
48	300-310	10.9	109	Slightly silty clay, shells throughout; darker interval; shell hash	5GY 4/1 dark greenish gray; 5Y 2.5/1 black	Kirkwood (Kw-C)
49	310-320	8.9	89	Silty clay, thin shells throughout, occasional dark lenses and thin organic-rich beds; shell hash	5GY 4/1 dark greenish gray; 5Y 2.5/1 black	Kirkwood (Kw-C)
50	320-326.5	7.6	117	Very slightly silty clay, shells throughout; silty fine sand; indurated at base	5Y 3/2-5Y 2/2 olive gray-black; 5Y 4/1-5Y 3/1 dark gray-very dark gray	Kirkwood (Kw-C)
51	326.5-330	0.7	20	Shell bed, indurated, fine sand matrix; silty fine sand; sequence boundary at 327.1 ft	5Y 3/2 dark olive gray; 5Y 2.5/1 black; 5Y 2.5/2 black	Kirkwood (Kw-C/Kw3)
52	330-340	9.4	94	Silty fine sand with clay and shells; silty fine sand with shells; slightly silty fine sand	5Y 3/2 dark olive gray; 5Y 2.5/1 black; 5Y 2.5/2 black	Kirkwood (Kw3)
53	340-350	1	10	Silty fine quartz sand; clayey fine quartz sand; shell hash	5Y 3/2 dark olive gray	Kirkwood (Kw3)
54	350-360	10.5	105	Micaceous very silty very fine sand to sandy silt, shells; shell hash; laminated clays	5Y 3/1 very dark gray to 5Y 2.5/1 black; 2.5Y 5/1 gray to 5Y 5/2 olive; 5Y 3/2 dark olive gray to 5Y 4/1 dark gray	Kirkwood (Kw3)
55	360-370	10.35	104	Laminated silty clay; silty clay; fine sandy silty clay with abundant shell fragments; shell hash	5Y 2.5/1 black to 5Y 3/2 dark olive gray to 5Y 5/1 gray; 5G 4/1 dark greenish gray; N2.5/ black; 5Y 2.5/1 black	Kirkwood (Kw3)
56	370-380	10	100	Slightly silty clay	5Y 3/2 dark olive gray; 5GY 4/1 dark greenish gray	Kirkwood (Kw3)
57	380-383	3.5	117	Slightly silty clay; shells 0-3.4 ft	5GY 4/1 dark greenish gray	Kirkwood (Kw3)
58	383-390	7.6	109	Slightly silty clay	5GY 4/1 dark greenish gray	Kirkwood (Kw3)
59	390-400	10.55	106	Slightly silty clay, shell debris in lower part	5GY 4/1 dark greenish gray	Kirkwood (Kw3)
60	400-410	9.75	98	Slightly silty clay with shell debris	5GY 4/1 dark greenish gray	Kirkwood (Kw3)
61	410-420	7.1	71	Clayey medium-coarse sand/sandy shelly clay; contact at 410.05 ft	5GY 3/2 dark olive gray; 5GY 4/1 dark greenish gray	Kirkwood (Kw3/Kw2b)
62	420-430	8.05	81	Shelly very clayey fine sand	5GY 4/1 dark greenish gray	Kirkwood (Kw2b)
63	430-440	9.9	99	Shelly clayey sand; large burrow at 433.25 ft; silty clay	5GY 4/1 dark greenish gray; 5Y 3/2 dark olive gray	Kirkwood (Kw2b)
64	440-450	1.5	15	Shelly clayey sand	5GY 4/1 dark greenish gray	Kirkwood (Kw2b)
65	450-460	9.2	92	Shelly clayey sand	N4 dark gray 5GY 4/1 dark gray	Kirkwood (Kw2b)
66	460-465	4.5	90	Clay with burrowed sand; sequence boundary at 465 ft	7.5YR 3/2 dark brown; 5Y 4/1 dark gray (burrow)	Kirkwood (Kw2b)

Table T1 (continued).

Core	Interval (ft)	Recovery (ft)	Recovery (%)	Primary lithology	Color (Munsell)	Formation
67	465-470	4.45	89	Shelly medium-coarse quartz sand; three fining upward cycles	5Y 4/1 dark gray; 10YR 4/1 interbeds	Kirkwood (Kw2a3)
68	470-480	7.3	73	Interbedded medium-very coarse sand; dark silty clay; lithology change at 477.1 ft to silt	5Y 4/1 dark gray; 10YR 4/1 interbeds	Kirkwood (Kw2a3)
69	480-490	2.3	23	Silt	5Y 3/2 dark olive gray	Kirkwood (Kw2a3)
70	490-500	10.4	104	Silt; lithology change at 495 ft; silty clay	5Y 3/2 dark olive gray; 2.5Y 3/2 very dark grayish brown	Kirkwood (Kw2a3)
71	500-507.5	6.65	89	Silty clay grading down to shell bed and shell hash; sequence boundary at 503.8 ft	5Y 3/2 dark olive gray; 2.5Y 3/2 very dark grayish brown	Kirkwood (Kw2a3/Kw2a2)
72	507.5-510	2.75	110	Shelly medium sand to sandy shell hash	5Y 3/2 dark olive gray	Kirkwood (Kw2a2)
73	510-520	7.55	76	Shelly medium sand to sandy shell hash	5Y 3/2 dark olive gray	Kirkwood (Kw2a2)
74	520-530	8.6	86	Clayey sand with shell hash; laminated clayey with shell hash; facies change at 524 ft	5Y 3/2 dark olive gray; 5Y 2.5/2 black	Kirkwood (Kw2a2)
75	530-534	3.1	78	Laminated clayey silt; sandy silt to silty sand; sequence boundary at 531.6 ft	5Y 2.5/2 black; 5Y 3/2 dark olive gray	Kirkwood (Kw2a2/Kw2a1)
76	534-540	5.1	85	Cross-bedded silty fine sand interbedded with laminated silty clay	5Y 2.5/2 black; 5Y 3/1 very dark gray	Kirkwood (Kw2a1)
77	540-550	10.2	102	Laminated to thin-bedded clay-silt	5Y 2.5/2 black	Kirkwood (Kw2a1)
78	550-560	4.9	49	Laminated silty-clay	5Y 3/2 dark olive gray	Kirkwood (Kw2a1)
79	560-570	9.4	94	Laminated silty-clay	5Y 3/2 dark olive gray; 5Y 2.5/2 black	Kirkwood (Kw2a1)
80	570-580	10.3	103	Laminated silty-clay; trace shell	5Y 3/2 dark olive gray; 5Y 2.5/2 black	Kirkwood (Kw2a1)
81	580-590	8.3	83	Laminated silty-clay; trace shell	5Y 3/2 dark olive gray	Kirkwood (Kw2a1)
82	590-600	10	100	Micaceous slightly silty clay	5Y 3/2 dark olive gray	Kirkwood (Kw2a1)
83	600-610	10.5	105	Micaceous slightly silty clay	5Y 3/2 dark olive gray	Kirkwood (Kw2a1)
84	610-619	8.1	90	Micaceous slightly silty clay	5Y 3/2 dark olive gray	Kirkwood (Kw2a1)
85	619-627	8.2	103	Micaceous slightly silty clay; contact clayey sand to sandy clay/shell bed/indurated zone; facies change at 627.0-627.2 ft	5Y 3/2 dark olive gray; 5Y 3/1 very dark gray to 5Y 2.5/1 very dark gray to 5Y 3/1 black; 5Y 6/2 light olive gray	Kirkwood (Kw2a1)
86	627-630	3	100	Indurated zone; sandy, shelly, clay; clayey fine sand	5Y 6/1 gray; 5Y 3/2 dark olive gray; 5Y 3/2	Kirkwood (Kw2a1)
87	630-636	6.25	104	Micaceous silty clay; clayey very fine sand; indurated zone	5Y 4/1 dark gray; 5Y 3/1 very dark gray; 5Y 6/1 gray	Kirkwood (Kw2a1)
88	636-640	3.6	90	Interbedded clay and sands	5Y 3/1 very dark gray to 5Y 2.5/1 black	Kirkwood (Kw2a1)
89	640-650	1.65	17	Clayey fine to medarkosic sand; shell hash; sequence boundary at 641.55 ft	5Y 3/2 dark olive gray	Kirkwood (Kw2a1/Kw1b)
90	650-660	7	70	Shell hash; shelly sand; shell bed; very shelly sand	5Y 3/2 dark olive gray	Kirkwood (Kw1b)
91	660-670	1.5	15	Shelly fine-medium sand	5Y 4/1 dark gray	Kirkwood (Kw1b)
92	670-675	4.95	99	Medium-coarse quartz	5Y 3/1 very dark gray	Kirkwood (Kw1b)
93	675-680	3.8	76	Alternations of fine-coarse sands	5Y 5/1 gray; 5Y 3/2 dark olive gray	Kirkwood (Kw1b)
94	680-687.5	7.3	97	Alternations of fine-coarse sands and clay	5Y 5/1 gray; 5Y 3/2 dark olive gray	Kirkwood (Kw1b)
95	687.5-695	7.6	101	Alternations of fine-coarse sands and clay	5Y 4/1 dark gray; 10YR 3/1 very dark gray	Kirkwood (Kw1b)
96	695-700	5.1	102	Alternations of fine-coarse sands and clay	5Y 3/1 to 5Y 2.5/2 very dark gray to black; 10YR 3/1 very dark gray	Kirkwood (Kw1b)
97	700-705	2.1	42	Mainly fine to medium quartz sand with clay laminations	5Y 3/2 dark olive gray to 5Y 3/2 dark olive gray	Kirkwood (Kw1b)
98	705-710	4.4	88	Slightly silty to sandy clays	10YR 3/1 very dark gray to 5Y 3/2 dark olive gray	Kirkwood (Kw1b)
99	710-713	3.9	130	Alternations of clayey silty fine sands and silty micaceous clay	10YR 3/1 very dark gray; 5Y 3/2 dark olive gray; 5Y 3/1 very dark gray	Kirkwood (Kw1b)
100	713-720	5.7	81	Clayey glauconitic fine quartz sand at top massive shell bed at bottom; sequence boundary 718.7 ft	5GY 4/1 dark greenish gray to 5Y 3/1 very dark gray	Kirkwood (Kw1b/Kw1a3)
101	720-730	2.3	23	Fine, medium to coarse quartz sand	5Y 4/1 dark gray	Kirkwood (Kw1a3)

Table T1 (continued).

Core	Interval (ft)	Recovery (ft)	Recovery (%)	Primary lithology	Color (Munsell)	Formation
102	730-735	4	80	Fine-medium quartz sand with clay interbeds	5Y 4/1 dark gray; 10YR 4/1 dark gray	Kirkwood (Kw1a3)
103	735-740	4.7	94	Fine-medium quartz sand with silty clay interbeds; sequence boundary at 740 ft	5Y 4/1 dark gray; 10YR 3/1 very dark gray	Kirkwood (Kw1a3)
104	740-750	1.6	16	Medium-very coarse quartz sand	5Y 4/1 dark gray	Kirkwood (Kw1a2)
105	750-760	9.1	91	Cross-bedded medium quartz sand; some medium-coarse sand	10YR 4/2 dark grayish brown	Kirkwood (Kw1a2)
106	760-765	4.6	92	Cross-bedded fine-medium sand	10YR 4/2 dark grayish brown; 10YR 5/1 gray	Kirkwood (Kw1a2)
107	765-775	10.05	101	Cross-bedded fine-medarkosic sand; clay at base	10YR 4/1 dark gray to 10YR 4/2 dark grayish brown; 10YR 3/1 very dark gray and 10YR 2/2 very dark brown	Kirkwood (Kw1a2)
108	775-780	0.9	18	Clay at top; silty fine sand to medarkosic-coarse sand; sequence boundary at 775.9-780 ft	10YR 3/1 very dark gray; 10YR 4/1 dark gray	Kirkwood (Kw1a2)
109	780-785	0.3	6	Clay at top; fine sandy clay with fine-medarkosic sand interbeds to fine-medarkosic sand	10YR 3/1 very dark gray; 10YR 3/2 very dark grayish brown to 10YR 4/1 dark gray	Kirkwood (Kw1a1)
110	785-790	4.1	82	Slightly silty fine-medium sand	10YR 3/2 very dark grayish brown	Kirkwood (Kw1a1)
111	790-800	9.15	92	Fine-medium sand	10YR 4/1 dark gray	Kirkwood (Kw1a1)
112	800-810	9.05	91	Fine-medium sand/interbedded sand and slightly silty clay	10YR 4/1 dark gray; 10YR 3/1 very dark gray	Kirkwood (Kw1a1)
113	810-820	10.3	103	Fine-medium sand/lithology change to sandy silty clay at 811.3 ft	10YR 4/1 dark gray; 10YR 3/1 very dark gray	Kirkwood (Kw1a1)
114	820-830	10.5	105	Silty clay with sandy interbeds	10YR 4/1 dark gray; 10YR 3/1 very dark gray	Kirkwood (Kw1a1)
115	830-840	8.8	88	Silty clay with sandy interbeds	10YR 3/1 very dark gray	Kirkwood (Kw1a1)
116	840-850	10.55	106	Laminated silty fine sand interbedded with laminated silty clay	dark gray-black	Kirkwood (Kw1a1)
117	850-860	9.65	97	Laminated silty fine sand interbedded with laminated silty clay	2.5Y 3/1 very dark gray; 25Y 4/1 dark gray	Kirkwood (Kw1a1)
118	860-870	3.55	36	Interbedded silty clay and silty fine sand	2.5Y 3.1 very dark gray; 25Y 4/1 dark gray	Kirkwood (Kw1a1)
119	870-880	9.1	91	Sandy glauconite silt overlying silty clay with shells	7.5YR 3/1 very dark gray/5G 4/1 dark greenish gray	Kirkwood (Kw1a1)
120	880-890	9.6	96	Shelly silty clay	7.5YR 3/1 very dark clay	Kirkwood (Kw1a1)
121	890-900	9.95	100	Silty clay/burrowed clay/shelly glauconite sand; sequence boundary at 891.65 ft; contact at 895.55 ft	2.5Y 3/2; 5Y 5; 5Y 3/2; 5GY 4/1	Kirkwood (Kw1a1/Kw0)/Atlantic City (O6)
122	900-906	5.7	95	Glauconitic medium-coarse sand with shells	5GY 4/1 dark greenish gray	Atlantic City (O6)
123	906-910	5.05	126	Slightly silty glauconitic medium-coarse sand	5GY 3/2 dark olive gray	Atlantic City (O6)
124	910-920	9.95	100	Slightly silty glauconitic medium-coarse sand	5GY 3/2 dark olive gray	Atlantic City (O6)
125	920-928	7.65	96	Slightly silty glauconitic medium-coarse sand; shell debris at lower part	5G 4/2 grayish green; 5Y 3/2 dark olive gray	Atlantic City (O6)
126	928-938	9.6	96	Slightly silty glauconitic medium-coarse sand; shell debris at lower part	5G 4/2 grayish green; 5Y 3/2 dark olive gray	Atlantic City (O6)
127	938-940	1.9	95	Slightly silty glauconitic medium-coarse sand; shell debris at lower part	5G 4/2 grayish green; 5Y 3/2 dark olive gray	Atlantic City (O6)
128	940-950	9.9	99	Slightly silty glauconitic medium-coarse sand; shell debris at lower part; sequence boundary at 950 ft	5G 4/2 grayish green; 5Y 3/2 dark olive gray	Atlantic City (O6)
129	950-960	9.2	92	Glauconitic medium-coarse sand with interbeds of sandy clay; shelly	5G 4/2 grayish green; 5Y 3/2 dark olive gray	Atlantic City (O5)
130	960-970	8.65	87	Clayey, glauconitic, medium-coarse sand with thin clays	5Y 4/2 olive gray	Atlantic City (O5)
131	970-975	4.25	85	Clayey, glauconitic, medium-coarse sand with thin clays	5Y 4/2 olive gray	Atlantic City (O5)
132	975-980	4.5	90	Slightly silty, glauconitic, medium-coarse sand with little clay and shell fragments	5GY 4/1 dark greenish gray	Atlantic City (O5)

Table T1 (continued).

Core	Interval (ft)	Recovery (ft)	Recovery (%)	Primary lithology	Color (Munsell)	Formation
133	980-990	9.4	94	Slightly silty, glauconitic medium-coarse sand grading to clayey glauconitic sand	2.5Y 2.5/1 black	Atlantic City (O5)
134	990-994	3.95	99	Glauconitic clay	5Y 3/1 very dark grey	Atlantic City (O5)
135	994-1005	10.65	97	Shelly glauconitic silty clay grading to clay with abundant coarse glauconite/sand contact at 1002 ft	5Y 3/2 dark olive gray	Atlantic City (O5)
136	1005-1007.5	2	80	Clayey very coarse glauconite sand	N 2.5/ black	Atlantic City (O5)
137	1007.5-1011.5	3.55	89	Slightly clayey very coarse glauconite/?goethite sand	N 2.5/ black	Atlantic City (O5)
138	1011.5-1020	5.8	68	Clayey coarse glauconite/?goethite; very coarse glauconite sand; sequence boundary at 1015.8 ft	5Y 2.5/2 black; N 2.5/ black	Atlantic City (O5/O3)
139	1020-1030	0.85	9	Glauconite mixed with drilling mud?		Atlantic City (O3)
140	1030-1033	1.7	57	Slightly clayey coarse glauconite/?goethite sand	5Y 2.5/2 black	Atlantic City (O3)
141	1033-1040	5.4	77	Shelly silty coarse glauconite sand	5Y 2.5/2 black	Atlantic City (O3)
142	1040-1045	4.3	86	Gravelly, clayey medium-coarse glauconite-quartz sands grading to sandy clay	5Y 2.5/2 black	Atlantic City (O3)
143	1045-1050	2.9	58	Slightly pebbly, sandy glauconite clay; sequence boundary at 1050.5 ft	5Y 4/2 olive gray	Atlantic City (O3/O2b)
144	1050-1053	3.1	103	Clayey, pebbly, slightly shelly, quartzose glauconite sand	5Y 3/2 dark olive gray; 5Y 6/1 gray	Atlantic City (O2b)
145	1053-1056.5	3.2	91	Clayey quartzose glauconite sand	7.5YR 2.5/1 black	Atlantic City (O2b)
146	1056.5-1060	3	86	Silty glauconitic medium-coarse quartz sand	2.5Y 3/2 dark grayish brown	Atlantic City (O2b)
147	1060-1070	10	100	Silty glauconitic medium-pebbly quartz sand	2.5Y 3/2 dark grayish brown	Atlantic City (O2b)
148	1070-1080	8.4	84	Silty glauconitic medium-coarse quartz sand with indurated zones	5Y 4/2 olive gray	Atlantic City (O2b)
149	1080-1090	6.4	64	Medium-coarse quartz glauconite sand over clayey glauconite sand with shells; sequence boundary at 1090 ft	5GY 4/1 dark greenish gray	Atlantic City (O2b)/Sewell Point (O2a)
150	1090-1100	10.7	107	Interbedded glauconitic clays and clayey sandy glauconite sand	10YR 2/2 very dark brown	Sewell Point (O2a)
151	1100-1106.5	6.5	100	Clayey glauconite fine sands	5Y 2.5/1 black	Sewell Point (O2a)
152	1106.5-1113	4.7	72	Clayey glauconite fine-very coarse sands	5Y 2.5/1 black	Sewell Point (O2a)
153	1113-1120	7.95	114	Clayey glauconite fine-very coarse sands	5Y 2.5/1 black	Sewell Point (O2a)
154	1120-1126	5.9	98	Clayey glauconite medium coarse sands	5Y 2.5/1 black	Sewell Point (O2a)
155	1126-1130	1.2	30	Clayey glauconite medium coarse sands; sequence boundary at 1126.3 ft	2.5Y 3/1 very dark gray	Sewell Point (O2a/O1)
156	1130-1135	0.4	8	Glauconitic clay	5Y 4/3 to 4/3 olive	Sewell Point
157	1135-1140	1.4	28	Glauconitic clay	5Y 4/3 to 4/3 olive	Sewell Point
158	1140-1145	4.1	82	Clayey glauconite medium coarse sands	5Y 4/3 to 4/3 olive	Sewell Point
159	1145-1150	4.8	96	Clayey glauconite sand	2.5Y 3/1 black	Sewell Point
160	1150-1160	8.1	81	Clayey glauconite sand	2.5Y 3/1 black	Sewell Point
161	1160-1162.5	2.4	96	Quartzose glauconite sand/sandy quartz; contact Sewell Point glauconite clay	2.5Y 3/1 black	Sewell Point
162	1162.5-1170	0.5	7	Clayey quartzose glauconite sand	2.5Y 3/1 black	Sewell Point
163	1170-1180	10.35	104	Quartzose glauconitic clay; sequence boundary 1171.5 ft; mica laminated clay	2.5Y 3/1 black; 5GY 4/1 dark greenish gray	Sewell Point/Absecon Inlet
164	1180-1190	9.4	94	Micaceous laminated silty clay to clay	5Y 3/2 dark olive gray	Absecon Inlet
165	1190-1200	10.4	104	Micaceous laminated silty clay to clay	5Y 3/2 dark olive gray	Absecon Inlet
166	1200-1210	10.5	105	Micaceous laminated silty clay	5Y 3/2 dark olive gray	Absecon Inlet
167	1210-1220	10.4	104	Micaceous laminated silty clay	5Y 3/2 dark olive gray	Absecon Inlet
168	1220-1230	9.4	94	Micaceous shelly laminated silty clay with clay interbeds	5Y 3/2 dark olive gray	Absecon Inlet

Table T1 (continued).

Core	Interval (ft)	Recovery (ft)	Recovery (%)	Primary lithology	Color (Munsell)	Formation
169	1230-1240	10.4	104	Micaceous shelly laminated silty clay with clay interbeds	5Y 3/2 dark olive gray	Absecon Inlet
170	1240-1250	3.25	33	Laminated silty micaceous clay	2.5Y 4/2 dark grayish brown to 2.5Y 4/1 very dark grayish brown	Absecon Inlet
171	1250-1260	6.8	68	Glauconitic sandy clay to silty micaceous glauconitic clay	Dark olive gray 5Y 3/2, dark greenish gray 5GY 4/1 to dark grayish brown 2.5Y 4/2	Absecon Inlet
172	1260-1270	10.5	105	Slightly glauconitic clay, occasional pyrite and shell fragments	Very dark gray 5Y 3/1 to dark olive gray 5Y 3/2	Absecon Inlet
173	1270-1280	9.2	92	Very slightly glauconitic clay, occasional thin shell fragments, occasional pyrite	Dark olive gray 5Y 3/2 to black 5Y 2.5/2	Absecon Inlet
174	1280-1290	10.5	105	Very slightly glauconitic clay, occasional thin shell fragments	Very dark gray 5Y 3/1 to dark olive gray 5Y 3/2	Absecon Inlet
175	1290-1300	10.45	105	Very slightly glauconitic clay, occasional thin shell fragments	Very dark gray 5Y 3/1 to dark olive gray 5Y 3/2	Absecon Inlet
176	1300-1310	8.3	83	Very slightly glauconitic clay, occasional thin shell fragments	5Y 3/1 very dark gray	Absecon Inlet
177	1310-1313	2.95	98	Very slightly glauconitic clay, occasional thin shell fragments	5Y 3/1 very dark gray	Absecon Inlet
178	1313-1320	5.2	74	Very slightly glauconitic clay, occasional thin shell fragments, *turritella* spp., schaphopod	5Y 3/2 dark olive gray	Absecon Inlet
179	1320-1330	10.5	105	Very slightly glauconitic clay, occasional thin shell fragments	5Y 3/2 dark olive gray	Absecon Inlet
180	1330-1340	10.2	102	Very slightly glauconitic clay, occasional thin shell fragments	5Y 3/2 dark olive gray	Absecon Inlet
181	1340-1350	7.7	77	Pyritic shelly silty clay to clay	5Y 3/2 dark olive gray to 5Y 3/1 very dark gray	Absecon Inlet
182	1350-1360	10.5	105	Pyritic shelly silty clay to clay	5Y 3/2 dark olive gray	Absecon Inlet
183	1360-1370	10.6	106	Pyritic shelly silty clay to clay	5Y 3/2 dark olive gray	Absecon Inlet
184	1370-1380	9.8	98	Pyritic shelly silty clay to clay; glauconitic clay; sequence boundary at 1375 ft; clayey glauconite sand; ash marl	5Y 3/2 dark olive gray (AI); 5Y 4/2 olive gray (upper SR); 5GY 5/1 greenish gray	Absecon Inlet/u Shark River
185	1380-1390	10.6	106	Glauconitic slightly silty clay to clay	5Y 4/2 olive gray; 5GY 5/1 greenish gray	u Shark River
186	1390-1400	10.25	103	Glauconitic silty clay to clay	5GY 5/1 greenish gray	u Shark River
187	1400-1410	10.2	102	Shelly glauconitic silty clay; sequence boundary at 1402.9 ft; slightly glauconitic silty clay	5Y 4/1 olive gray; 5Y 3/2 dark olive gray	u Shark River
188	1410-1420	9.9	99	Slightly glauconitic shelly silty dry clay	5Y 3/2 dark olive gray	u Shark River
189	1420-1430	3.7	37	Clay to glauconitic clay	5Y 3/2 dark olive gray	u Shark River
190	1430-1440	7.7	96	Slightly glauconitic clay to clayey glauconite sand; sequence boundary at 1434.4 ft	5Y 5/2 olive gray; 5Y 3/2 dark olive gray	u Shark River
191	1438-1448	10	100	Slightly glauconitic uniform silty clay	5Y 5/2 olive gray	l Shark River
192	1448-1453	5.3	106	Slightly glauconitic uniform silty clay	5Y 4/2 olive gray	l Shark River
193	1453-1460	0.15	2	Somewhat indurated silty clay	5Y 4/2 olive gray	l Shark River
194	1460-1463	0.4	13	Porcellanitic slightly glauconitic shelly clay	5Y 4/2 olive gray	l Shark River
195	1463-1470	2.2	31	Somewhat indurated/porcellanitic slightly glauconitic clay	5Y 4/2 olive gray	l Shark River
196	1470-1480	0.4	4	Somewhat indurated silty clay	5Y 4/2 olive gray	l Shark River
197	1480-1484	0.1	3	Indurated silty clay	5Y 4/2 olive gray	l Shark River
198	1484-1487	2.87	96	Indurated clayey silt to silty clay	5Y 6/2 light olive gray	l Shark River
199	1487-1490	3.6	120	Indurated porcellanitic clay to clayey porcellanite	5Y 6/2 light olive gray to 5Y 7/1 light gray	l Shark River
200	1490-1500	8.5	85	Indurated foraminiferal porcellanitic clay	5Y 6/2 light olive gray to 5Y 7/1 light gray	l Shark River
201	1500-1509	10.43	116	Indurated foraminiferal porcellanitic clay	5Y 6/2 light olive gray to 5Y 7/1 light gray	l Shark River
202	1509-1519.3	8.37	81	Indurated foraminiferal porcellanitic clay	5Y 6/2 light olive gray to 5Y 7/1 light gray	l Shark River
203	1519.3-1527.5	6.8	83	Indurated foraminiferal porcellanitic clay	5Y 6/2 light olive gray to 5Y 7/1 light gray	l Shark River
204	1527.5-1536	10.5	124	Indurated foraminiferal porcellanitic clay	5Y 6/2 light olive gray to 5Y 7/1 light gray	l Shark River

Table T1 (continued).

Core	Interval (ft)	Recovery (ft)	Recovery (%)	Primary lithology	Color (Munsell)	Formation
205	1536-1540	4.2	105	Indurated foraminiferal porcellanitic clay	5Y 6/2 light olive gray to 5Y 7/1 light gray	l Shark River
206	1540-1550	9.6	96	Indurated foraminiferal porcellanitic clay to slightly glauconitic foraminiferal clay	5Y 6/2 light olive gray to 5Y 7/1 light gray; 5GY 6/1 to 5GY 5/1 greenish gray	l Shark River
207	1550-1560	10.4	104	Glauconitic clay; sequence boundary at 9.0 ft; porcellanitic clay	5Y 6/2 light olive gray; 5Y 5/2 olive gray	l Shark River
208	1560-1570	8.7	87	Indurated foraminiferal porcellanitic clay to slightly glauconitic foraminiferal clay	5Y 6/2 light olive gray to 5Y 7/1 light gray	l Shark River
209	1570-1580	3.5	70	Glauconitic foraminiferal clay and silty clay	5Y 6/2 light olive gray to 5Y 7/1 light gray	Shark River
			Totals:			
			Recovered (ft):	1271.14		
			Drilled (ft):	1575		
			Recovery (%):	80.71		
			Median recovery (%):	91		
Hole B						
1	0-2.9	2.9	100	Soil and fill	Not recorded	Fill
2	2.9-4.0	1.1	100	Gravelly sand	Not recorded	Unnamed gravel member, Cape May
3	4.0-6.0	2	100	Sandy gravel	Not recorded	Unnamed gravel member, Cape May
4	6.0-7.0	1	100	Gravelly sand	Not recorded	Unnamed gravel member, Cape May
5	7.0-8.0	1	100	Medium-coarse quartz sand	Not recorded	Unnamed gravel member, Cape May
6	8.0-9.0	1	100	Gravelly sand	Not recorded	Unnamed gravel member, Cape May
7	9.0-11.1	2.1	100	Slightly gravelly fine-very coarse sand	Not recorded	Unnamed gravel member, Cape May
8	11.1-12.25	1.15	100	Well-sorted fine sand	Not recorded	Cape May
9	12.25-13.1	0.85	100	Sandy gravel	Not recorded	Cape May
10	13.1-13.7	0.6	100	Gravelly sand	Not recorded	Cape May
11	13.7-13.9	0.2	100	Fine sand	Not recorded	Cape May
12	13.9-16.1	2.2	100	Sandy gravel grading to gravely sand	Not recorded	Cape May
13	16.1-19.4	3.3	100	Medium sand; contact at 19.4 ft	Not recorded	Cape May
14	19.4-22.7	3.3	100	Slightly micaceous silty clay	Not recorded	Cape May
15	22.7-23.4	0.7	100	Silty fine sand	Not recorded	Cape May
16	23.4-24.0	0.6	100	Fine-medium sand	Not recorded	Cape May
17	24.0-25.0	1	100	Occasionally pebbly medium sand	Not recorded	Cape May
18	25.0-25.5	0.5	100	Fe-stained occasionally pebbly medium sand	Not recorded	Cape May
19	25.5-27.0	1.5	100	Occasionally pebbly medium sand	Not recorded	Cape May
20	27.0-29.0	2	100	Medium sand	2.5Y 8/2 pale yellow	Cape May
21	29.0-30.0	1	100	Medium-coarse sand	5YR 5/8 yellowish red	Cape May
22	30-30.5	0.5	100	Gravelly sand	Not recorded	Cape May
23	30.5-34.0	3.5	100	Medium-very coarse sand	Not recorded	Cape May
24	34.0-38.0	4	100	Medium sand	2.5Y 8/2 pale yellow	Cape May
25	38.0-39.0	1	100	Medium sand	5YR 5/8 yellowish red	Cape May
26	39.0-49.0	10	100	Medium-coarse sand	2.5Y 8/2 pale yellow	Cape May
27	49.0-51.0	2	100	Silty micaceous fine sand	2.5Y 7/8 yellow	Cape May
28	51.0-51.8	0.8	100	Fine-coarse sand	Brownish yellow	Cape May
29	51.8-61.0	9.2	100	Coarse-very coarse sand	Not recorded	Cape May
30	61.0-73.0	12	100	Medium-very coarse sand	Not recorded	Cape May
			Totals			
			Recovered (ft):	73		
			Drilled (ft):	73		
			Recovery (%):	100		
			Median recovery (%):	100		

Note: AI = Absecon Inlet, SR = Shark River.

Table T2. Dinocyst occurrences in the Ocean View borehole, Leg 174AX.

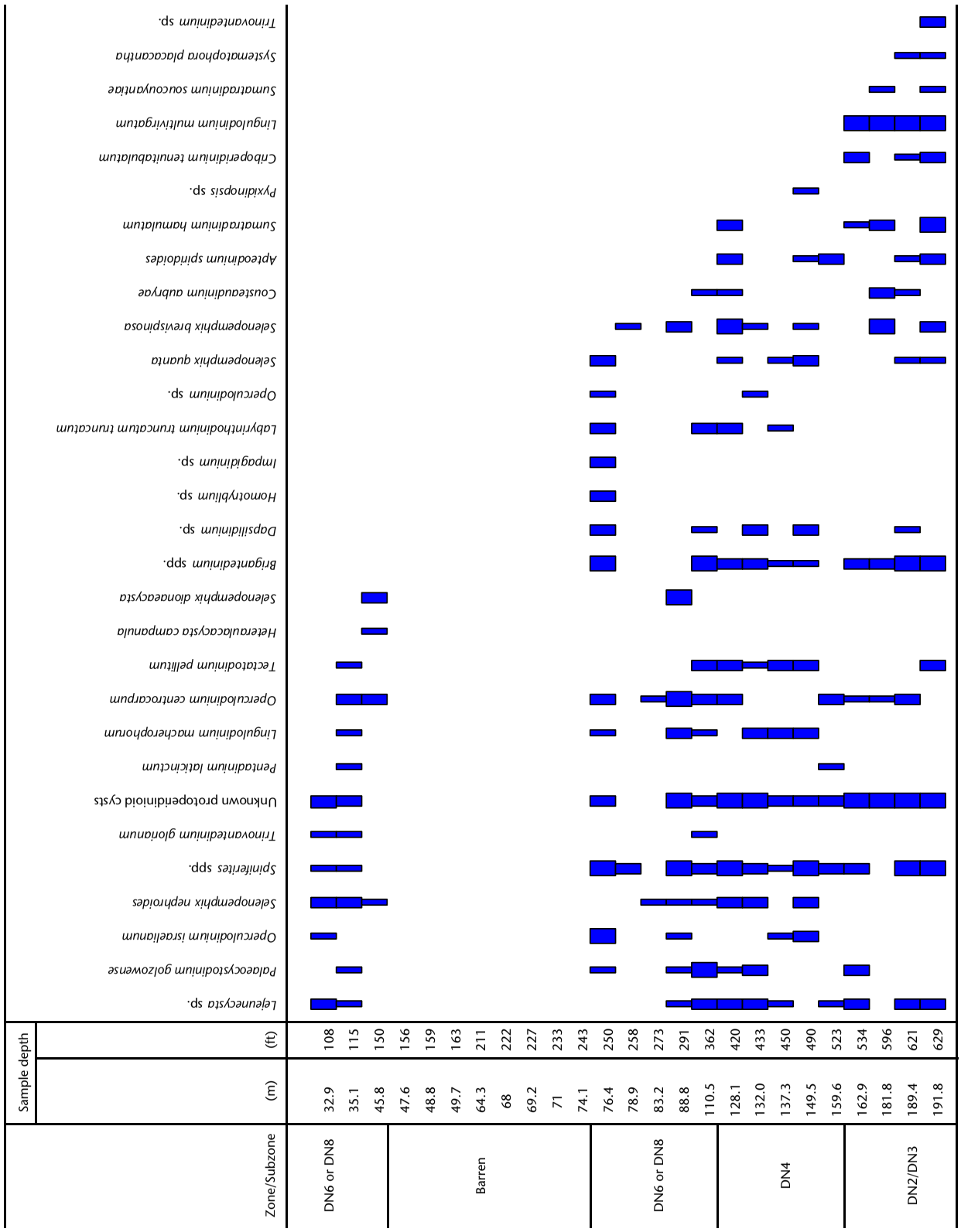

Table T3. Eocene planktonic foraminiferal occurrences in the Ocean View borehole, Leg 174AX. (See table note. Continued on next page.)

Species	Sample depth (ft)																																							
	1552	1545.6	1542	1532	1522	1512.5	1502.5	1501	1470	1463	1451	1441	1431	1421	1411	1401	1391	1381	1361	1351	1341	1331	1321	1311	1301	1291	1281	1271	1261	1251	1241	1231	1221	1211	1201	1191	1181	1177.2	1175.2	1173	1172.1
Acarinina bullbrooki				x		x		x	x	x	x		x	x	x																										
Acarinina matthewsae								x		x	x																														
Acarinina pentacamerata			x	x	x	x	x	x	x				x	x	x	x																									
Acarinina quetra		x	x	x	x																																				
Acarinina rohri									x		x	x																													
Acarinina soldadoensis	x				x																																				
Acarinina topilensis								x	x	x	x	x	x	x																											
Cassigerinella chipolensis																					x																				
Catapsydrax dissimilis																																							x		
Catapsydrax globiformis													x	x		x	x	x			x	x	x												x	x					
Catapsydrax hardingae																																						x	x	x	x
Catapsydrax pera																		x																							
Chiloguembelina ototara																x		x			x						x				x				x				x	x	
Chiloguembelina victoriana									x			x		x		x	x	x								x											x				
Dentoglobigerina galavisis																x	x	x	x	x	x	x	x	x	x		x		x						x			x	x	x	
Dentoglobigerina globularis																			?	x		x			?														x	x	
Dentoglobigerina pseudovenezuelana																									x						x				x					x	x
Globigerina officinalis																															x			x	x	x	x	x	x	x	
Globigerina praebulloides																																						x	x	x	x
Globigerinatheka index									x				x	x	x	x	x	x			x	x		x		x	x														
Globigerinatheka kugleri								x	x	x	x	x			x	x																									
Globigerinatheka mexicana								x																																	
Globigerinatheka semiinvoluta																	x					x				x															
Globigerinatheka subconglobata			x		x																																				
Globorotaloides carcosellensis					x			x	x		x						x	x																							
Globoturborotalita? ampliapertura																																						x	x		
Globoturborotalita ouachitatensis																	x	x			x										x	x			x		x	x	x	x	
Guembelitrioides lozanoi			x					x																																	
Hantkenina alabamensis																												x			x	x								x	x
Hantkenina nuttalli		x	x																																						
Hantkenina primitiva								x	x	x																															
Morozovella gracilis		x	x		x																																				
Morozovella formosa		x	x	x	x																																				
Morozovella lehneri								x		x																															
Morozovella spinulosa								x		x	x		x	x	x																										
Paragloborotalia griffinae			x		x																																		x	x	x
Paragloborotalia nana																															x	x		x	x	x		x	x		
Planorotalites pseudoscitula				x	x																																				
Pseudohastigerina micra				x	x	x	x	x	x	x	x	x	x	x	x	x	x	x			x	x				x	x	x			x	x	x		x		x	x	x	x	
Pseudohastigerina sharkriverensis				x																																					
Pseudohastigerina wilcoxensis		x	x	x					?																																
Subbotina cryptomphala									x		x		x																												
Subbotina eocaena	x		x	x	x	x	x	x	x	x	x	x	x	x	x	x	x	x	x	x	x	x	x	x	x	x	x	x	x	x	x	x	x	x		x	x	x	x	x	x
Subbotina frontosa		x	x	x	x	x		x			x																														
Subbotina hagni			x	x				x	x	x	x	x	x	x	x		x																								
Subbotina linaperta																x		x		x		x									x										
Subbotina praeturritilina																																								x	

Table T3 (continued).

Species	Sample depth (ft)																																							
	1552	1545.6	1542	1532	1522	1512.5	1502.5	1501	1470	1463	1451	1441	1431	1421	1411	1401	1391	1381	1361	1351	1341	1331	1321	1311	1301	1291	1281	1271	1261	1251	1241	1231	1221	1211	1201	1191	1181	1177.2	1175.2	1173	1172.1
Subbotina senni		x	x	x	x				x	x	x	x																													
Subbotina utilisindex															x	x	x	x	x						x		x	x	x	x	x	x									
Subbotina yeguaensis									x		x	x	x							x						x					x										
Tenuitella gemma																																						x	x	x	x
Tenuitella insolita																										x					x				x						
Turborotalia cerroazulensis																	x	x			x	x	x			x	x	x	x	x	x	x	x				x		x		
Turborotalia cocoaensis																																x					x				
Turborotalia increbescens																																									x
Turborotalia pomeroli									?	x		x	x	x	x		x	x	x	x			x	x	x	x	x	x	x										x	x	
Turborotalia possagnoensis								x		x	x	x	x	x	x																										
Turborotalia pseudoampliapertura																															x	x	x	x	x	x	x		x	x	x
genus? *aculeata*																x				x						x	x														

Note: x = occurrence of taxon in sample, ? = questionable identification.

Table T4. Eocene benthic foraminiferal occurrences in the Ocean View borehole, Leg 174AX. (Continued on next page.)

Species	Sample depth (ft)																																
	1552	1542	1532	1522	1512.5	1502.5	1501	1470	1463	1451	1441	1431	1421	1411	1401	1391	1381	1361	1351	1341	1331	1321	1311	1301	1291	1281	1271	1261	1251	1241	1231	1221	1211
Alabamina		F	R		X									VR							VR		VR					VR					
Anomalinoides							X	F	C	F			F																				
Bolivina sp. (>125 µm)															C	C	C												VR				
Bolivina sp. (<125 µm)								C	C		C	F	A	A	R	R																	
Bulimina cacumenata morph											F																						
Bulimina			R					R	R			F	R		VR					C	VR					X				F	R		
Bulimina sp. (<125 µm)		A	A	C																													
Bulimina jacksonensis																A	A	R					VR			X	C	F	F/C				
Buliminella													R																				
Cassidulina																	R								X	X				F/C			
Ceratobulimina																				VR		VR			X	X				R/F	R	C	R
Chilostomella														VR						VR						X							
Cibicides								C			C	A	A	A	C	F	F	R		C					X		C	C	F	C	C	C	
Cibicidoides	X	A	A	C	X	C	X	C	C	A	F				A	C	A	C	F	F	F	F	F	F	X		C	C	C	C	F		C
Dentalina		R		VR			X	VR		VR			R	R	R		R	R	R	R	R			R	X	X	F	R	R	R/F	F	R	C
Epistomina																		R	R	VR		R	F		X		R	R		VR		R	F
Epistominella																R				VR	VR	VR		R									
Frondicularia																									X		VR	VR	VR				VR
Gaudryina	X												C	C	R													F					
Gavelinella		R	F	R		VR			F		R		R		R	R	R						R						F		F	VR	
Globulina															R	R		R		R		R	R	R	X	X	R	F		R/F	F	C	R
Guttulina			C		X					VR					R			R	R		R	R	R	R	X		F	R	R		F	R	R
Gyroidinoides	X		C					C	C	R			C	C	C	C	F	C	C	F	R	R	R	F	X	X	F	R	R	F	F	C	R
Lagena												C																	VR				
Lenticulina	X	C	F	F	X		X	R	R	F	F		F	F	R			R	R	R	F	R	F	R	X	X	R	VR	R	R/F		C	C
Marginulina	X	R						VR			R						VR					VR		VR				VR					VR
Melonis planatum		F	R		X	VR					R			C											X	X	VR	R	R		VR	VR	VR
Nodosaria	X											VR	VR		VR														VR		R		R
Oolina																																	VR
Oridorsalis																			R	VR	R	VR		F	X	X	R	R	R/F	F	VR	VR	
Osangularia																		VR						F									
Pamula																																	
Pullenia				R										VR												X				VR			
Rectonodosaria																			VR														
Saracenaria																				VR											VR		
Siphonina danvillensis								R		R	R	R	R																			C	F
Spiroplectammina		F	C				X	VR	VR			F	VR			VR	R			VR			VR								VR		
Stilostomella		C					X	R			R	R		R	F	F	C	VR	R	R	R	R	R/F	F	X		VR	VR	R	R		VR	VR
Uvigerina								C		C		C	C	F	R/F	R	F					A	VR		X	X	F	F		R	R/F	VR	C
Planktonic foraminifers (<125 µm)		A	A	C			A	A	A	A	A	A	A	A	A	A	A	C	C	A					R								
Planktonic foraminifers (>125 µm)		A	A	C			A	A	A	A	A	A	A	A	A	A	A	C	A	F	C	C	R	F	C	A	C	R	R	R	R	R	R

Note: A = abundant, C = common, F = frequent, R = rare, VR = very rare, X = present.

Table T4 (continued).

Species	Sample depth (ft)		
	1201	1191	1181
Alabamina			
Anomalinoides			
Bolivina sp. (>125 µm)	VR	R	
Bolivina sp. (>125 µm)			
Bulimina cacumenata morph			
Bulimina	R		
Bulimina sp. (>125 µm)			
Bulimina jacksonensis			
Buliminella			
Cassidulina		F	
Ceratobulimina	F	F	C
Chilostomella			
Cibicides	C/A	F	F
Cibicidoides	C/A	C	C
Dentalina	F/C	R	R
Epistomina		R	
Epistominella			
Frondicularia	R	R	
Gaudryina			
Gavelinella			
Globulina	F/C		R
Guttulina	F/C	F	R
Gyroidinoides	F/C	F	C
Lagena			R
Lenticulina	F/C	F	R
Marginulina		F	
Melonis planatum	R	F	C
Nodosaria		F	
Oolina			
Oridorsalis			
Osangularia			
Pamula			
Pullenia	R		
Rectonodosaria			VR
Saracenaria			
Siphonina danvillensis	F/C	F	C
Spiroplectammina			VR
Stilostomella	R		VR
Uvigerina	F	R	VR
Planktonic foraminifers (>125 µm)			
Planktonic foraminifers (>125 µm)	R	R	R

Table T5. Sr-isotopic data, Ocean View borehole, Leg 174AX. (See table note. Continued on next page.)

Sample depth (ft)	Sample depth (m)	Material	$^{87}Sr/^{86}Sr$ ratio	Analytical error (2σ)	CK92 age Oslick (Ma)	CK92 age Martin (Ma)	BKSA95 age Reilly (Ma)	
293.3	89.4	Shell	0.708834	0.000005	13.5	11.6	—	
309.4	94.31	Shell	0.708865	0.000010	12.4	10.0	—	
312.1	95.13	Shell	0.708834	0.000050	13.5	11.6	—	
312.1	95.13	Shell	0.708821	0.000005	14.0	12.2	—	Duplicate
325.3	99.15	Shell	0.708846	0.000005	13.1	11.0	—	
326.9	99.64	Shell	0.708829	0.000015	13.7	11.8	—	
326.9	99.64	Shell	0.708824	0.000006	13.9	12.1	—	Duplicate
327	99.67	Shell	0.708837	0.000006	13.4	11.4	—	
335.8	102.35	Shell	0.708847	0.000008	13.1	10.9	—	
335.8	102.35	Shell	0.708844	0.000005	13.2	11.1	—	Duplicate
369.9	112.75	Shell	0.708864	0.000011	12.4	10.1	—	
369.9	112.75	Shell	0.708832	0.000004	13.6	11.7	—	Duplicate
397.12	121.04	Shell	0.708819	0.000008	14.1	12.3	—	
427.1	130.18	Shell	0.708769	0.000009	15.9	—	—	
428	130.45	Shell	0.708773	0.000006	15.8	—	—	
431	131.37	Shell	0.708792	0.000006	15.1	—	—	
441.5	134.57	Shell	0.708769	0.000014	15.9	—	—	
460.65	140.41	Shell	0.708760	0.000006	16.0	—	—	
465.1	141.76	Shell	0.708700	0.000006	16.9	—	—	
475	144.78	Shell	0.708734	0.000005	16.4	—	—	
480.7	146.52	Shell	0.708692	0.000005	17.0	—	—	
490.9	149.63	Shell	0.708700	0.000005	16.9	—	—	
497.7	151.7	Shell	0.708703	0.000005	16.9	—	—	
502.91	153.29	Shell	0.708695	0.000007	17.0	—	—	
514.5	156.82	Shell	0.708715	0.000008	16.7	—	—	
515	156.97	Shell	0.708674	0.000005	17.3	—	—	
522.37	159.22	Shell	0.708680	0.000005	17.2	—	—	
526.42	160.45	Shell	0.708676	0.000005	17.3	—	—	
531.6	162.03	Shell	0.708677	0.000006	17.2	—	—	
563.75	171.83	Shell	0.708654	0.000005	17.6	—	—	
563.75	171.83	Shell	0.708654	0.000005	17.6	—	—	Duplicate
600.75	183.11	Shell	0.708668	0.000006	17.4	—	—	
609.58	185.8	Shell	0.708665	0.000005	17.4	—	—	
609.58	185.8	Shell	0.708777	0.000010	15.8	—	—	Duplicate
623.38	190.01	Shell	0.708659	0.000006	17.5	—	—	
625.75	190.73	Shell	0.708631	0.000005	17.9	—	—	
632.29	192.72	Shell	0.708644	0.000007	17.7	—	—	
633.06	192.96	Shell	0.708639	0.000005	17.8	—	—	
641	195.38	Shell	0.708511	0.000007	19.7	—	—	
651.5	198.58	Shell	0.708489	0.000006	20.0	—	—	
655.5	199.8	Shell	0.708491	0.000010	20.0	—	—	
661.5	201.63	Shell	0.708486	0.000011	20.0	—	—	
676.35	206.15	Shell	0.708493	0.000006	19.9	—	—	
676.35	206.15	Shell	0.708445	0.000005	20.6	—	—	Duplicate
681.8	207.81	Shell	0.708455	0.000007	20.5	—	—	
681.8	207.81	Shell	0.708459	0.000015	20.4	—	—	Duplicate
701.9	213.94	Shell	0.708455	0.000004	20.5	—	—	
717.13	218.58	Shell	0.708473	0.000005	20.2	—	—	
735.5	224.18	Shell	0.708461	0.000006	20.4	—	—	
735.5	224.18	Shell	0.708465	0.000006	20.3	—	—	Duplicate
737.35	224.74	Shell	0.708445	0.000006	20.6	—	—	
825.25	251.54	Shell	0.708518	0.000009	19.6	—	—	
825.25	251.54	Shell	0.708458	0.000006	20.5	—	—	Duplicate
828.45	252.51	Shell	0.708442	0.000004	20.7	—	—	Duplicate
844.6	257.43	Shell	0.708459	0.000004	20.4	—	—	
844.6	257.43	Shell	0.708433	0.000006	20.8	—	—	Duplicate
844.6	257.43	Shell	0.708482	0.000005	20.1	—	—	Duplicate
861.55	262.6	Shell	0.708426	0.000013	20.9	—	—	
871	265.48	Shell	0.708449	0.000005	20.6	—	—	
878.6	267.8	Shell	0.708445	0.000006	20.6	—	—	
878.6	267.8	Shell	0.708403	0.000007	21.3	—	—	Duplicate
878.6	267.8	Shell	0.708472	0.000004	20.2	—	—	Duplicate
890	271.27	Shell	0.708424	0.000008	20.9	—	—	
892	271.88	Shell	0.708400	0.000005	21.3	—	—	
895	272.8	Shell	0.708318	0.000009	22.5	—	23.0	
895.3	272.89	Shell	0.708280	0.000006	23.8	—	23.7	
895.5	272.95	Shell	0.708318	0.000009	22.5	—	23.0	
897	273.41	Shell	0.708214	0.000008	25.0	—	25.0	

Table T5 (continued).

Sample depth (ft)	Sample depth (m)	Material	$^{87}Sr/^{86}Sr$ ratio	Analytical error (2σ)	CK92 age Oslick (Ma)	CK92 age Martin (Ma)	BKSA95 age Reilly (Ma)
900.6	274.5	Shell	0.708197	0.000018	25.4	—	25.3
901	274.62	Shell	0.708220	0.000007	24.9	—	24.9
911	277.67	Shell	0.708221	0.000010	24.9	—	24.9
931	283.77	Shell	0.708210	0.000005	25.1	—	25.1
941	286.82	Shell	0.708202	0.000006	25.3	—	25.2
956	291.39	Shell	0.708133	0.000005	26.6	—	26.6
978	298.09	Shell	0.708143	0.000006	26.4	—	26.4
999	304.5	Shell	0.708130	0.000006	26.7	—	26.7
1031	314.25	Shell	0.708059	0.000006	28.3	—	28.4
1050.7	320.24	Shell	0.708035	0.000005	29.0	—	29.0
1076	327.96	Shell	0.707994	0.000006	30.1	—	30.1
1086	331.01	Shell	0.707983	0.000005	30.4	—	30.4
1096	334.06	Shell	0.707960	0.000006	31.0	—	31.0
1135.7	346.16	Shell	0.707893	0.000007	32.9	—	32.8
1141	347.78	Shell	0.707898	0.000008	32.7	—	32.6
1151	350.8	Shell	0.707877	0.000006	33.3	—	33.2
1155.5	352.3	Shell	0.707832	0.000006	34.5	—	34.4

Note: — = outside of meaningful range.